Quantum Dissipation
at the Nanoscale

CANDIDATE
Franco Pellegrini

SUPERVISORS
Prof. Erio Tosatti
Prof. Giuseppe E. Santoro

Contents

Introduction

The study of dissipation is of great theoretical and technological importance. While physics often models a system as isolated, with all the relevant degrees of freedom accounted for, in most realistic cases the "interesting" part of the system is coupled to many external degrees of freedom, often referred to as the *environment*. When we try to manipulate our system, in most cases we will also be acting on the environment. The most direct effect of this is that some of the energy we put in the system will be shared with a large number of degrees of freedom and thus, to all intents and purposes, will be *dissipated* in the environment. While we are typically not interested in the precise dynamics of the irrelevant degrees of freedom, an accurate description of the out-of-equilibrium *dynamics* of our system requires us to add some terms in our model to account for this coupling and energy loss. As in many physical problems, the main issue is the presence of a large amount of degrees of freedom that cannot be handled exactly and the need for a description able to represent the essential features of anything we are not specifically interested in: this of course represents a well known line of problems in modern physics [1, 2].

In parallel with the theoretical interest, the study of dissipation is of the utmost importance in many applications. One of the macroscopic effects of dissipation is friction: the conversion of kinetic energy into thermal energy due to the relative motion of two bodies. Many theories have been created to address this issue: from the simplest empirical observations of Leonardo da Vinci, to the most sophisticated microscopic theories describing friction through large scale classical atomistic simulations. Still, many problems remain unsolved and most theories aim at obtaining simpler models to take into account dissipative effects and, if possible, find ways to reduce their complexity.

Moving to the quantum world, the basic idea remains the same, but things often become much more complicated: while in a classical system we can often afford to construct reasonably simple models to mimic the presence of the environment, in quantum systems the dimension of the Hilbert space grows

so rapidly that we are forced to be much more efficient in the description of the non-relevant degrees of freedom. Moreover, while for classical systems the environment is an external term added to the standard description of the system, for quantum mechanics the presence of degrees of freedom which are not treated explicitly forces us to move from a "pure-state description" of our system to a statistical mixture of states.

The most common starting point for the description of quantum dissipative systems is, as for the general case, the separation of a complex model in two parts: the system we are interested in describing and the environment, which is typically assumed to be in thermodynamical equilibrium and large enough to keep its state under the influence of the system. From this common starting point, most approaches focus on the elimination of the irrelevant degrees of freedom through various schemes, appropriate to the specific problem under exam. In our application we will follow this general idea.

Quantum dissipative systems have been receiving more and more attention, since the development of nanotechnology requires a better understanding of dissipative effects at scales where a quantum description becomes essential. Many state-of-the-art applications, from atomic force microscopy to quantum computation, require a profound understanding of these effects for a reliable description. The models we will consider in this thesis fall into these categories: in one application, analyzing a recent atomic force microscopy experiment, we provide a theoretical description for a dissipation channel unaccounted so far; in the other we construct a model taking into account dissipative effects for electrons circulating a nanoscopic device of probable experimental feasibility. In the first case [3] we will consider the energy loss of a tip oscillating over a surface; this system is usually described in a mostly classical framework in the known theories of *nanotribology*: the study of the microscopic mechanisms and energy dissipation channels leading to the effects macroscopically characterized as friction. In our case we will see how the central role of the spins of the surface and their coupling to the internal degrees of freedom of the system will require an *ad hoc* quantum model. With the second system [4], we will explore the effects of electronic dissipation over the observables of a system explicitly kept in a nonequilibrium state through an external cyclic perturbation generally referred to as *pumping*. In this case, more than exploring the energy dissipation itself, our focus will be on the effects of a dissipative coupling of the electron motion on the steady state of the system. Once more, quantum mechanics will play a fundamental role in our description.

While our two starting points will be very different, we will show how they can both be reduced in the end to the most simple quantum system, a single spin-$\frac{1}{2}$, and how the presence of the bath will modify the simple dynamics

of this spin in very interesting ways. Although our final Hamiltonian will be similar in both cases, the different nature of the coupling will require two very different approaches: in one case we will derive a master equation for the spin density matrix, a quite intuitive and general approach valid for weak coupling to the environment; while in the other case the presence of a strong coupling will force use to resort to a path integral technique, a heavier and more specific approach able to describe a wider range of parameters.

The outline of this work will be as follows: in chapter 1, after a brief overview of the systems studied and a preview of the results obtained, we will introduce the general models and methods we are going to use to tackle the systems considered, hopefully providing enough theory to understand our later extensive treatment, without entering in too much detail in the widely studied general theories of our models. In chapter 2 we will show our first application: the description of a spin-sensitive dissipation channel compatible with the experimental findings of an atomic force microscopy experiment. We will describe in some detail the experiment and the system under study and why some direct approaches are unable to account for the observed effect; we will then specialize the previously described path integral technique to obtain a numerical description of the system, highlighting our proposed dissipation mechanism. In chapter 3 we will consider electron current pumping in a three-site system and how it can be affected by the presence of an environment. We will first obtain and solve a simple equation for the isolated system, then couple a bath to this and specialize the master equation theory to obtain an analytical result for the system in presence of an environment, observing some interesting changes it its behavior. The experimental feasibility of the proposed setup will be explored. Finally, in chapter 4 we will briefly present another model for the description of dissipative systems which has been investigated but, for now, is not complete enough to produce interesting results: inspired from another atomic force microscopy experiment where frictional effects of hydrogen atoms on a surface are observed, we will try to investigate the possibility of inherently quantum effects in a similar system, where a light particle is coupled to other heavier atoms, treated classically. We will propose a model and a technique for its simulation, though this will prove too computationally demanding to be of practical use.

Chapter 1

Models and Methods for Dissipative Quantum Systems

There is no standard model to tackle a general dissipative system. However, one general concept behind the description of a dissipative quantum system is the possibility to construct a model in which a small number of interesting degrees of freedom (usually referred to as the *system* itself) is coupled to a much larger number of less interesting degrees of freedom that can be treated as a *bath*. The aim of dissipative models is to take into account the presence of the bath and its effects on the system without the need for a precise description of all its degrees of freedom, but just referring to its general properties such as temperature, density of states and coupling.

In section 1.1 we will present a general overview of the systems studied to provide a structure of what will be explained in more details in the rest of the thesis. The rest of the chapter will be quite technical: in section 1.2 we will describe the general characteristics of a bath and compute some quantities that will later prove useful, we will then considers two different procedures to compute the time evolution of a system represented by a simple spin-$\frac{1}{2}$ in contact with a bath composed of bosons with different spectra and coupling limits. Specifically, in section 1.3 we will consider the case of weak coupling through the Master Equation formalism, while in section 1.4 we will consider the path integral approach which, although more technically involved, can handle a wider range of couplings and can still be recast in a rather simple form in some limiting cases.

1.1 Overview

We will now briefly introduce the two models that will be considered in this thesis and the general strategies that will be used to extract the relevant physics. While both models will described in much more detail in the respective chapters (2 and 3), this introduction will give the reader a general idea of the whole procedure, which might get obscured by the technicalities of the complete treatment.

The first system we investigated is inspired by an experiment of non contact atomic force microscopy [14] where an atomically sharp Fe tip is oscillated over a NiO sample, achieving a sufficient accuracy to distinguish between inequivalent spins in the antiferromagnetic structure of NiO. Our aim is to find a channel of dissipation of the mechanically oscillating tip, which is capable of accounting for the different energy loss observed in correspondence with different spins. This task is far from trivial, since the observed force is due to exchange interaction between the spins of Fe and Ni atoms and the oscillation frequency of the tip is so slow that purely taking into account the gapped spin excitations would lead to a very small effect, while the observed energy dissipation per cycle is of the order of the exchange parameter itself. In order to describe this system, we therefore need to consider the coupling of the Ni spin to some other degree of freedom of the crystal: we find a suitable coupling to the phonons, mediated by the presence of the tip magnetization, and so reduce our system to the study of a single spin strongly coupled to a bosonic bath. We will show that while one spin direction is always close to its minimum with respect to the tip, the other may flip under the external perturbation and in doing so dissipates energy through the phonons.

The procedure to understand the motion of the spin under the effect of the environment is complicated by the strength of the coupling: since a perturbative treatment is not possible, we need to resort to a more complex description of the density matrix of the system in terms of path integrals. As will be explained in detail, in this framework the effect of the bath can be accounted for exactly, but leads to a rather complex summation over the possible paths. In the limit of slow external perturbation and for our specific spin-phonon coupling, it is possible to resum the series and obtain much simpler equations for the spin dynamics, which can be numerically integrated. Aside from the numerical details, the physical effect of this strong coupling is the introduction of a new "slow" timescale for the relaxation of the spin, which is comparable to the frequency of the external perturbation. This effective "self-trapping" of the spin leads to a hysteretical response of the turning spin: its position during approach and retraction of the tip is different, and this difference is proportional to the energy dissipated in the system. Numer-
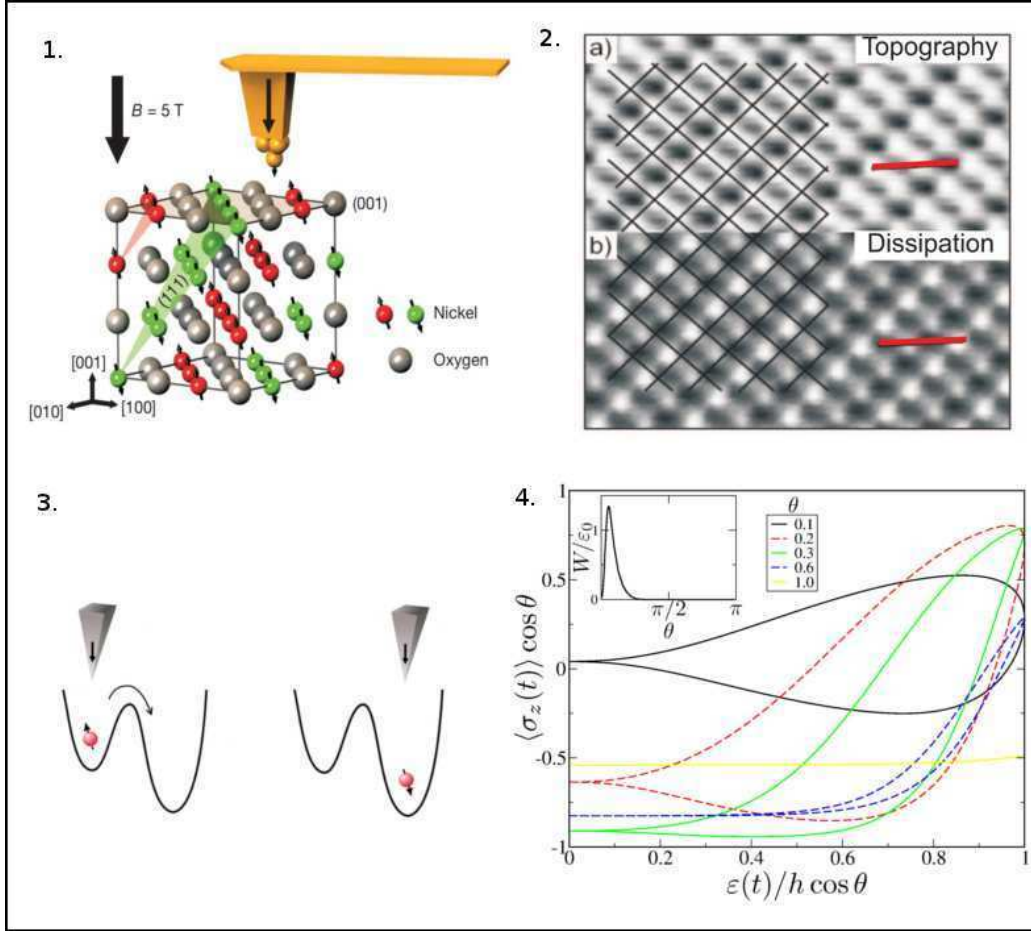
Figure 1.1: Main steps for the spin sensitive dissipation: (1) the experimental setup [14], (2) the measured force and dissipation maps [15], (3) our proposed model, (4) the numerical hysteresis cycles. For further details see chapter 2.

ical calculations confirm the effective frequency and order of magnitude of this effect to be comparable with the experimental findings, thus configuring our model as a viable explanation for spin sensitive dissipation.

The second system we consider is purely electronic dissipation in a three-site, three-electron model in a triangular setup, under the action of a cyclic potential designed to pump current through the ring: such a model could be used to represent a triple quantum dot. It is fairly easy to reduce the three sites to a simple two level system, and estimate the pumped current in the perfectly isolated case: the rotating perturbation acts as an effective potential in the rotating frame of reference, the dynamics is therefore a simple precession, leading to an oscillating current that never stabilizes due to the
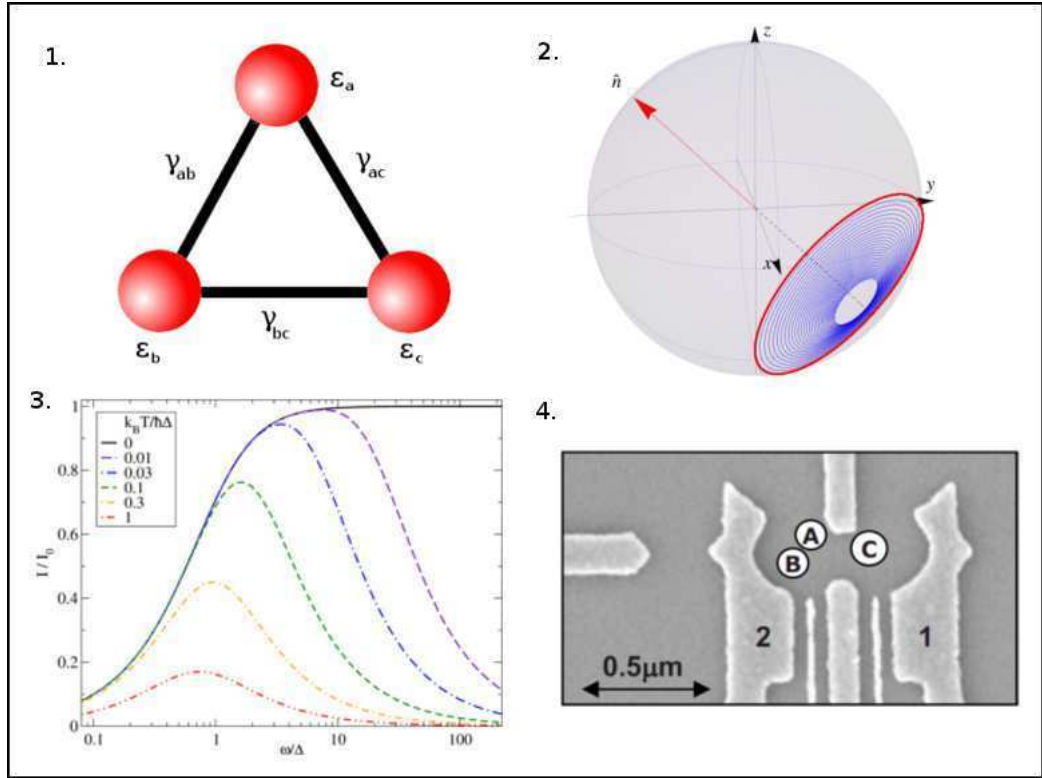
Figure 1.2: Main steps for the quantum pumping: (1) the three site model, (2) solution in the spin space, (3) current in the coupled system for various temperatures, (4) possible experimental setup. For further details see chapter 3.

precessional motion. It is quite clear that a perfectly isolated trimer is far from realistic: to support this current the quantum state of the system should remain unperturbed at all times. In reality one must therefore introduce dissipation. To test the stability of the uncoupled result in presence of an environment, we weakly couple our system to a bosonic bath: we expect this to allow the system to relax to the thermal equilibrium state, affecting the resulting pumped current.

Since we want to investigate the effect of a weak coupling, we can solve this system by expanding the contribution of the bath in powers of the coupling parameter and keeping terms up to the second order. The equation we obtain for the density matrix is quite simple and the asymptotic current can be expressed analytically: we indeed find that the system thermalizes to the bath temperature, and a standard current increase with frequency, at low frequencies, but we also observe a final decrease of the current for high

frequencies, a regime where thermal fluctuations make an unexpected return in the rotating frame of reference of the pumping. This result highlights the importance of properly accounting for the dissipation channels in quantum systems, and suggests an interesting effect amenable to experimental test.

1.2 The bath

We will now enter in more detail in the description of what we refer to as *bath*. Throughout this work, we will consider Hamiltonians of the general form:

$$\mathcal{H}(t) = \mathcal{H}_S(t) + \mathcal{H}_B + \mathcal{H}_{SB} , \tag{1.1}$$

where $\mathcal{H}_S(t)$ is the (possibly time-dependent) Hamiltonian of the system, $\mathcal{H}_B$ is the Hamiltonian of the bath and $\mathcal{H}_{SB}$ is the interaction Hamiltonian, of general form

$$\mathcal{H}_{SB} = \sum_p S_p B_p , \tag{1.2}$$

S_p and B_p being system and bath operators, respectively.

The whole system plus bath model can be described by the density matrix $\rho(t) = \sum_\mu |\psi_\mu(t)\rangle \langle \psi_\mu(t)|$, but we will be interested in tracing out the degrees of freedom of the bath, obtaining an expression for $\rho_S(t) = \text{Tr}_B \rho(t)$. In order to do this, we will need a few assumptions on the nature of the bath itself.

For the sake of the later treatment, we will pass to the interaction picture with respect to $\mathcal{H}_0 = \mathcal{H}_S + \mathcal{H}_B$. We will start by assuming that the bath is almost unperturbed by the interaction with the system, so that the reduced density matrix always reads:

$$\rho_B^{(I)}(t) = \text{Tr}_S \rho^{(I)}(t) \approx \rho_B(t) = \sum_\nu p_\nu |\Phi_\nu\rangle \langle \Phi_\nu| , \tag{1.3}$$

and we will consider the state of the bath to be in the thermodynamic equilibrium state at temperature T, so that $p_\nu = e^{-E_\nu^{(B)}/k_B T}/Z$, where $E_\nu^{(B)}$ and $|\Phi_\nu\rangle$ are eigenvalues and eigenstates of $\mathcal{H}_B$.

Our general aim will be to take care of the terms in the interaction Hamiltonian $\mathcal{H}_{SB}$. To do that we will need to calculate the one and two operator averages of the B_p's. We can assume without loss of generality (allowing for a renormalization of $\mathcal{H}_S$) that the first order averages are zero:

$$\text{Tr}_B \left[\rho_B^{(I)}(t) B_p^{(I)}(t) \right] = 0 \tag{1.4}$$

and we will define the second order averages

$$g_{pq}(t, t') = \text{Tr}_B \left[\rho_B^{(I)} B_p^{(I)}(t) B_q^{(I)}(t') \right] = g_{pq}(t - t') = g_{pq}(\tau) , \tag{1.5}$$

where $\tau = t - t'$. It is easy to explicit the form of g_{pq} in terms of the eigenvectors of $\mathcal{H}_B$ as

$$g_{pq}(\tau) = \sum_{\nu\nu'} p_\nu (B_p)_{\nu\nu'} (B_q)_{\nu'\nu} e^{i(E_\nu^{(B)} - E_{\nu'}^{(B)})\tau/\hbar} , \qquad (1.6)$$

which clearly shows the general property $g_{pq}^*(\tau) = g_{qp}(-\tau)$. We will further assume that $g_{pq}(\tau)$ tends to 0 rapidly for $\tau >> \tau_c$, where τ_c is a characteristic small time-scale of the fluctuation of the bath.

We will now derive an expression for the correlation function assuming the bath to be composed of free bosons and the coupling operators to be displacement operators of the form:

$$\begin{aligned} B(\tau) &= \sum_\nu \lambda_\nu \left(b_\nu^\dagger(\tau) + b_\nu(\tau) \right) = \\ &= \sum_\nu \lambda_\nu \left(e^{i\omega_\nu\tau} b_\nu^\dagger + e^{-i\omega_\nu\tau} b_\nu \right) , \end{aligned} \qquad (1.7)$$

where $b_\nu^\dagger$ and b_ν are bosonic creation and annihilation operators and we consider the presence of only one operator.

By using the Bose-Einstein distribution

$$\left\langle b_\nu^\dagger b_\nu \right\rangle_B = \frac{1}{e^{\beta\omega_\nu} - 1} \equiv f_B(\omega_\nu) \qquad (1.8)$$

at inverse temperature $\beta = 1/k_B T$ as our probability distribution we obtain

$$g(\tau) = \sum_\nu \lambda_\nu^2 \left[e^{i\omega_\nu\tau} f_B(\omega_\nu) + e^{-i\omega_\nu\tau} \left(f_B(\omega_\nu) + 1 \right) \right] . \qquad (1.9)$$

Baths are more commonly treated by considering the energy levels to be dense enough to be considered a continuum and are usually identified by the spectral density

$$J(\omega) = \sum_\nu \frac{\lambda_\nu^2}{2} \delta(\omega - \omega_\nu) = \frac{1}{2} \hbar^2 \alpha \frac{\omega^s}{\omega_c^{s-1}} e^{-\omega/\omega_c} \qquad (1.10)$$

where the last term is the general shape typically used with a power-law dispersion characterized by the exponent s at low frequency and a cutoff frequency ω_c introduced to avoid divergences. The $s = 1$ case (linear dispersion) is usually referred to as the *ohmic* case, $s < 1$ is called *subohmic* while $s > 1$ is *superohmic*.

The summation over the bath states can therefore be converted in an integral, obtaining

$$g(\tau) = \int_0^\infty d\omega \, J(\omega) \cos(\omega\tau) \coth\frac{\beta\omega}{2} - i \int_0^\infty d\omega \, J(\omega) \sin(\omega\tau) . \qquad (1.11)$$

We will derive here some noteworthy integrals of the correlation function multiplied by sine and cosine functions as they will be useful in the treatment of the master equation. Let us introduce the Laplace transform of $g(\tau)$:

$$
\begin{aligned}
\hat{g}(z) &= \int_0^\infty e^{-z\tau} g(\tau) d\tau = \\
&= \int_0^\infty d\omega J(\omega) \left[\frac{f_B(\omega)}{z - i\omega} + \frac{f_B(\omega) + 1}{z + i\omega} \right] ,
\end{aligned}
\tag{1.12}
$$

and define:

$$
\begin{aligned}
g_\pm(\Omega) &= \int_0^\infty g(\tau) e^{\pm i\Omega\tau} d\tau \\
g_0 &= \int_0^\infty g(\tau) d\tau .
\end{aligned}
\tag{1.13}
$$

We can now compute these integrals as Laplace transforms for $z = \mp 2i\Omega + 0^+$ (0^+ being an infinitesimal real part added for integral convergence) to get:

$$
\begin{aligned}
g_\pm(\Omega) &= \int_0^\infty i J(\omega) d\omega \left[\frac{f_B(\omega)}{\pm\Omega + \omega + i0^+} + \frac{f_B(\omega) + 1}{\pm\Omega - \omega + i0^+} \right] = \\
&= \fint_0^\infty i J(\omega) d\omega \left[\frac{f_B(\omega)}{\pm\Omega + \omega} + \frac{f_B(\omega) + 1}{\pm\Omega - \omega} \right] + \\
&\quad + \pi \left[J(\pm\Omega) f_B(\mp\Omega) + J(\pm\Omega) \left(f_B(\pm\Omega) + 1 \right) \right] ,
\end{aligned}
\tag{1.14}
$$

where $\fint$ indicates the principal part integral. This finally gives us a very simple expression for the real part of $g_\pm$:

$$
\begin{cases}
\Re g_+(\Omega) &= \pi \left[J(\Omega) - J(-\Omega) \right] \left(f_B(\Omega) + 1 \right) \\
\Re g_-(\Omega) &= \pi \left[J(\Omega) - J(-\Omega) \right] f_B(\Omega) .
\end{cases}
\tag{1.15}
$$

Moreover, introducing the sine and cosine combinations:

$$
\begin{cases}
g_c(\Omega) &= \frac{1}{2} \left(g_+(\Omega) + g_-(\Omega) \right) = \int_0^\infty g(\tau) \cos(\Omega\tau) d\tau \\
g_s(\Omega) &= \frac{1}{2i} \left(g_+(\Omega) - g_-(\Omega) \right) = \int_0^\infty g(\tau) \sin(\Omega\tau) d\tau ,
\end{cases}
\tag{1.16}
$$

we get simple expressions for

$$
\begin{cases}
\Re g_c(\Omega) &= \frac{\pi}{2} \left[J(\Omega) - J(-\Omega) \right] \coth(\beta\Omega/2) \\
\Im g_s(\Omega) &= -\frac{\pi}{2} \left[J(\Omega) - J(-\Omega) \right] ,
\end{cases}
\tag{1.17}
$$

and finally an expression that will be useful later:

$$
-\frac{\Im g_s(\Omega)}{\Re g_c(\Omega)} = \tanh \frac{\beta\Omega}{2} .
\tag{1.18}
$$

1.3 The Master Equation

1.3.1 Derivation

To derive the Master Equation (ME) we will follow the book of Cohen-Tannoudji *et al.* [5], with a little generalization to the time dependent case as we will need it in our applications.

Let us consider a Hamiltonian of the form (1.1), and let the system be represented by the density matrix $\rho(t) = \sum_\mu |\psi_\mu(t)\rangle \langle\psi_\mu(t)|$; we will pass to the interaction representation with respect to $\mathcal{H}_0(t) = \mathcal{H}_S(t) + \mathcal{H}_B$, i.e. through the correspondent evolution operator

$$U_0(t,0) = T\exp\left(-\frac{i}{\hbar}\int_0^t \mathcal{H}_0(t')dt'\right) = U_{0,S}(t,0) \times U_{0,B}(t,0) . \qquad (1.19)$$

The evolution equation for the density matrix $\rho^{(I)}(t) = U_0^\dagger(t,0)\rho(t)U_0(t,0)$ is given by:

$$i\hbar\frac{\mathrm{d}}{\mathrm{d}t}\rho^{(I)}(t) = \left[\mathcal{H}_{SB}^{(I)}(t), \rho^{(I)}(t)\right] , \qquad (1.20)$$

where $\mathcal{H}_{SB}^{(I)}(t) = U_0^\dagger(t,0)\mathcal{H}_{SB}U_0(t,0)$ is the system-bath interaction, in interaction picture.

Integrating Eq. (1.20) between t and $t + \Delta t$ leads to

$$\rho^{(I)}(t+\Delta t) = \rho^{(I)}(t) + \frac{1}{i\hbar}\int_t^{t+\Delta t} dt' \left[\mathcal{H}_{SB}^{(I)}(t'), \rho^{(I)}(t')\right] \qquad (1.21)$$

and iterating (substituting for $\rho^{(I)}(t')$) we obtain for $\Delta\rho^{(I)}(t) = \rho^{(I)}(t+\Delta t) - \rho^{(I)}(t)$:

$$\begin{aligned}
\Delta\rho^{(I)}(t) &= \frac{1}{i\hbar}\int_t^{t+\Delta t} dt' \left[\mathcal{H}_{SB}^{(I)}(t'), \rho^{(I)}(t)\right] + \\
&+ \frac{1}{(i\hbar)^2}\int_t^{t+\Delta t} dt' \int_t^{t'} dt'' \left[\mathcal{H}_{SB}^{(I)}(t'), \left[\mathcal{H}_{SB}^{(I)}(t''), \rho^{(I)}(t'')\right]\right] .
\end{aligned}$$
$$(1.22)$$

Since we will be considering the case of weak coupling, this expression clearly goes in the direction of an expansion in orders of $\mathcal{H}_{SB}$.

To further simplify this equation and eliminate the explicit dependence on the degrees of freedom of the bath, we will take the trace with respect to them in eq. (1.22) to obtain an expression for $\Delta\rho_S^{(I)}(t) = \mathrm{Tr_B}[\Delta\rho^{(I)}(t)]$:

$$\begin{aligned}
\Delta\rho_S^{(I)}(t) &= \frac{1}{i\hbar}\int_t^{t+\Delta t} dt' \mathrm{Tr_B}\left[\mathcal{H}_{SB}^{(I)}(t'), \rho^{(I)}(t)\right] + \qquad (1.23) \\
&+ \frac{1}{(i\hbar)^2}\int_t^{t+\Delta t} dt' \int_t^{t'} dt'' \mathrm{Tr_B}\left[\mathcal{H}_{SB}^{(I)}(t'), \left[\mathcal{H}_{SB}^{(I)}(t''), \rho^{(I)}(t)\right]\right] ,
\end{aligned}$$

where we have substituted the last $\rho^{(I)}(t'') \approx \rho^{(I)}(t)$ to truncate the expansion to second order; this is always legitimate if the interaction is small and we consider Δt to be much smaller than the typical timescale t_S of evolution of $\rho^{(I)}(t)$.

To be able to use the averages (1.4) and (1.5) we would like to factorize the density matrix in two terms corresponding to bath and system. While this can be simply assumed for $t = 0$, at later times its form generally is

$$\rho^{(I)}(t) = \rho_S^{(I)}(t) \times \rho_B^{(I)}(t) + \rho_{\mathrm{corr}}^{(I)}(t) . \qquad (1.24)$$

However, the correlation acquired in an interval Δt is at most of order $\tau_c/\Delta t$, so that for $\tau_c \ll \Delta t$ the fast decaying bath correlations ensure that we can neglect $\rho_{\mathrm{corr}}(t)$. We can therefore factorize $\rho^{(I)}(t)$ and we realize that the first term on the r.h.s. of (1.23) vanishes exactly, and substituting (1.5) we obtain:

$$\frac{\Delta \rho_S^{(I)}(t)}{\Delta t} \approx -\frac{1}{\hbar^2 \Delta t} \int_t^{t+\Delta t} dt' \int_t^{t'} dt'' \sum_{pq} \qquad (1.25)$$

$$\left\{ g_{pq}(t' - t'') \left[S_p(t') S_q(t'') \rho_S^{(I)}(t) - S_q(t'') \rho_S^{(I)}(t) S_p(t') \right] + \right.$$
$$\left. + g_{qp}(t'' - t') \left[\rho_S^{(I)}(t) S_q(t'') S_p(t') - S_p(t') \rho_S^{(I)}(t) S_q(t'') \right] \right\} .$$

A change of variables to $\tau = t' - t''$ and t' and extending the integrals by taking into account the fast decay of $g_{pq}(\tau)$ yields

$$\frac{1}{\Delta t} \int_t^{t+\Delta t} dt' \int_t^{t'} dt'' \rightarrow \int_0^{\Delta t} d\tau \frac{1}{\Delta t} \int_{t+\tau}^{t+\Delta t} dt' \approx \int_0^\infty d\tau \frac{1}{\Delta t} \int_t^{t+\Delta t} dt' \quad (1.26)$$

which recasts eq.(1.25) as

$$\frac{\Delta \rho_S^{(I)}(t)}{\Delta t} \approx -\frac{1}{\hbar^2 \Delta t} \int_0^\infty d\tau \int_t^{t+\Delta t} dt' \sum_{pq} \qquad (1.27)$$

$$\left\{ g_{pq}(\tau) \left[S_p(t') S_q(t' - \tau) \rho_S^{(I)}(t) - S_q(t' - \tau) \rho_S^{(I)}(t) S_p(t') \right] + \right.$$
$$\left. + g_{qp}(\tau) \left[\rho_S^{(I)}(t) S_q(t' - \tau) S_p(t') - S_p(t') \rho_S^{(I)}(t) S_q(t' - \tau) \right] \right\} .$$

This can be considered as the derivative of the density matrix in interaction picture as long as $\mathcal{H}_{SB}$ is small (justifying the second order expansion) and as long as we are interested in finite differences of order Δt where $\tau_c \ll \Delta t \ll t_S$, τ_c being the correlation time of the bath and t_S the typical

timescale of the system. In this way we can remove one integral and obtain the final form:

$$
\frac{\partial \rho_S^{(I)}(t)}{\partial t} \approx -\frac{1}{\hbar^2} \int_0^\infty d\tau \sum_{pq} \tag{1.28}
$$
$$
\left\{ g_{pq}(\tau) \left[S_p(t)S_q(t-\tau)\rho_S^{(I)}(t) - S_q(t-\tau)\rho_S^{(I)}(t)S_p(t) \right] + \right.
$$
$$
\left. + g_{qp}(\tau) \left[\rho_S^{(I)}(t)S_q(t-\tau)S_p(t) - S_p(t)\rho_S^{(I)}(t)S_q(t-\tau) \right] \right\} .
$$

Moreover, if the bath operators couple in the same way to all the system operators we can clearly take the bath degrees of freedom out of the summation over p, q and use eq. (1.11).

As a last remark, we can notice that in some cases it is more useful to turn back to the Schrödinger picture with respect to the system and recast eq. (1.28) as:

$$
\frac{\partial \rho_S(t)}{\partial t} \approx \frac{1}{i\hbar} [\mathcal{H}_S, \rho_S(t)] - \frac{1}{\hbar^2} \int_0^\infty d\tau \sum_{pq} \tag{1.29}
$$
$$
\{ g_{pq}(\tau) [S_p S_q(-\tau)\rho_S(t) - S_q(-\tau)\rho_S(t)S_p] +
$$
$$
+ g_{qp}(\tau) [\rho_S(t)S_q(-\tau)S_p - S_p\rho_S(t)S_q(-\tau)] \} .
$$

1.3.2   The Spin-1/2 case

We will now specialize the last form of the ME (1.29) to the case in which the system is represented by a single spin-$\frac{1}{2}$, as this will be the case of our interest. Specifically we will consider the simplest spin Hamiltonians and analyze its behavior in presence of different bath couplings to gain some understanding on the possible effects of environment on this kind of systems.

We will consider the general Hamiltonian form (1.1) and for the system part we will take the simplest case:

$$
\mathcal{H}_S = \frac{\Delta}{2} \sigma^z . \tag{1.30}
$$

It is clear that the solution of this Hamiltonian alone is simply a precession around the z axis with frequency $\Delta/\hbar$. To exemplify the evolution of the density matrix, throughout this subsection we will consider the effect of the evolution equation on the generic state:

$$
\bar{\rho} = \frac{1}{2}(\mathbb{I} + a\sigma^x + b\sigma^y + c\sigma^z) . \tag{1.31}
$$

For example, in the absence of a bath, the precession is clearly exemplified by:

$$\frac{\partial \bar{\rho}}{\partial t} = -i\left[\mathcal{H}_S, \bar{\rho}\right] = \frac{\Delta}{2}\left(a\sigma^y - b\sigma^x\right), \tag{1.32}$$

where we have taken, as we will do henceforth, $\hbar = 1$.

Let us now proceed by considering the coupling with a ohmic bath through the operator σ^z:

$$\mathcal{H}_{SB} = \sum_\nu \lambda_\nu a_\nu \sigma^z, \tag{1.33}$$

where a_ν are creation operators of a bath characterized by the spectral density $J(\omega) = \alpha\omega e^{-\omega/\omega_c}$.

Using the ME (1.29) and the integrals (1.13) we simply get:

$$\frac{\partial \rho(t)}{\partial t} = -i\frac{\Delta}{2}\left[\sigma^z, \rho(t)\right] - g_0\left[\sigma^z, \sigma^z\rho(t)\right] - g_0^*\left[\rho(t)\sigma^z, \sigma^z\right]. \tag{1.34}$$

which for our generic $\bar{\rho}$ gives:

$$\frac{\partial \bar{\rho}}{\partial t} = \frac{\Delta}{2}\left(a\sigma^y - b\sigma^x\right) - 2\Re g_0\left(a\sigma^x + b\sigma^y\right). \tag{1.35}$$

From this we can see that the evolution is still characterized by a rotation around the z axis, but this time coupled to a decay of the component in the xy plane with a rate $2\Re g_0$. It is generally said that this form of coupling destroys the *coherences* of the system (out of diagonal elements of the density matrix).

Let us now see what changes if the coupling is along the x axis instead:

$$\mathcal{H}_{SB} = \sum_\nu \lambda_\nu a_\nu \sigma^x. \tag{1.36}$$

The application of (1.29) is in this case slightly more complicated because of the time dependence introduced in σ^x by $\mathcal{H}_S$:

$$\sigma^x(t) = \cos(\Delta t)\sigma^x - \sin(\Delta t)\sigma^y, \tag{1.37}$$

so that the final ME takes the shape:

$$\begin{aligned}
\frac{\partial \rho(t)}{\partial t} &= -i\frac{\Delta}{2}\left[\sigma^z, \rho(t)\right] - g_c\left[\sigma^x, \sigma^x\rho(t)\right] - g_c^*\left[\sigma^x\rho(t), \sigma^x\right] \\
&\quad + g_s\left[\sigma^x, \sigma^y\rho(t)\right] + g_s^*\left[\sigma^y\rho(t), \sigma^x\right],
\end{aligned} \tag{1.38}$$

where all the g's are intended as $g(\Delta)$.

To get some further insight in what this means for the evolution of the system, we apply this again to $\bar{\rho}$:

$$
\begin{aligned}
\frac{\partial \bar{\rho}}{\partial t} &= \tfrac{\Delta}{2}\left(a\sigma^y - b\sigma^x\right) - 2\Re g_c\left(c\sigma^z + b\sigma^y\right) - 2\Re g_s a\sigma^y - 2\Im g_s \sigma^z = \\
&= -\tfrac{\Delta}{2}b\sigma^x + \left(\tfrac{\Delta}{2}a - 2\Re g_c b - 2\Re g_s a\right)\sigma^y - 2\left(\Re g_c c + \Im g_s\right)\sigma^z \ .
\end{aligned}
\tag{1.39}
$$

Apart from the standard precession around z, we can now see two different effects: the perpendicular xy component is once more damped to 0, but in this case also the z component is affected by the presence of the bath. We can easily see that the equilibrium state for z is given by (see eq. (1.18))

$$
c = -\frac{\Im g_s}{\Re g_c} = \tanh\left(\frac{\Delta\beta}{2}\right) \ .
\tag{1.40}
$$

This means that the *populations* of the system (diagonal terms) are brought to an asymptotic state, which is exactly the thermalized state for the system at the temperature T of the bath.

If we now want to consider more complex couplings, there are two things that can be done: the direct combination of the previous cases would be to take

$$
\mathcal{H}_{SB} = \frac{1}{2}\sum_\nu \lambda_\nu a_\nu \sigma^x + \frac{1}{2}\sum_\nu \lambda_\nu b_\nu \sigma^z \ ,
\tag{1.41}
$$

i.e. two separated baths, one along each direction. It is quite straightforward to see that in this case the final ME is a simple sum of the previous ones:

$$
\begin{aligned}
\frac{\partial \bar{\rho}}{\partial t} &= -\left(\tfrac{\Delta}{2}b + \Re g_0 a\right)\sigma^x + \left(\tfrac{\Delta}{2}a - (\Re g_c + \Re g_0)b - \Re g_s a\right)\sigma^y \\
&\quad - \left(\Re g_c c + \Im g_s\right)\sigma^z \ ,
\end{aligned}
\tag{1.42}
$$

so that the final behavior is the same of the perpendicular coupling, albeit with different coefficients.

The second and more interesting case is a single bath with an intermediate coupling direction:

$$
\mathcal{H}_{SB} = \frac{1}{2}\sum_\nu \lambda_\nu a_\nu \left(\sigma^x + \sigma^z\right) \ .
\tag{1.43}
$$

In this case, the correlation function gives rise to some new terms in the ME, which reads:

$$
\begin{aligned}
\frac{\partial \bar{\rho}}{\partial t} &= -i\tfrac{\Delta}{2}\left[\sigma^z, \rho\right] - \tfrac{1}{2}\left(g_0\left[\sigma^z + \sigma^x, \sigma^z\rho\right] + g_0^*\left[\rho\sigma^z, \sigma^z + \sigma^x\right] + \right. \\
&\quad + g_c\left[\sigma^x + \sigma^z, \sigma^x\rho\right] + g_c^*\left[\sigma^x\rho, \sigma^x + \sigma^z\right] + \\
&\quad \left. - g_s\left[\sigma^x + \sigma^z, \sigma^y\rho\right] - g_s^*\left[\sigma^y\rho, \sigma^x + \sigma^z\right]\right) \ .
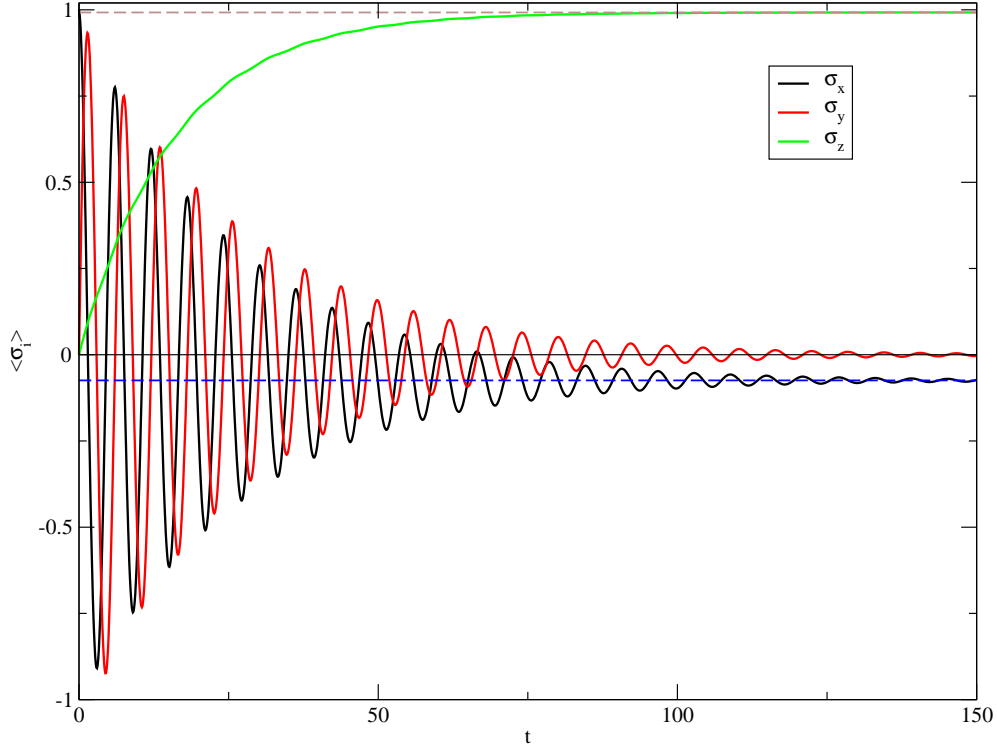\end{aligned}
\tag{1.44}
$$

Figure 1.3: Time evolution of the components of the spin for the interaction Hamiltonian (1.43) (full lines) and asymptotic estimate according to (1.46) (dashed lines).

To find the equilibrium value, again we consider our generic density matrix:

$$
\frac{\partial \bar{\rho}}{\partial t} = -\left(\frac{\Delta}{2}b + \Re g_0 a - \Re g_c c - \Im g_s\right)\sigma^x - \left(\Re g_c c + \Im g_s - \Re g_0 a\right)\sigma^z +
$$
$$
-\left(-\frac{\Delta}{2}a + (\Re g_c + \Re g_0)b + \Re g_s(a+c) + \Im g_0 - \Im g_c\right)\sigma^y, \quad (1.45)
$$

and since the solution is slightly more complex we set to 0 all derivatives to find the stable state:

$$
\begin{cases}
a = & \dfrac{-\Re g_s \Im g_s + \Re g_c(\Im g_0 - \Im g_c)}{\Delta \Re g_c - \Re g_s(\Re g_0 + \Re g_c)} \\[2mm]
b = & 0 \\[2mm]
c = & \tanh\left(\dfrac{\Delta\beta}{2}\right) + \dfrac{\Re g_0}{\Re g_c}\dfrac{-\Re g_s \Im g_s + \Re g_c(\Im g_0 - \Im g_c)}{\Delta \Re g_c - \Re g_s(\Re g_0 + \Re g_c)}.
\end{cases} \quad (1.46)
$$

As we can see, in this case the presence of the bath altered the equilibrium state of the system: the correction to the thermodynamical state is of first

order in α and thus goes to 0 in the limit of weak coupling, but it can nevertheless be observed for any finite value, as is shown in a simple example in Fig. 1.3.

This simple examples showed us how there are two essential types of damping due to a weak coupling to a bath: a decay to 0 of the directions perpendicular to the quantization axis and a decay to the thermodynamic state along the quantization direction. Moreover, we have seen how the presence of a bath can change the final thermalization axis of a spin from that of the original unperturbed Hamiltonian, but only at first order in the spin-bath coupling.

1.4 The Driven Spin-Boson Model

1.4.1 The Model

We will present here a simple Hamiltonian generally known as the driven spin-boson (SB) model. This system belongs to the more general family of Caldeira-Leggett models [6], which try to describe quantum systems coupled to external baths to get a description of quantum dissipation, the issue we are interested in. Although it will soon become clear that this model could in the limit of weak coupling be handled with the ME techniques previously presented, we will introduce here another formalism which, applied specifically to this system, will prove fit to explore different regimes, which will be important in our later applications.

Let us start by introducing the original SB Hamiltonian:

$$\mathcal{H} = \frac{1}{2}\varepsilon\sigma^z + \frac{1}{2}\hbar\Delta\sigma^x + \sigma^z \sum_i \lambda_i \left(b_i + b_i^\dagger \right) + \sum_i \omega_i \left(b_i^\dagger b_i + \frac{1}{2} \right) , \quad (1.47)$$

which describes a spin-$\frac{1}{2}$ (σ^i operators) with a splitting ε and a hopping Δ coupled via σ^z to a bosonic bath characterized by creation and annihilation operators $b_i^\dagger$, b_i.

Since in the experimental case of our interest the external perturbation is time dependent, in the final Hamiltonian we will substitute the spin parameters with the time-dependent version:

$$\begin{cases} \varepsilon & \to & \varepsilon_0 + \varepsilon(t) \\ \Delta & \to & \Delta(t) , \end{cases} \quad (1.48)$$

which results in the *driven* SB model.

The method we will apply to this system works, with the due changes, for different forms of the bath spectral density. However, for the case of our

interest, we will concentrate in the following on the case of a *ohmic* bath (see Eq. (1.10)):

$$J(\omega) = \frac{1}{2}\hbar^2 \alpha \omega e^{-\omega/\omega_c} \ . \tag{1.49}$$

1.4.2 The Real-Time Path Integral Solution

The path integral description of quantum mechanics introduced by Feynman [9] starts from the possibility of computing the probability of evolution of a wavefunction between two states as a sum over all the possible paths connecting them weighted by the exponential of the action over each path. One of the main simplification in this theory comes in the form of "influence functionals" that can take into account some of the degrees of freedom of the system as an effective interaction among more interesting degrees of freedom. Without entering too deeply in the detail of this technique, we will try in the following to justify the application of this scheme to our model and its reduction to a set of quite manageable equations. For a schematic derivation of the influence functional use we refer the reader to Appendix A.

For the real-time path integral treatment of the spin-boson model we start by considering the amplitude for an isolated two-state system in state σ' at time 0 to make a transition to a state σ at a subsequent time t as:

$$A_{\sigma'\sigma} = \int \mathcal{D}q \exp\left(\frac{i}{\hbar}S[q]\right) \equiv \int \mathcal{D}q \mathcal{A}[q] \tag{1.50}$$

where $\mathcal{D}q$ represents an integral over all the possible paths for the two-state system discreet variable q with constraints $q(0) = \sigma'/2$, $q(t) = \sigma/2$, and $\mathcal{A}[q]$ represents the free evolution of the system, which is the exponential of the classical action $S[q]$.

We will now start from this expression to justify the more complex equation for the probability of a two-state system coupled to a harmonic bath and under the effect of an external force to pass from state σ' at time 0 to a state σ at a subsequent time t. Computing a probability $|A_{\sigma'\sigma}|^2$ will require a double integral over paths q and q', the effect of the external perturbation will be accounted in the $\mathcal{A}[q]$ term and the presence of the bath will be represented by the introduction of the appropriate influence functional $\mathcal{F}[q, q']$; the final expression will therefore have the form:

$$P(\sigma, t; \sigma', 0) = \int \mathcal{D}q \int \mathcal{D}q' \ \mathcal{A}[q] \ \mathcal{A}^*[q'] \ \mathcal{F}[q, q'] \ . \tag{1.51}$$

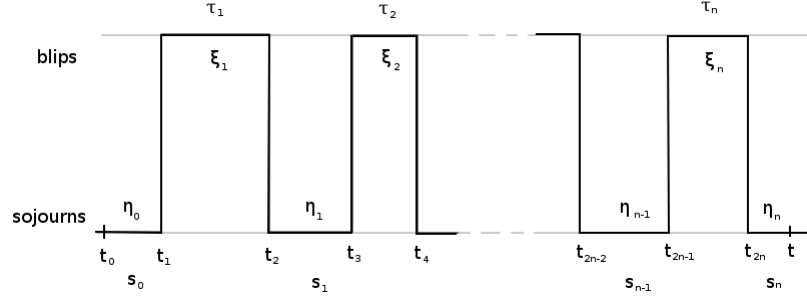As explained in more detail in Appendix A, the form of the influence func-

Figure 1.4: Sojourns and blips in the path integral computation of $\langle \sigma^z(t) \rangle$.

tional for a harmonic bath is given by [10]:

$$
\begin{aligned}
\mathcal{F}[q, q'] \;\; = \;\; & \exp \left\{ - \int_0^t dt' \int_0^{t'} dt'' \, [q(t') - q'(t')] \right. \\
& \left. [L(t' - t'')q(t'') - L^*(t' - t'')q'(t'')] \right\}
\end{aligned}
\tag{1.52}
$$

with

$$
L(t) = \frac{1}{\pi} \int_0^\infty d\omega J(\omega) \left(\coth \frac{\omega\beta}{2} \cos(\omega t) - i \sin(\omega t) \right) ,
\tag{1.53}
$$

[cf. Eq. (1.11)].

We can now introduce the symmetric and antisymmetric combinations $\eta(t) = q(t) + q'(t)$ and $\xi(t) = q(t) - q'(t)$ and consider the two paths as a single path made of steps were $\eta = \pm 1$ and $\xi = 0$, that we will call *sojourn* as they correspond to the populations (diagonal terms) of the density matrix, and steps were $\xi = \pm 1$ and $\eta = 0$, which will be called *blips* and correspond to coherences (off-diagonal terms). We can now label the sojourns and blips as shown in Fig. 1.4 and explicit the path integrals as: a sum over the possible number of "jumps" between blips and sojourns, a series of integrals over the time of the jumps and a further summation over the possible values of $\xi_j = \xi(t_{2j} - t_{2j-1})$ and $\eta_j = \eta(t_{2j+1} - t_{2j})$:

$$
\int \mathcal{D}q \mathcal{D}q' \;\; \to \;\; \sum_{n=0}^\infty \int \mathcal{D}_n\{t_j\} \sum_{\{\xi_j = \pm 1\}} \sum_{\{\eta_j = \pm 1\}} .
\tag{1.54}
$$

By further defining the integral concerning the spectral density

$$
Q(t) = \int_0^\infty d\omega \frac{J(\omega)}{\omega^2} (1 - \cos \omega t) \coth(\frac{1}{2}\beta\omega) + i \int_0^\infty d\omega \frac{J(\omega)}{\omega^2} \sin \omega t , \tag{1.55}
$$

we can separate the contributions to the path integral as: interactions of a blip with itself

$$S_{j,k} = S(t_j - t_k) = \Re\, Q(t_j - t_k) \,, \tag{1.56}$$

interactions of pairs of blips

$$\Lambda_{j,k} = S_{2j,2k-1} + S_{2j-1,2k} - S_{2j,2k} - S_{2j-1,2k-1} \,, \tag{1.57}$$

and interactions of a blip with the preceding sojourns

$$X_{j,k} = R_{2j,2k+1} + R_{2j-1,2k} - R_{2j,2k} - R_{2j-1,2k+1}, \tag{1.58}$$

with $R_{j,k} = R(t_j - t_k) = \Im\, Q(t_j - t_k)$.

With all these definitions we can recast the influence functional in the form:

$$\mathcal{F}_n = \exp\left\{ -\sum_{j=1}^{n} S_{2j,2j-1} - \sum_{j=2}^{n}\sum_{k=1}^{j-1} \xi_j \xi_k \Lambda_{j,k} + i \sum_{j=1}^{n}\sum_{k=1}^{j-1} \xi_j \eta_k X_{j,k} \right\} \,, \tag{1.59}$$

and the final probability takes the form:

$$
\begin{aligned}
P(\sigma,t;\sigma',0) &= \delta_{\sigma,\sigma'} + \sigma\sigma' \sum_{n=1}^{\infty} \left(-\frac{1}{4}\right)^n \int_0^t \mathcal{D}_n\{t_j\}\Delta(t_j) \sum_{\{\xi_j\}}\sum_{\{\eta_j\}} \\
&\quad \mathcal{F}_n \exp\left\{ i \sum_{k=1}^{n} \xi_k \int_{t_{2k-1}}^{t_{2k}} \varepsilon(t')dt' \right\}.
\end{aligned}
\tag{1.60}
$$

With this expression we can compute the z-component of the spin at any time for a system starting at time 0 from the up state, as $\langle\sigma^z(t)\rangle = P(\uparrow,t;\uparrow,0) - P(\downarrow,t;\uparrow,0)$. To get a compact expression for $\langle\sigma^z(t)\rangle$ it is convenient to take the Laplace transform of the probability:

$$P(\lambda) = \int_0^{\infty} P(t)e^{-\lambda t}dt \,. \tag{1.61}$$

Defining the time intervals of the sojourns $s_j = t_{2j+1} - t_{2j}$ and those of the blips $\tau_j = t_{2j} - t_{2j-1}$, after Laplace transform and summation over the sojourn states $\{\eta_j\}$, we get:

$$
\begin{aligned}
\langle\sigma^z(\lambda)\rangle &= \frac{1}{\lambda} + \frac{1}{\lambda}\sum_{n=1}^{\infty}\left(-\frac{1}{2}\right)^n \int_0^{\infty} \tilde{\mathcal{D}}_n(\lambda)\Delta_{2n} \sum_{\{\xi_j\}} \\
&\quad Q_n \cos\left(\Phi_n + \sum_{j=1}^{n} \xi_j X_{j,0}\right) \prod_{k=1}^{n-1} \cos\left(\sum_{j=k+1}^{n} \xi_j X_{j,k}\right) \,,
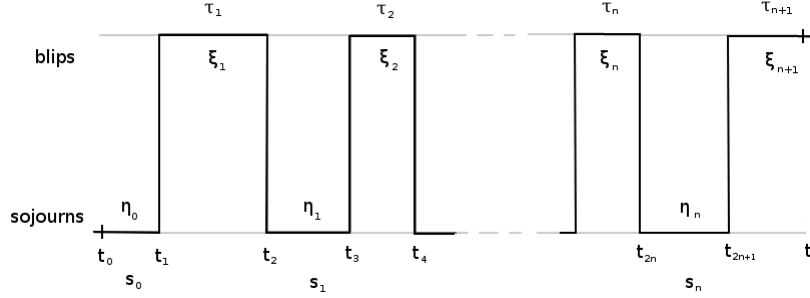\end{aligned}
\tag{1.62}
$$

Figure 1.5: Sojourns and blips in the path integral computation of $\langle \sigma^x(t) \rangle$.

where the integration $\tilde{\mathcal{D}}_n(\lambda) = \prod_{i=1}^{n} d\tau_i ds_i e^{-\lambda(\tau_i + s_i)}$ includes the transform coefficients, Δ_{2n} represent the $2n$ Δ contributions at the time of the flips, $Q_n = \exp\left\{ -\sum_j S_{2j,2j-1} - \sum_{j,k} \xi_j \xi_k \Lambda_{j,k} \right\}$ is the blip pair and self interaction and $\Phi_n = \sum_{j=1}^{n} \xi_j \int \varepsilon(t') dt'$ are the integrals of the z external perturbation over the n blips.

Up to now all the equations we derived are exact and quite general, to go further into the analysis of the system we will consider some simplifications: the first approximation we make is the so called *noninteracting blip approximation* (NIBA) [7]. This approximation, which consists in considering the length of the blips τ_i much shorter than the length of the sojourns s_i, is quite generally used in the treatment of the spin-boson model and has been shown to be valid also in the driven case in the limits we will consider in section 2.3 [8, 11, 12]. We will thus neglect all blip pair interaction ($\Lambda_{j,k} = 0$) and consider only interaction of a blip with the previous sojourn: $X_{j,k} = 0$ for $j \neq k+1$, $X_{k+1,k} = R(\tau_{k+1})$. This simplifies Eq. 1.62 to:

$$
\begin{aligned}
\langle \sigma^z(\lambda) \rangle &= \frac{1}{\lambda} + \frac{1}{\lambda} \sum_{n=1}^{\infty} (-1)^n \int_0^{\infty} \tilde{\mathcal{D}}_n(\lambda) \Delta_{2n} e^{-S(\tau_1)} \cos\left(\phi_1 + R(\tau_1)\right) \\
&\quad \prod_{k=2}^{n} \cos\left(R(\tau_k)\right) \cos \phi_k e^{-S(\tau_k)} ,
\end{aligned}
\tag{1.63}
$$

where the ϕ_j's are the integrals of the external z perturbation over the blips: $\phi_j = \int_{\tau_j} \varepsilon(t') dt'$.

This expression is considerably simpler to compute than the original one. Moreover, we will see in 2.3 how specializing it for low frequency and Ohmic dissipation leads to an equation that can be integrated numerically in a straightforward way.

We will now briefly expose the modifications in the treatment needed to compute $\langle \sigma^x(t) \rangle$. As $\sigma^x = \rho_{-1,1} + \rho_{1,-1}$ is made up of off-diagonal terms of

the density matrix, the path integral expression requires in this case an odd number of transition, so that the paths end up in a blip state (see Fig. 1.5). After taking the Laplace transform and summing over the η's, the equivalent of eq.(1.62) becomes:

$$
\begin{aligned}
\langle \sigma^x(\lambda) \rangle \;=\;& \sum_{n=0}^{\infty} \left(-\frac{1}{2} \right)^{n+1} \int_0^{\infty} \tilde{\mathcal{D}}_{n+1}(\lambda) \Delta_{2n+1} \sum_{\{\xi_j\}} \xi_{n+1} Q_{n+1} \\
& \sin \left(\Phi_n + \sum_{j=1}^{n} \xi_j X_{j,0} \right) \prod_{k=1}^{n} \cos \left(\sum_{j=k+1}^{n} \xi_j X_{j,k} \right) ,
\end{aligned}
\tag{1.64}
$$

with the same notation as before, except for everything being rescaled for $n+1$ steps. Again, we can apply the NIBA and sum over $\{\xi_j\}$ to obtain:

$$
\begin{aligned}
\langle \sigma^x(\lambda) \rangle \;=\;& \sum_{n=0}^{\infty} (-1)^{n+1} \int_0^{\infty} \tilde{\mathcal{D}}_{n+1}(\lambda) \Delta_{2n+1} e^{-S(\tau_1)} \cos \left(\phi_1 + R(\tau_1) \right) \\
& \prod_{k=2}^{n+1} \cos \left(R(\tau_k) \right) \sin \phi_k e^{-S(\tau_k)} .
\end{aligned}
\tag{1.65}
$$

This is the equivalent of (1.63) for $\langle \sigma^x \rangle$ and will undergo a similar simplification.

Chapter 2

Atomic spin sensitive dissipation on magnetic surfaces

The dissipation mechanism proposed in this chapter is born from the observation of a comparably large and unexplained energy dissipation in a recent atomic force microscopy experiment [14]. In section 2.1 we will describe such experiment, in section 2.2 we will describe in more detail the material in which the dissipation takes place and why standard dissipation mechanisms do not give a satisfactory explanation; finally in section 2.3 we will propose the dissipation mechanism we consider most relevant for this system [3].

2.1 Magnetic Exchange Force Microscopy of NiO

In a recent and very accurate experiment, spin resolution in atomic force microscopy (AFM) has been achieved thanks to a refined experimental setup named magnetic exchange force microscopy (MExFM) [14]. In this experiment, an atomically sharp iron tip was used to probe the surface of a nickel oxide sample, showing not only a sufficient resolution to distinguish between Ni and O atoms, but the ability to differentiate inequivalent spin direction of the Ni atoms according to the known antiferromagnetic structure of this crystal (explained in detail in 2.2) as can be seen in Fig. 2.1, reproduced from the original article.

The experiment basically consists in oscillating a tip at constant amplitude at different distances from the NiO sample and measuring the deviations of the oscillation frequency from the resonance frequency of the free can-
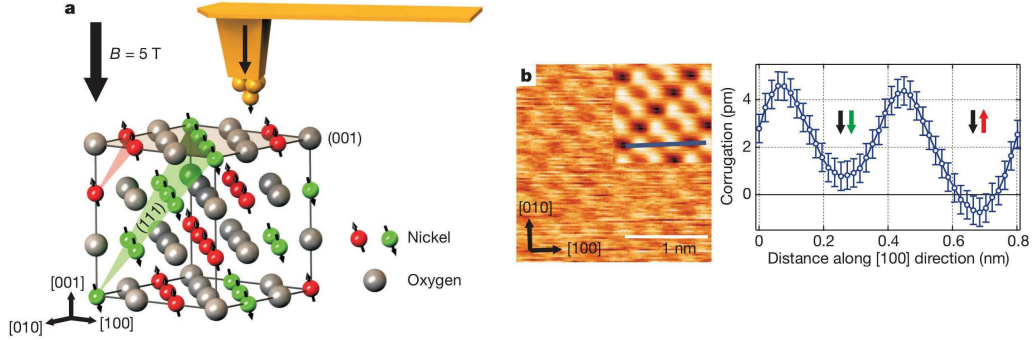
Figure 2.1: (a) Setup of the MExFM experiment. (b) Measured topography of the NiO surface (multiple cell average in the upper right corner) and corrugation as a function of position for the line marked in the topography. Reproduced from [14].

tilever, due to the tip-sample interaction. While this is one of the standard setups of AFM, very high sensitivity and the possibility to achieve very short tip-sample distances (smaller than 3Å) increase the importance of exchange interaction: as the electronic clouds of the tip and the substrate obtain a considerable overlap we get a chance to observe spin-dependent effects. In this particular experiment, the Fe tip is magnetized through an external 5T magnetic field, such that we can reasonably assume the foremost electron to posses a definite spin direction perpendicular to the surface. When such spin gets a non negligible overlap with the spin of the Ni in the sample (whose direction will be better explained in 2.2), depending on its direction a different interaction changes the oscillation frequency, giving a measurable effects.

The resulting force map shown in Fig. 2.1 clearly shows a different corrugation (distance needed to achieve a given frequency shift) for "up" and "down" spins, found in alternating lines on the (001) surface of NiO.

A first principles calculation of the tip-surface interaction was carried out in [16] to help with the interpretation of this experiment. Their calculations (reproduced in Fig. 2.2) clearly show the different force curves as a function of probe height for opposite spin directions. Specifically, we can see how antiparallel spins show a stronger interaction: this is due to the hybridization between Fe and Ni d-orbitals resulting in an exchange effect favoring parallel spins. If we also consider the stronger interaction with oxygen, the force topography of Fig. 2.1 can be clearly explained.

There is another effect which was originally not so clear in this experiment: by measuring the amount of energy needed to keep the cantilever oscillations at constant amplitude, it is possible to estimate the energy dissi-
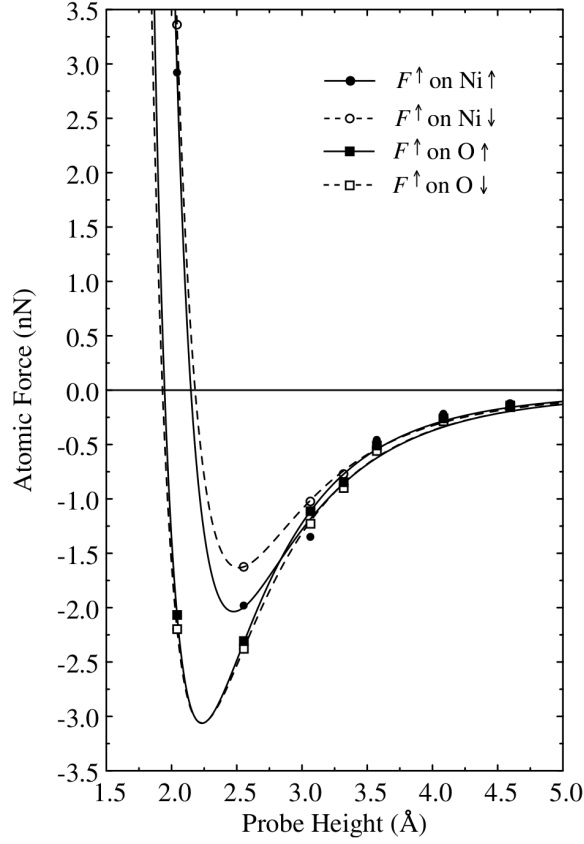
Figure 2.2: Calculated force curves as a function of the distance for a ↑-spin Fe atom over the four inequivalent atoms of the NiO surface (a small spin is observed for oxygen due to interactions with the underlying Ni). Reproduced from [16].

pated in a cycle. As shown in Fig. 2.3 (reproduced from [15]), the dissipation is clearly different for the two spin directions and in particular is larger for antiparallel spins. This is the problem we are going to tackle in section 2.3. As will be clear from a better description of the magnetic structure of NiO given in section 2.2, obtaining this large difference in dissipation at the "slow" experimental frequency (~ 160 kHz) cannot be explained through standard spin wave theory and will require a more complete treatment taking into account the coupling of the spin to the phononic degrees of freedom of the system.
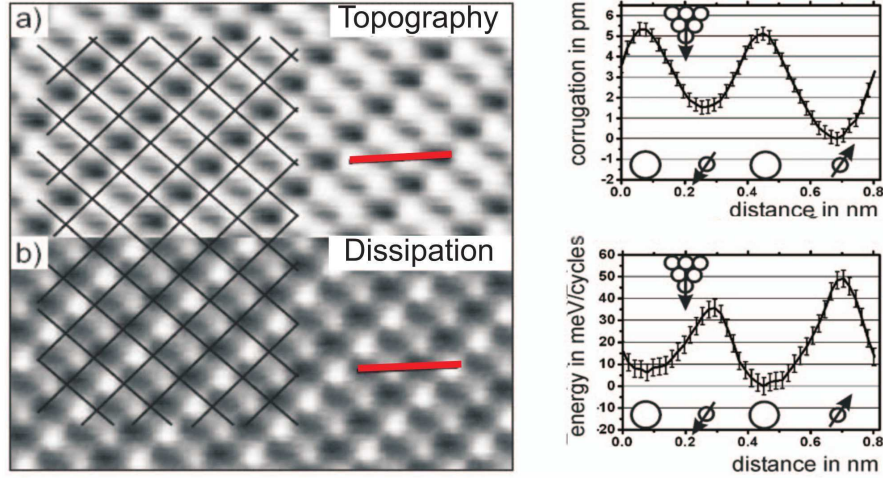
Figure 2.3: (a) Topography of the NiO surface. (b) Energy dissipation map of the same surface, and the same quantity as a function of position for the line marked in the map. Reproduced from [15].

2.2   Nickel Oxide

2.2.1   The Structure

Nickel oxide (NiO) is a crystal that shows the typical rock salt structure of two compenetrating fcc lattices of oxygen and nickel atoms. From an electronic point of view, NiO is generally considered a charge-transfer insulator [17], but what we are more interested in is the magnetic structure. Due to the spin distribution in the d states of nickel, NiO shows a magnetic structure and due to superexchange effects through the oxygen atoms the structure is antiferromagnetic, and more specifically it exhibits antiferromagnetic ordering of type 2 (AF2) [18] with a Néel temperature of 525 K. The AF2 structure in the nickel sublattice is characterized by planes of opposite spins alternating along the [111] direction or, equivalently, four compenetrating simple cubic lattices with alternating spins, as shown in Fig. 2.5. This structure emerges from the interplay of different exchange mechanisms: a strong antiferromagnetic superexchange J_2 between a Ni atom and its 6 next nearest neighbors (NNN) Ni in the same sublattice, forming a 180° angle with the oxygen in the middle, and two smaller interaction with the 12 nearest neighbors (NN) belonging to the other 3 sublattices and forming 90° angles with the oxygens: a ferromagnetic one J_1^- with 6 of them and an antiferromagnetic J_1^+ with the remaining 6. An experimental estimate of the exchange parameters can

be found in Fig. 2.4.

There have been many discussions regarding the specific form of the NiO magnetic anisotropy [18, 19, 20, 21], but the accepted structure defines the spins as lying in the (111) plane and, within the plane, pointing along one of the three in-plane $\langle\bar{2}11\rangle$ directions (there seems to be a very slight deviation from the plane, but it represent a minor correction and can be safely disregarded). This structure seems to ultimately be the effect of a long range dipolar interaction between spins of different sublattices and can be mimicked by considering an out-of-plane anisotropy parameter D_1 and a triangular in-plane parameter D_2. Experimental estimates of these parameters can be found in table 2.4.

The presence of this different possible orientation leads in most crystals to the creation of domains where different minima are chosen and domain walls between them. There are two kinds of domain walls [22]: T walls and S walls. T walls, also called twinning walls, are characterized by different (111) planes of parallel spins, they require more energy to form and are correlated with some little magnetostrictive effect in the [111] direction; S walls are generated by different $\langle\bar{2}11\rangle$ orientations within the same plane, they are less energetic and therefore harder to completely remove from a sample.

In our treatment we will consider the sample as a magnetic (as well as chemical) single crystal, by assuming that any interesting effect happens on such a short scale that it is reasonable to assume to be working with a single domain. Of course the presence of domain walls or impurities causing the pinning of domains would open many interesting channels of dissipation. Within our approximation, we can model the system in terms of an fcc lattice of spins $\vec{S}_i$ with NN and NNN interaction and asymmetric anisotropy. A

N_p	D_1	D_2	J_1^+	J_1^-	$J_1^+ - J_1^-$	J_2
3	1.13	0.06[a]	−15.7	−16.1	0.45	221
	(±0.04)	(±0.05)	(− 6.0)	(− 6.0)		
			(+10.0)	(+10.0)	(±0.20)	(±4)

Figure 2.4: Anisotropy parameters D_i and exchange couplings J_i (in K) as measured by neutron scattering. Reproduced from [21].
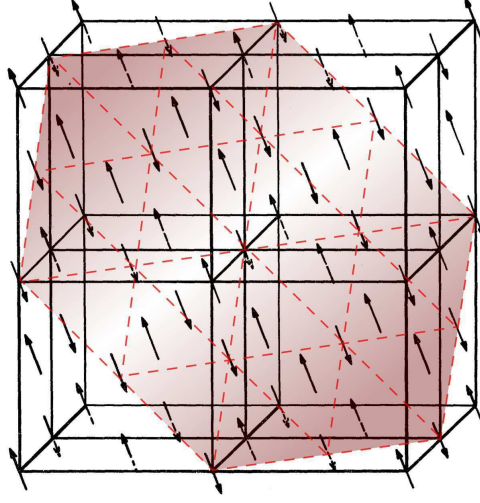
Figure 2.5: The AF2 spin structure of Ni in NiO (oxygens now shown) with one of the (111) planes highlighted. Modified from [21].

possible Hamiltonian reads [23]:

$$
\begin{aligned}
\mathcal{H}_0 &= J_1^- \sum_{i,\delta_p} \vec{S}_i \cdot \vec{S}_{i+\delta_p} + J_1^+ \sum_{i,\delta_a} \vec{S}_i \cdot \vec{S}_{i+\delta_a} + J_2 \sum_{i,\delta_2} \vec{S}_i \cdot \vec{S}_{i+\delta_2} + \\
&\quad + D_1 \sum_i (S_i^x)^2 + D_2 \sum_i (S_i^y)^2 \ ,
\end{aligned}
\tag{2.1}
$$

where S_z is taken as the minimum position, S_x being the out-of-plane and S_y the in-plane direction, and the vectors δ_p, δ_a and δ_2 connect ferromagnetic NN, antiferromagnetic NN and NNN, respectively.

2.2.2   Spin-Wave Description

To get some insight on the localization of the effect of the tip on the NiO sample, we will consider the linear spin-wave (LSW) theory for an antiferromagnet [24]. We will show how this is implemented on the basic simple cubic Heisenberg antiferromagnet (HAF) to estimate the perturbation of the tip and the time evolution due to its oscillations. We will not explicitly derive the same equations for the complete system, but we will show that it can be reduced to a Hamiltonian of the same form, so that the same qualitative results are expected to apply.

Linear spin-wave thory for the Heisenberg antiferromagnet in presence of anisotropy — We want to describe a system of spins S interacting through an antiferromagnetic Heisenberg interaction and subject to an on-site magnetic

field generating an unidirectional anisotropy. In order to do this we will use the Holstein-Primakoff (HP) transformation [25] to construct a linear spin-wave theory of our system.

We start from the Hamiltonian:

$$\mathcal{H} = J \sum_{i,\delta} \vec{S}_i \cdot \vec{S}_{i+\delta} - D \sum_i (S_i^z)^2, \qquad (2.2)$$

where $J > 0$ represents the antiferromagnetic coupling, $D > 0$ is the anisotropy (along the z direction) and δ represents all the possible vectors joining the nearest-neighboring (NN) sites (we will assume a M dimensional cubic structure with lattice spacing a). To start with we will apply to the spins the so-called Holstein-Primakoff transformation for the antiferromagnet:

$$\begin{cases} S_i^z &= (-1)^i \left(S - \hat{n}_i \right) \\ S_i^\pm &= \frac{1 \mp (-1)^i}{2} \, \hat{d}_i^\dagger \, \sqrt{2S - \hat{n}_i} + \frac{1 \pm (-1)^i}{2} \, \sqrt{2S - \hat{n}_i} \, \hat{d}_i \, , \end{cases} \qquad (2.3)$$

where the $\hat{d}_i$'s are bosonic operators satisfying the usual commutation relations and the $\hat{n}_i$'s are the corresponding number operators $\hat{d}_i^\dagger \hat{d}_i$. This transformation casts our Hamiltonian in the form:

$$\begin{aligned} \mathcal{H} &= -J \sum_{i,\delta} (S - \hat{n}_i)(S - \hat{n}_{i+\delta}) + \\ &+ \frac{J}{8} \sum_{i,\delta} \left[(1 - (-1)^i)^2 \, \hat{d}_i^\dagger \, \sqrt{2S - \hat{n}_i} \, \hat{d}_{i+\delta}^\dagger \, \sqrt{2S - \hat{n}_{i+\delta}} + \right. \\ &\left. + (1 + (-1)^i)^2 \, \sqrt{2S - \hat{n}_i} \, \hat{d}_i \, \sqrt{2S - \hat{n}_{i+\delta}} \, \hat{d}_{i+\delta} \right] + \\ &- D \sum_i (S - \hat{n}_i)^2. \end{aligned} \qquad (2.4)$$

Assuming low occupation numbers, we can take the limit $\langle \hat{n} \rangle / S \ll 1$ and, keeping only terms up to order S, our Hamiltonian simplifies to:

$$\mathcal{H} = -NJS^2(M + D^*) + 2JS(M + D^*) \sum_i \hat{d}_i^\dagger \hat{d}_i + JS \sum_{i,\delta} \left[\hat{d}_i^\dagger \hat{d}_{i+\delta}^\dagger + \hat{d}_i \hat{d}_{i+\delta} \right], \qquad (2.5)$$

where once more M is the dimensionality of the system and $D^* = D/J$ is the rescaled anisotropy parameter. Moving to k-space, we have

$$\begin{aligned} \mathcal{H} &= -NJS^2(M + D^*) + 2JS(M + D^*) \sum_k \hat{d}_k^\dagger \hat{d}_k + \\ &+ JS \sum_{k,\delta} \left[\hat{d}_k^\dagger \hat{d}_{-k}^\dagger \, e^{i\vec{k}\cdot\vec{\delta}} + \hat{d}_k \hat{d}_{-k} \, e^{-i\vec{k}\cdot\vec{\delta}} \right]. \end{aligned} \qquad (2.6)$$

We can now diagonalize this Hamiltonian by means of a Bogoliubov transformation in terms of the new bosonic operators $\hat{b}_k$ and parameters $u_k = u_{-k}$:

$$\begin{cases} \hat{d}_k & = \cosh u_k \, \hat{b}_k + \sinh u_k \, \hat{b}^\dagger_{-k} \\ \hat{d}^\dagger_k & = \cosh u_k \, \hat{b}^\dagger_k + \sinh u_k \, \hat{b}_{-k}. \end{cases} \qquad (2.7)$$

We find that for this transformation to diagonalize the system, the u_k's must satisfy the condition

$$\tanh 2u_k = -\frac{\sum_\delta \cos(\vec{k} \cdot \vec{\delta})}{M + D^*}, \qquad (2.8)$$

reducing the Hamiltonian to the final diagonal form

$$\begin{aligned} \mathcal{H} & = -NJS^2(M + D^*) - NJS(M + D^*)+ \\ & \quad +2JS(M + D^*)\sum_k \left(\hat{n}_k + \frac{1}{2}\right)\sqrt{1 - \left(\frac{\sum_\delta \cos(\vec{k} \cdot \vec{\delta})}{M + D^*}\right)^2} \equiv \\ & \equiv E_0 + \sum_k \left(\hat{n}_k + \frac{1}{2}\right)\omega_k . \end{aligned} \qquad (2.9)$$

An example of the dispersion ω_k for different values of D for the 1-dimensional case is shown in Fig. 2.6. As we can see the dispersion is gapless and linear for small k in the isotropic case, while the anisotropy opens a gap in the spectrum.

Interaction with a magnetic tip — We now want to model the interaction of our antiferromagnetic surface with an external magnetic tip by adding a term to the hamiltonian in the form:

$$\mathcal{H}_{int} = -H_z S^z_0 - H_x S^x_0, \qquad (2.10)$$

that is a Heisenberg interaction of one single (0) spin with an external magnetic field along the z and x direction (due to the experimental setup we want to describe). We will try to find the ground state of this new Hamiltonian within the LSW theory; we will thus expect our result to be accurate at least for small external perturbations, when we can consider the low occupation needed for this theory to still hold.

In the spin-wave $\hat{b}_k$ basis of (2.9), our Hamiltonian now reads:

$$\begin{aligned} \mathcal{H} & = E'_0 + \sum_k \omega_k \hat{b}^\dagger_k \hat{b}_k - \frac{H_z}{N}\sum_{k,k'}\cosh(u_k + u_{k'})\hat{b}^\dagger_k \hat{b}_{k'}+ \\ & \quad -H_x\sqrt{\frac{S}{2N}}\sum_k (\cosh u_k + \sinh u_k)\left(\hat{b}^\dagger_k + \hat{b}_k\right), \end{aligned} \qquad (2.11)$$
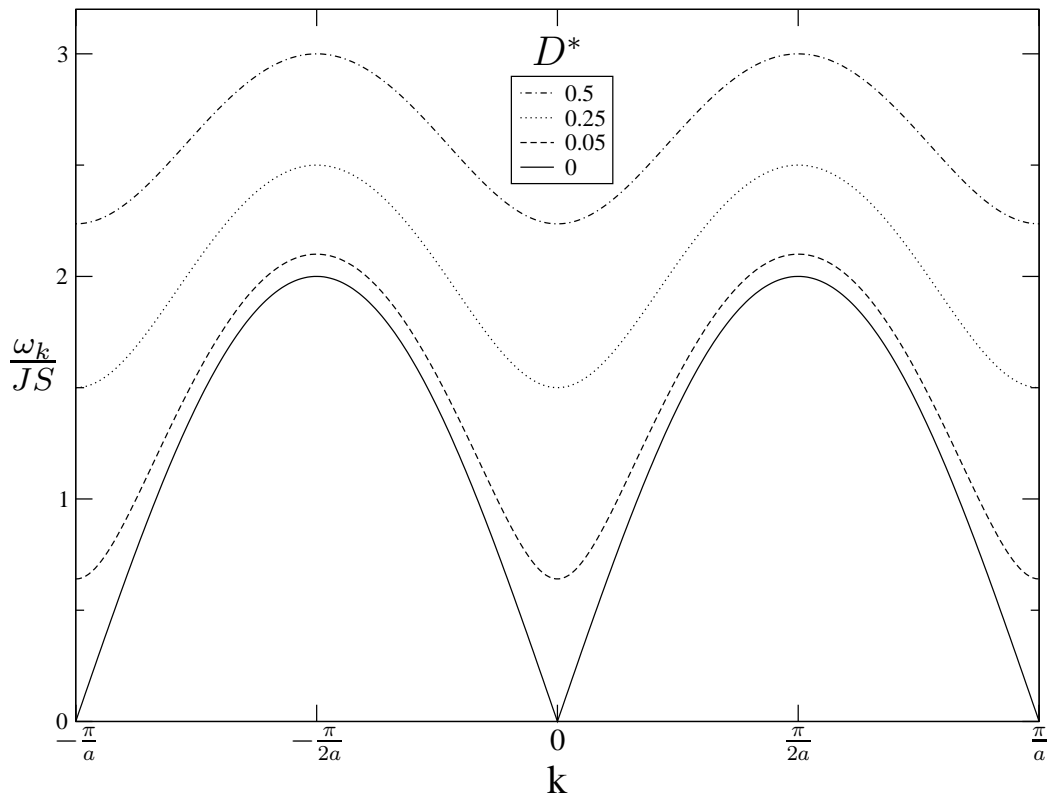
Figure 2.6: Spin-waves dispersion for the 1-dimensional HAF for different values of the anisotropy D^* (see legend).

where $E_0' = E_0 + H_z(S - \langle S_0^z \rangle_0)$ with E_0 and ω_k from (2.9) and $\langle S_0^z \rangle_0$ the average spin in the unperturbed system (the first order correction in energy), and with the u_k's as defined by the Bogoliubov transformation (2.7), and N the total number of spins in the system.

We now look for the lowest eigenstate of this Hamiltonian which has the form:

$$|\psi\rangle = f_{GS} |0\rangle + \sum_k f_k \hat{b}_k^\dagger |0\rangle . \qquad (2.12)$$

where $|0\rangle$ is the spin-wave vacuum (ground state of the unperturbed system) and we have introduced the $N + 1$ parameters $\{f_{k,GS}\}$, subject to the normalization constraint $|f_{GS}|^2 + \sum_k |f_k|^2 = 1$. It has to be noted that, due to the presence of terms $\hat{b}_k^\dagger$ in the Hamiltonian, this combination of one-magnon states cannot be an exact eigenstate of the system; anyway, as long as H_x is small enough and so are the f_k's (which is the limit in which we expect our theory to be valid), the higher magnon states can be safely neglected in the determination of the ground state of the system. This condition will be

taken into account in the following calculations.

Evaluating the energy of a set of coefficients $\{f_{k,GS}\}$ as $E[\{f_{k,GS}\}] = \langle\psi|\mathcal{H}|\psi\rangle / \langle\psi|\psi\rangle$ using Hamiltonian (2.11) over the trial state (2.12) gives:

$$
\begin{aligned}
E[\{f_{k,GS}\}] &= E'_0 + \sum_k |f_k|^2\,\omega_k - \frac{H_z}{N}\,{}_z\sum_{k,k'}\cosh(u_k + u_{k'})f_k^* f_{k'} + \\
&\quad -H_x\sqrt{\frac{S}{2N}}\sum_k \left(\cosh u_k + \sinh u_k\right)\left(f_{GS}f_k^* + f_k f_{GS}^*\right) = \\
&\equiv E'_0 + \Delta[\{f_{k,GS}\}]\;.
\end{aligned}
\tag{2.13}
$$

To find the minimum configuration for the coefficients $\{f_{k,GS}\}$, we impose the variation on the energy to go to zero:

$$
\delta E[\{f_{k,GS}\}] = 0 \;\Rightarrow\; \langle\delta\psi|\mathcal{H} - E|\psi\rangle = 0
\tag{2.14}
$$

By considering a real variation of $f_{\bar{k}}$ or of f_{GS} we get

$$
\begin{cases}
f_{\bar{k}} &= \dfrac{1}{\omega_{\bar{k}} - \Delta}\left[\dfrac{H_z}{N}\sum_k f_k \cosh(u_k + u_{\bar{k}}) + \right. \\
&\quad \left. + \sqrt{\dfrac{S}{2N}}H_x\left(\cosh u_{\bar{k}} + \sinh u_{\bar{k}}\right)f_{GS}\right] \\[2mm]
f_{GS} &= -\dfrac{1}{\Delta}\sqrt{\dfrac{S}{2N}}H_x\sum_k\left(\cosh u_k + \sinh u_k\right)f_k.
\end{cases}
\tag{2.15}
$$

This is a set of $N+1$ equations that need to be satisfied self-consistently. We found solutions for these equations for different parameters H_z and H_x and varying degrees of anisotropy D (taken into account in ω_k and u_k) with respect to the initial J coupling constant. In Fig.(2.7) we can see an example of the absolute difference in the S_z and S_x components of the spins from the unperturbed values for different perturbations H in a 2-dimensional system.

We can see that the decay in both components of the spin is exponential, with a slight deviation near the interacting site (the slight deviation for boundary sites is just a finite-size effect). We can further see that the decay rate does not seem to depend on the perturbation strength (it is instead related to the coupling-anisotropy ratio), while the rotation of the spin of the perturbed site does. For perturbations stronger than the ones shown, the rotation of the perturbed spin does not seem to increase further and the decay rate slightly decreases; this is probably due to the breakdown of the LSW theory.

Expanding the theory to include two-magnon states does not seem to substantially change the shape of the perturbed ground state, which can
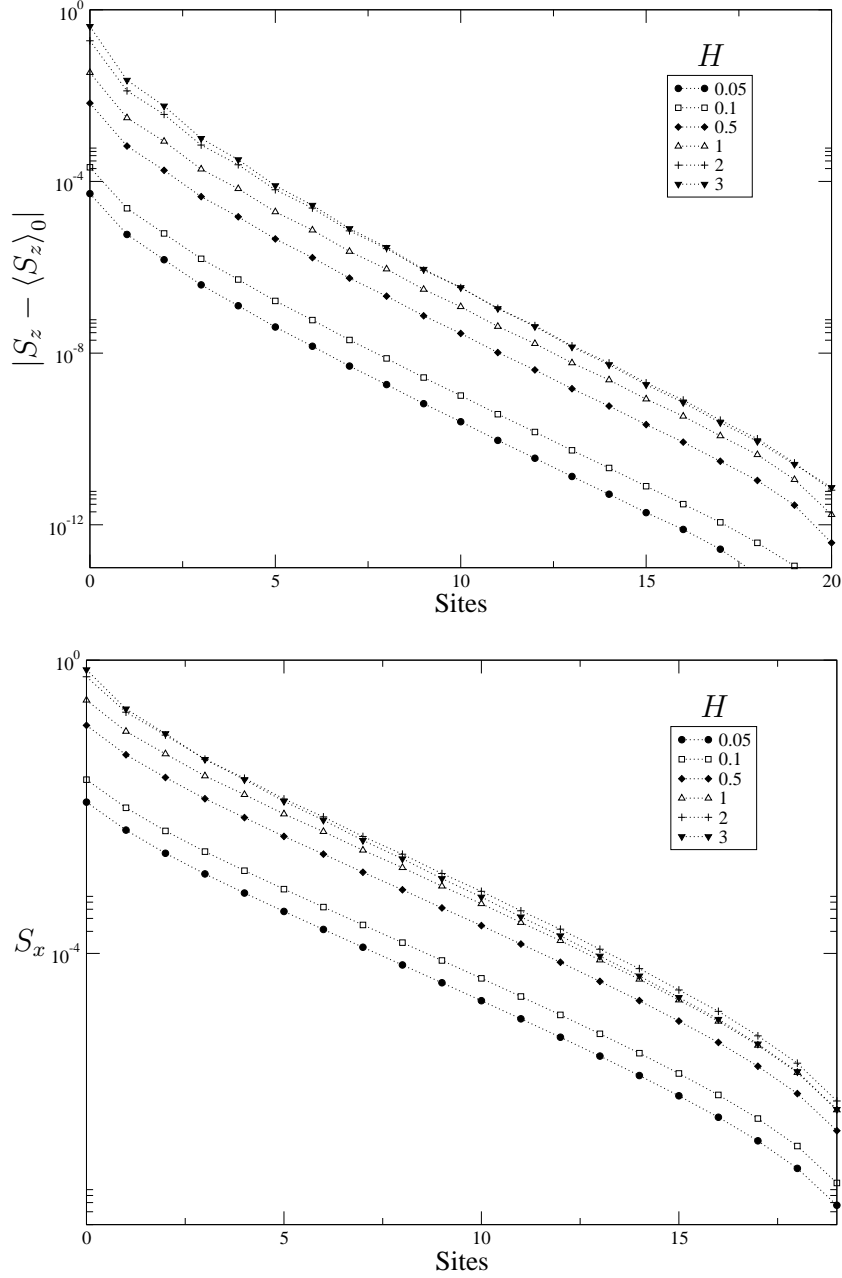
Figure 2.7: Absolute difference in the S_z and S_x components of the spins from the unperturbed values for a 2-dimensional 41×41 spins system in term of sites i along the $\hat{x}$ direction. We considered an anisotropy parameter $D^* = 0.1$ and different values of the perturbation H in the xz plane with $H_z = \sqrt{2}H_x$ (in the legend $H = \sqrt{H_z^2 + H_x^2}$).

therefore be considered the correct state of the system for small perturbations.

We will now consider the time-dependence of the external perturbation and compute the dynamics of the system. In order to do this we take a time-dependent version of the trial wavefunction (2.12):

$$|\psi(t)\rangle = f_{GS}(t)\,|0\rangle + \sum_k f_k(t)\hat{b}_k^\dagger\,|0\rangle \tag{2.16}$$

and we impose the time-dependent version of the variational principle:

$$\langle\delta\psi(t)|\,i\hbar\frac{\partial}{\partial t} - \mathcal{H}(t)\,|\psi(t)\rangle = 0 \,. \tag{2.17}$$

In this way we find equations for the derivatives of the coefficients:

$$\begin{cases} \dfrac{\partial f_{\bar{k}}(t)}{\partial t} &= \left(\omega_{\bar{k}} + E_0'\right)f_{\bar{k}}(t) - \dfrac{H_z}{N}\sum_k f_k \cosh(u_k + u_{\bar{k}}) + \\[2mm] & \quad -\sqrt{\dfrac{S}{2N}}H_x e^{u_{\bar{k}}} f_{GS}(t) \\[3mm] \dfrac{\partial f_{GS}(t)}{\partial t} &= E_0' f_{GS}(t) - \dfrac{1}{\Delta}\sqrt{\dfrac{S}{2N}}H_x \sum_k e^{u_k} f_k(t) \,. \end{cases} \tag{2.18}$$

By numerically integrating this equations for a time-dependent perturbation we can see how the system responds to tips oscillating at different frequencies. An example for a 'slow' and a 'fast' perturbation behaving like $H(t) = H\sin^2(\omega t)$ is shown in Fig. 2.8. We can clearly see how in the case of slow perturbation the system can follow essentially adiabatically and is always in the ground state with respect to the position of the tip. On the contrary, for faster perturbations the system 'lags' behind and is not allowed to reach the ground state; this means that the tip sees a different state while approaching to and receding from the surface, giving rise to a hysteresis loop that can account for dissipation.

To understand the regime relevant to the experimental case under exam, we should construct a spin-wave theory for the more complex structure of NiO. Luckily, it is possible to do so as shown in [23] starting from the Hamiltonian (2.1) we previously derived. We will omit here the tedious detail of the derivation and just say that the final result is in the usual form

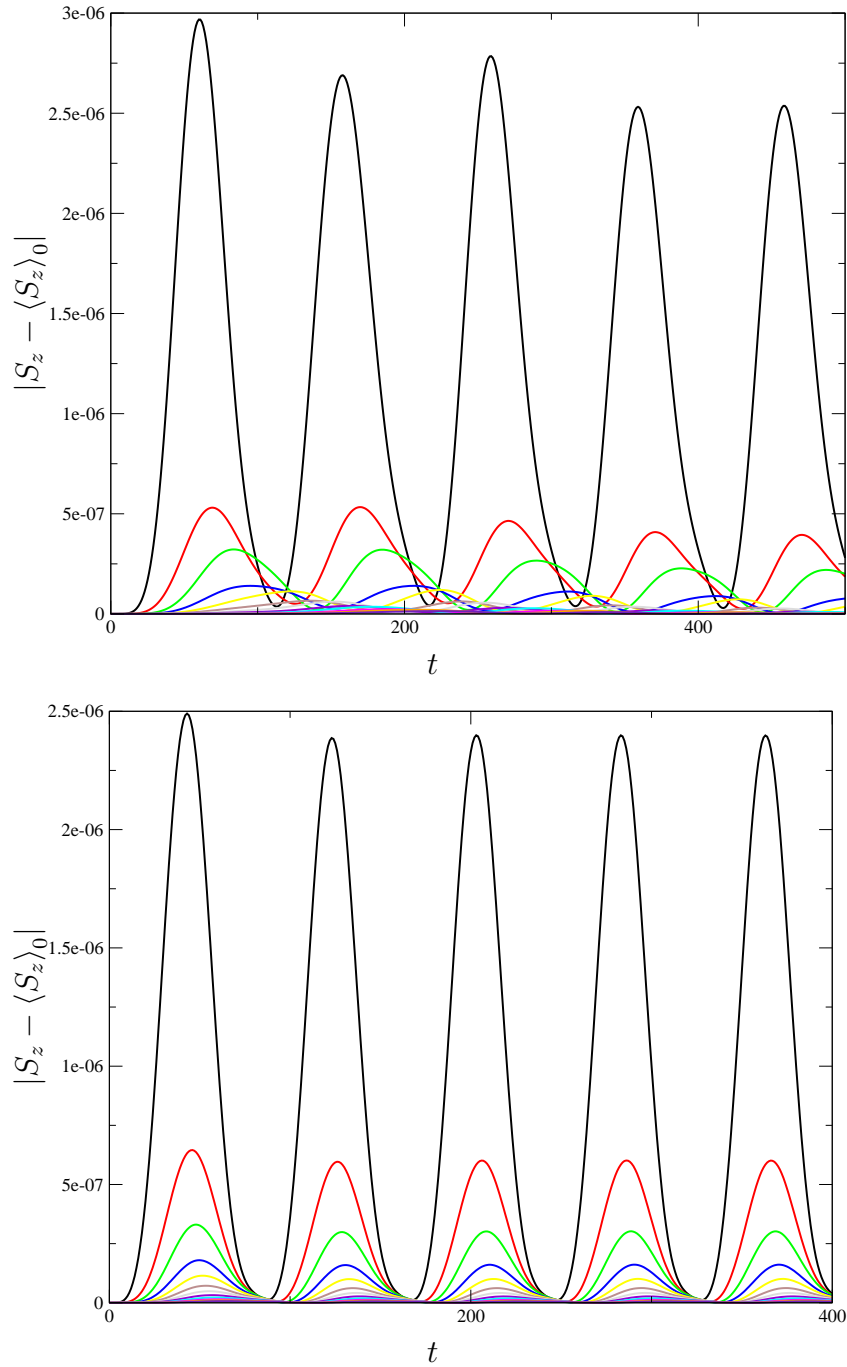$$E_0 + \sum_k \left(\hat{n}_k + \frac{1}{2}\right)\omega_k \,, \tag{2.19}$$

Figure 2.8: Time evolution of the z component of the spin obtained integrating Eq. (2.18), with $D^* = 0.01$ under an external perturbation $H(t) = H\sin^2(\omega t)$ with $H = 0.008$ (again $H_z = \sqrt{2}H_x$) and different frequencies $\omega = 2\pi/10$ (upper panel) and $\omega = 2\pi/40$ (lower panel).

with the rather complicated coefficients:

$$\begin{cases} E_0 &= -\frac{1}{2}NS(S+1)\left[z_2J_2 + \frac{1}{2}z_1(J_1^+ - J_1^-)\right] \\ \omega_k &= \left[(\beta_1 + \gamma)(\beta_2 - \gamma)\right]^{1/2} \\ \beta_{1,2} &= z_2J_2 + \frac{1}{2}z_1(J_1^+ - J_1^-) + J_1^- \sum_{\delta_p} e^{ik\delta_p} + 2D_{1,2} \\ \gamma &= J_1^+ \sum_{\delta_a} e^{ik\delta_a} + J_2^- \sum_{\delta_2} e^{ik\delta_2} \, , \end{cases} \qquad (2.20)$$

where all the quantities have the same definitions of (2.1) and $z_{1,2}$ is the number of NN and NNN (12 and 6, respectively).

Considering this spin-wave spectrum with the values of NiO and the experimental tip frequency around 160 kHz, it is easy to see that the MExFM setup is clearly in the adiabatic limit and therefore no relevant dissipation can come from this channel (even taking into account a possible discrepancy due to the roughness of our model).

It is interesting to see that this result could have been predicted in a much easier way just by considering the gap in the AF spin-wave spectrum: from our theory or directly from experimental measurements we can see that this gap is of the order of 1.5 meV, corresponding to a frequency of more than 2 THz. A perturbation at a frequency of 160 kHz is therefore clearly unable to directly couple to any magnon mode within the sample and can be safely considered adiabatic with respect to this kind of excitation, leading to no direct dissipation from this channel. Dissipation could still in principle come from the decay of the excited spin-waves, but this is a much smaller effect and cannot be held responsible for the huge observed dissipation.

2.3   The Dissipation Mechanism

2.3.1   Coupling Mechanism

To provide a realistic mechanism able to describe the energy dissipation observed in the MExFM experiment described in section 2.1, we will need to take into account the coupling of the spin to some gapless excitations of the system: in this case, phonons. To illustrate this coupling, let us consider a $\downarrow$-polarized Fe tip oscillating over a Ni spin $\vec{S}_i$ and define the exchange potential

$$V^{\text{ex}}(z) = V^{\downarrow\downarrow}(z) - V^{\uparrow\downarrow}(z) \, . \qquad (2.21)$$

This potential can be estimated to yield an exchange force $f^{\text{ex}} = -\frac{\partial V^{\text{ex}}}{\partial z}$ of ~ 0.3 nN when the tip edge is closer than 3Å to the surface Ni [16], which

in turn produces a small displacement $u_z(i)$ of the Ni-atom from its equilibrium position ultimately resulting in a potential of the form $-f^{\text{ex}}S_i^z u_z(i)$ (neglecting an unimportant spin-independent term). We can now express this potential in terms of phonon creation $(a_{\mathbf{k}s}^\dagger)$ and annihilation $(a_{\mathbf{k}s})$ operators ($\mathbf{k}s$ being wavevector and polarization of the phonon mode) by writing

$$u_z(i) = \sum_{\mathbf{k}s} \sqrt{\frac{\hbar}{2NM\omega_{\mathbf{k}s}}} e_z(\mathbf{k}s)(a_{\mathbf{k}s} + a_{-\mathbf{k}s}^\dagger)e^{i\mathbf{k}\cdot\mathbf{r}_i} \, , \qquad (2.22)$$

$e_z(\mathbf{k}s)$ and $\omega_{\mathbf{k}s}$ being the eigenvector and eigenvalue of the $\mathbf{k}s$ phonon mode, N the number of atoms in the chain, M their mass and r_i the position of atom i.

This gives us a simple form for the coupling of the Ni-spin to the Ni acoustic phonons:

$$H_{\text{spin}-\text{phonons}} = \sigma_i^z \sum_{\mathbf{k}s} \lambda_{\mathbf{k}s}^{(i)}(a_{\mathbf{k}s} + a_{-\mathbf{k}s}^\dagger) \qquad (2.23)$$

where

$$\lambda_{\mathbf{k}s}^{(i)} = -f^{\text{ex}}e^{i\mathbf{k}\cdot\mathbf{r}_i}\sqrt{\frac{\hbar}{8NM\omega_{\mathbf{k}s}}} e_z(\mathbf{k}s) \, . \qquad (2.24)$$

As explained in section 1.2, the most important quantity for a compact description of a bath is its spectral density (1.10). From the previous derivation we can easily estimate:

$$J(\omega) = (f^{\text{ex}})^2 \frac{\hbar}{8MN} \sum_{\mathbf{k}s} \delta(\omega - \omega_{\mathbf{k}s}) \frac{|e_z(\mathbf{k}s)|^2}{\omega_{\mathbf{k}s}} \, . \qquad (2.25)$$

By assuming the standard Debye form for the low-energy acoustic phonons in three-dimensions, we find that the small-ω limit of $J(\omega)$ is precisely *Ohmic* $J(\omega) = \hbar^2\alpha\omega + \cdots$ with

$$\alpha = (f^{\text{ex}})^2 \frac{3\hbar^2}{8Mk^3 T_D^3} \, , \qquad (2.26)$$

where T_D is the Debye temperature. An estimate, with $f^{\text{ex}} \sim 0.3$ nN, gives a value of α close to 1, which can be easily made > 1 by a slightly larger f^{ex} or by a better account of the (softer) surface phonon modes. It should be noted that we purposely ignored all complications related to the surface projection of bulk phonons, which would call for a much more cumbersome treatment, without essentially changing the physics.

We thus reduced our problem to the study of a slowly driven spin-boson model with a Ohmic bath and a rather strong coupling. We will now refine the path-integral theory of section 1.4 to tackle this limit in the most convenient form.

2.3.2 Path Integral Description

We will start our description from the last expression of section 1.4 for the Laplace transform of $\langle \sigma^z \rangle$ within the NIBA, Eq. (1.63) that we repeat here for convenience (we refer to that section for notation and terminology):

$$
\begin{aligned}
\langle \sigma^z(\lambda) \rangle &= \frac{1}{\lambda} + \frac{1}{\lambda} \sum_{n=1}^{\infty} (-1)^n \int_0^{\infty} \tilde{\mathcal{D}}_n(\lambda) \Delta_{2n} e^{-S(\tau_1)} \cos\left(\phi_1 + R(\tau_1)\right) \\
&\quad \prod_{k=2}^{n} \cos\left(R(\tau_k)\right) \cos \phi_k e^{-S(\tau_k)} .
\end{aligned}
\tag{2.27}
$$

We will make four approximations to obtain our final result, justified by the specifics of the system under study as presented in section 2.1. The first one has already been presented as the NIBA and, as mentioned, is justified in our case, namely by considering a Ohmic bath and a coupling $\alpha > 1$. The second approximation is allowed by the very slow oscillation frequency of the cantilever, making our characteristic frequency ω such that $\omega \langle \tau \rangle \ll 1$, where $\langle \tau \rangle$ is the average blip length. We can therefore replace the ϕ_k's and Δ_{2n} with the average value of the perturbation during the blip itself:

$$
\begin{cases}
\phi_j \simeq \varepsilon \tau_j \sum_{k=0}^{j-1} s_k \\
\Delta_{2n} \simeq \prod_{j=0}^{n} \Delta^2 \sum_{k=0}^{j} s_k .
\end{cases}
\tag{2.28}
$$

In this limit it becomes possible to analytically compute the series: considering only the antisymmetric contribution of the external perturbation (a similar result can be found for the symmetric part, which can be proved to decay rapidly) and defining $\rho_j = \sum_{k=0}^{j} s_k$ and the functions

$$
\begin{aligned}
F_\lambda(\rho) &= \Delta^2(\rho) \int_0^{\infty} \sin R(\tau) e^{-\lambda \tau - S(\tau)} \sin\left(\varepsilon(\rho)\tau\right) d\tau \\
G_\lambda(\rho) &= \Delta^2(\rho) \int_0^{\infty} \cos R(\tau) e^{-\lambda \tau - S(\tau)} \cos\left(\varepsilon(\rho)\tau\right) d\tau,
\end{aligned}
\tag{2.29}
$$

we find $\langle \sigma^z(\lambda) \rangle$ in the form:

$$
\langle \sigma^z(\lambda) \rangle^{(a)} = \int_0^{\infty} d\rho_0 F_\lambda(\rho_0) e^{-\lambda \rho_0} \int_0^{\infty} d\rho_1 e^{-\lambda \rho_1} \exp\left[-\int_{\rho_0}^{\rho_0 + \rho_1} d\rho\, G_\lambda(\rho) \right] .
\tag{2.30}
$$

We now need to introduce the specific form of the spectral density which we found to be Ohmic (2.25), and calculate the functions $S(\tau)$ and $R(\tau)$, which, we recall, are real and imaginary part of the spectral density integral (1.55). For this case we can explicitly compute

$$
\begin{aligned}
S(\tau) &= 2\alpha \left[\frac{\hbar\beta}{\pi\tau} \sinh\left(\frac{\pi\tau}{\hbar\beta}\right) \right] + \alpha \ln\left(1 + \omega_c^2\tau^2\right) \\
R(\tau) &= 2\alpha \arctan\left(\omega_c\tau\right) ,
\end{aligned}
\tag{2.31}
$$

which can be further simplified for τ such that $\omega_c\tau \gg 1$, our third approximation and quite general, since ω_c is supposed to be a high energy cutoff. We obtain

$$
\begin{aligned}
S(\tau) &= 2\alpha \left[\frac{\hbar\beta}{\pi\tau} \sinh\left(\frac{\pi\tau}{\hbar\beta}\right) \right] \\
R(\tau) &= \pi\alpha .
\end{aligned}
\tag{2.32}
$$

To get a simplified expression for G_λ and F_λ we will define the useful integral:

$$
\begin{aligned}
\Sigma(\lambda) &= \Delta^2(\rho)\cos(\pi\alpha) \int_0^\infty d\tau e^{-\lambda\tau} \left[\frac{\beta\omega_c}{\pi} \sinh\left(\frac{\pi\tau}{\beta}\right) \right]^{-2\alpha} = \\
&= \Delta_e \left(\frac{\beta\Delta_e}{2\pi}\right) \frac{\Gamma\left(\alpha + \beta\lambda/2\pi\right)}{\Gamma\left(1 - \alpha + \beta\lambda/2\pi\right)},
\end{aligned}
\tag{2.33}
$$

Γ being the gamma function and

$$
\Delta_e = \Delta \left(\frac{\Delta}{\omega_c}\right)^{\frac{\alpha}{1-\alpha}} \left[\cos(\pi\alpha)\Gamma(1 - 2\alpha)\right]^{\frac{1}{2-2\alpha}} .
\tag{2.34}
$$

This allows us to explicit G_λ and F_λ as

$$
\begin{aligned}
G_\lambda(\rho) &= \frac{1}{2} \left[\Sigma(\lambda + i\varepsilon(\rho)) + \Sigma(\lambda - i\varepsilon(\rho)) \right] \\
F_\lambda(\rho) &= \frac{\tan(\pi\alpha)}{2i} \left[\Sigma(\lambda + i\varepsilon(\rho)) - \Sigma(\lambda - i\varepsilon(\rho)) \right] .
\end{aligned}
\tag{2.35}
$$

The fourth and last approximation we will make is to consider G and F not strongly dependent on λ: this is a rather drastic approximation, but it can be shown to be true for the strong damping Ohmic case we are interested in [12] and allows us to write a very simple rate equation governing $\langle\sigma^z(t)\rangle$. If fact upon taking $G_\lambda(\rho) \simeq G_0(\rho)$ and $F_\lambda(\rho) \simeq F_0(\rho)$ we can perform an inverse Laplace transform and get

$$
\langle\sigma^z(t)\rangle^{(a)} = \int_0^t d\rho F_0(\rho) \exp\left[-\int_\rho^t d\rho_0 G_0(\rho_0) \right] ,
\tag{2.36}
$$

which in turn obeys the simple rate equation:

$$\frac{\mathrm{d}}{\mathrm{d}t} \langle \sigma^z(t) \rangle^{(a)} = -G_0(t) \langle \sigma^z(t) \rangle^{(a)} + F_0(t) \ . \tag{2.37}$$

Eq.(2.37) can be easily integrated numerically for a given low frequency time-dependent perturbation to obtain the time evolution of the z component of the spin.

We will now briefly show how to obtain a similar result for $\langle \sigma^x \rangle$. We will start from Eq. (1.65) and follow the same steps and the same approximations presented for $\langle \sigma^z \rangle$: we will consider a low frequency perturbation and define

$$
\begin{aligned}
\tilde{F}_\lambda(\rho) &= \Delta^2(\rho) \int_0^\infty \sin R(\tau) e^{-\lambda\tau - S(\tau)} \cos \left(\varepsilon(\rho)\tau \right) d\tau \\
\tilde{G}_\lambda(\rho) &= \Delta^2(\rho) \int_0^\infty \cos R(\tau) e^{-\lambda\tau - S(\tau)} \sin \left(\varepsilon(\rho)\tau \right) d\tau \ .
\end{aligned}
\tag{2.38}
$$

In terms of these we can find for the symmetric contribution (similar equations can be written for the antisymmetric, which is the decaying one in this case):

$$
\begin{aligned}
\langle \sigma^x(\lambda) \rangle^{(s)} &= \int_0^\infty d\rho_0 F_\lambda(\rho_0) e^{-\lambda\rho_0} \int_0^\infty d\rho_1 e^{-\lambda\rho_1} \frac{\tilde{G}_\lambda(\rho_0 + \rho_1)}{\Delta(\rho_0 + \rho_1)} \\
&\quad \exp \left[- \int_{\rho_0}^{\rho_0 + \rho_1} d\rho \, G_\lambda(\rho) \right] .
\end{aligned}
\tag{2.39}
$$

We can still write $\tilde{F}_\lambda$ and $\tilde{G}_\lambda$ in terms of $\Sigma(\lambda)$ of Eq. (2.33) and take them as almost constant in λ to get:

$$\langle \sigma^x(t) \rangle^{(s)} = \int_0^t d\rho F_0(\rho) \frac{\tilde{G}_0(t)}{\Delta(t)} \exp \left[- \int_\rho^t d\rho_0 G_0(\rho_0) \right] , \tag{2.40}$$

which can be cast as another rate equation:

$$\frac{\mathrm{d}}{\mathrm{d}t} \langle \sigma^x(t) \rangle^{(s)} = -G_0(t) \langle \sigma^x(t) \rangle^{(s)} + \frac{F_0(t) \tilde{G}_0(t)}{\Delta(t)} . \tag{2.41}$$

The last component of the spin $\langle \sigma^y(t) \rangle$ can be easily evaluated from $\langle \sigma^z(t) \rangle$ by using the simple relation [13]

$$\langle \sigma^y(t) \rangle = -\frac{1}{\Delta(t)} \frac{\mathrm{d} \langle \sigma^z(t) \rangle}{\mathrm{d}t} \ . \tag{2.42}$$

2.3.3   Numerical Results

We can now apply the rate equations obtained for all the components of the spin in the spin-boson model specialized to our system, to understand how the coupling to phonons can account for the energy dissipation reported in the experimental setup described in section 2.1.

Before considering the experimental time-dependent perturbation, it is a good idea to start analyzing the behavior of the system under an external perturbation turned on at $t = 0$ and having a constant value $\bar{\varepsilon} - \varepsilon_0$ thereafter. In this case eq.(2.37) can be considerably simplified and the equilibrium value

$$\langle \sigma^z(\infty) \rangle = -F_0/G_0 = -\tanh(\frac{1}{2}\beta\bar{\varepsilon}) \ , \qquad (2.43)$$

as well known in literature [7], and as we have found for similar systems subject to thermalization in section 1.3 through a totally different formalism (see Eq. (1.40)). Concerning the way in which the system reaches the equilibrium value, the spin boson system is know to present different regimes: in particular in the ohmic case for $\alpha > 1$ the system shows an overdamped behavior reaching the equilibrium value exponentially with a decay rate given, for low temperatures, by

$$\Gamma = \frac{\pi\Delta^2\,\bar{\varepsilon}^{2\alpha-1}}{2\Gamma(2\alpha)\omega_c^{2\alpha}}\left[1 + \frac{\pi^2\alpha(2\alpha-1)(2\alpha-2)}{3(\beta\bar{\varepsilon})^2}\right] \ . \qquad (2.44)$$

This gives us an idea of how in the overdamped regime the decay rate can take quite large values; this means that, even when subject to a comparably slow external perturbation, the system can be out of its instantaneous equilibrium value. This is the basis of the hysteretical behavior of this system, which we have excluded in terms of spin-wave excitations in section 2.2, but becomes now realistic in presence of this new timescale.

Before presenting the results of our analysis a remark about the role of ω_c is required: as we can see from Eq. (1.10), ω_c acts as a high energy cutoff to avoid the divergence of the spectral density. This cutoff can either be a true characteristic of the system or, as is the case in many application of the spin-boson model, an external artifact created while reducing a more general system at low energy to a two-state system. In this second case, one usually divides the density in a low energy component, treated as shown in the previous section, and a high energy component, which merely renormalizes the value of such quantities as Δ, which in the ohmic case is indeed found to scale as $\Delta \propto \omega_c^\alpha$. We can thus find a combination $\Delta_r = \Delta\,(\Delta/\omega_c)^{\alpha/(1-\alpha)}$ which is effectively independent of the chosen cutoff frequency: we will call quantities dependent on ω_c only through Δ_r *universal*. As can be clearly seen

from the explicit equations for the time-independent perturbation (2.43), $\langle\sigma^z(t)\rangle$ is in fact universal; contrariwise, as first noted in [26], $\langle\sigma^x(t)\rangle$ and $\langle\sigma^y(t)\rangle$ are not universal quantities, as their behavior strongly depends on the high energy part of the spectrum. For this reason, as we will see in the following, $\langle\sigma^x(t)\rangle$ and $\langle\sigma^y(t)\rangle$ will always be very small in our simulation, and the dissipated energy will be in fact dominated by the $\langle\sigma^z(t)\rangle$ behavior. This is not surprising, since a strong damping tends to suppress the coherences of the system [cf. section 1.3].

We will now consider a time-dependent perturbation simulating the real action of the tip. To do this we will start from the original Hamiltonian (1.47), which we report here for convenience:

$$\mathcal{H} = \frac{1}{2}\varepsilon(t)\sigma^z + \frac{1}{2}\hbar\Delta(t)\sigma^x + \sigma^z\sum_i \lambda_i\left(b_i + b_i^\dagger\right) + \sum_i \omega_i\left(b_i^\dagger b_i + \frac{1}{2}\right) \ , \ (2.45)$$

and take the external perturbation in the form

$$\left\{ \begin{array}{rcl} \varepsilon(t) & = & \varepsilon_0 + h\cos\theta\sin^2(\omega t) \\ \Delta(t) & = & h\sin\theta\sin^2(\omega t) \ , \end{array} \right. \qquad (2.46)$$

where ε_0 is the fixed potential on the spin due to the neighboring spins (we take it as constant since we saw in section 2.2 that nearest neighbors are only slightly affected by the perturbation), h is the maximum amplitude of the perturbation due to the tip, which we take as oscillating with frequency ω but always positive and θ is the angle the tip forms with the original spin direction.

We start from the initial condition $\sigma^z(0) = -1$ and integrate numerically equations (2.37) and (2.41) for values compatible with the experimental data. Numerical integration was performed through a simple implementation of the Runge-Kutta algorithm [27]. A sample time evolution for $\langle\sigma^z\rangle$ and $\langle\sigma^x\rangle$ is shown in Fig. 2.9 ($\langle\sigma^y\rangle$, not shown, is of the order of $\langle\sigma^x\rangle$): concentrating on the σ^z component (in black), we can clearly see how, at regime, the response of the system is "slower" than the perturbation, meaning that the system cannot respond to the tip instantaneously and the interactions during the approach and retraction phases are different. This is the typical case of hysteresis.

We can therefore now propose our model for dissipation in this system on more solid bases: the Ni spins are coupled through the action of the tip to the phonons of NiO, due to this coupling the effective response to the external tip perturbation is not instantaneous and any rotation of the spin leads to dissipation of energy through hysteresis; since the coupling is ferromagnetic, spins parallel to the tip are subject to a very small rotation and thus show
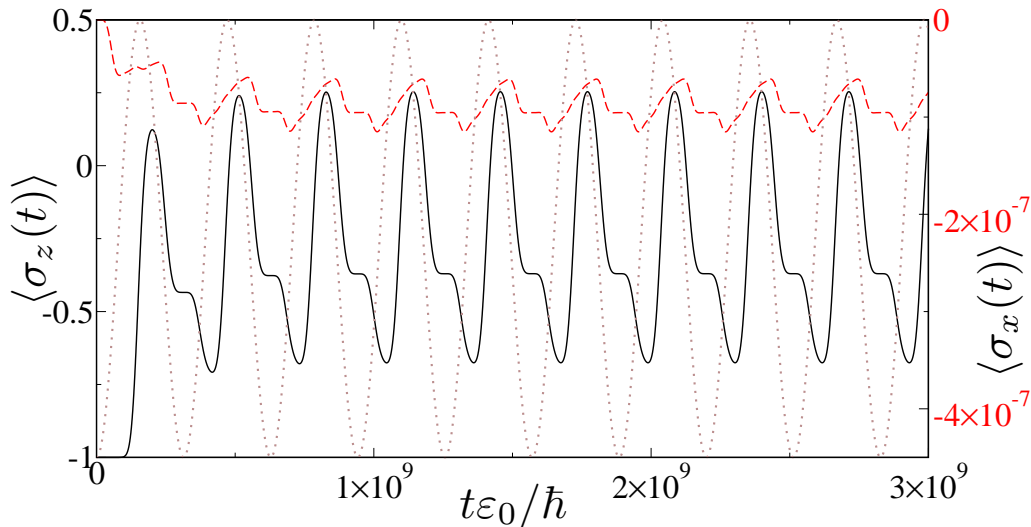
Figure 2.9: Time evolution of $\langle\sigma^z(t)\rangle$ (black full line, left axis) and $\langle\sigma^x(t)\rangle$ (dashed red line, right axis) for $\varepsilon_0 = 1$, $\omega_c = 20\varepsilon_0$, $\alpha = 2.1$, $h = 1.5\varepsilon_0$, $\theta = 0.6$, $\omega = 10^{-8}\varepsilon_0$, $\beta\varepsilon_0 = 20$. The dotted line shows the shape of the external perturbation.

low dissipation from this channel whereas antiparallel spins undergo a much greater movement to try to align to the tip magnetization direction and show therefore a much larger dissipation.

To numerically support this model and check that the spin-dependent dissipation is consistent with the experimental findings shown in Fig. 2.3, we computed evolutions for different tip-sample angles θ and calculated the energy dissipated in a cycle as:

$$W = \int_0^{2\pi/\omega} dt \left[\langle\sigma^z(t)\rangle \frac{\mathrm{d}\varepsilon(t)}{\mathrm{d}t} + \langle\sigma^x(t)\rangle \frac{\mathrm{d}\Delta(t)}{\mathrm{d}t} \right] , \qquad (2.47)$$

which also corresponds to the area of the hysteresis cycle as seen in a state-perturbation diagram. Such curves and the corresponding dissipated energy as a function of θ are shown in Fig. 2.10. It is necessary to point out that only the data for the z component are reported, since the x contribution is, as we have seen, negligible. Moreover, the curves represent the behavior of the system in the steady state, which depending on the parameters may take a few to a few tens of oscillation to be reached. We can clearly see that the dissipation has a maximum near $\theta = 0$ (not exactly at 0, where no rotation is allowed) and decreases for larger angles, just as expected from our description. Furthermore, the area of the hysteresis cycle for the most dissipative cases is of the order of magnitude of the antiferromagnetic coupling
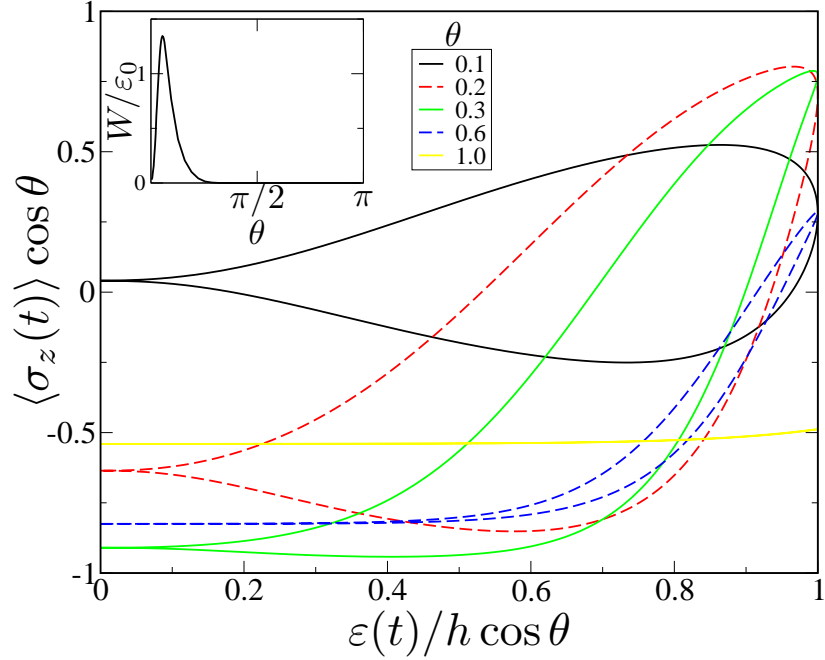
Figure 2.10: Hysteresis cycle for the z component of the external perturbation for different angles θ (see legend) for $\varepsilon_0 = 1$, $\omega_c = 100\varepsilon_0$, $\alpha = 2.1$, $h = 1.3\varepsilon_0$, $\omega = 10^{-12}\varepsilon_0$. Inset: angular dependence of the hysteresis area W.

ε_0, which we saw in 2.2 to be of the order of 20 meV, and therefore perfectly compatible with the dissipation difference of ~ 15 meV reported in [15] (see again Fig. 2.3).

In order to investigate some other features of this dissipation, we performed calculations at different frequencies ω and inverse temperatures β, as reported in Fig. 2.11 (in terms of energy dissipated per cycle W and of dissipated power $P = \omega W$). This results clearly show the presence of an "optimal" frequency attaining maximum dissipation. This can be easily explained by considering the new timescale Γ^{-1} (see Eq. (2.44)) due to the bosonic coupling: for frequencies of the order of (or slightly higher than) Γ, dissipation is high because the response of the system is hysteretic, but for slower frequencies the system can easily follow the external perturbation and the area of the hysteresis loop goes to zero, in accordance with the general principle that there is no zero-frequency dissipation in a thermal system. On the other side, for frequencies much higher than Γ the system has no time to really evolve during an oscillation of the tip and only sees an average perturbation in which it is effectively "frozen", leading to a slow decay to a position which is, in the steady state, almost fixed and producing no energy
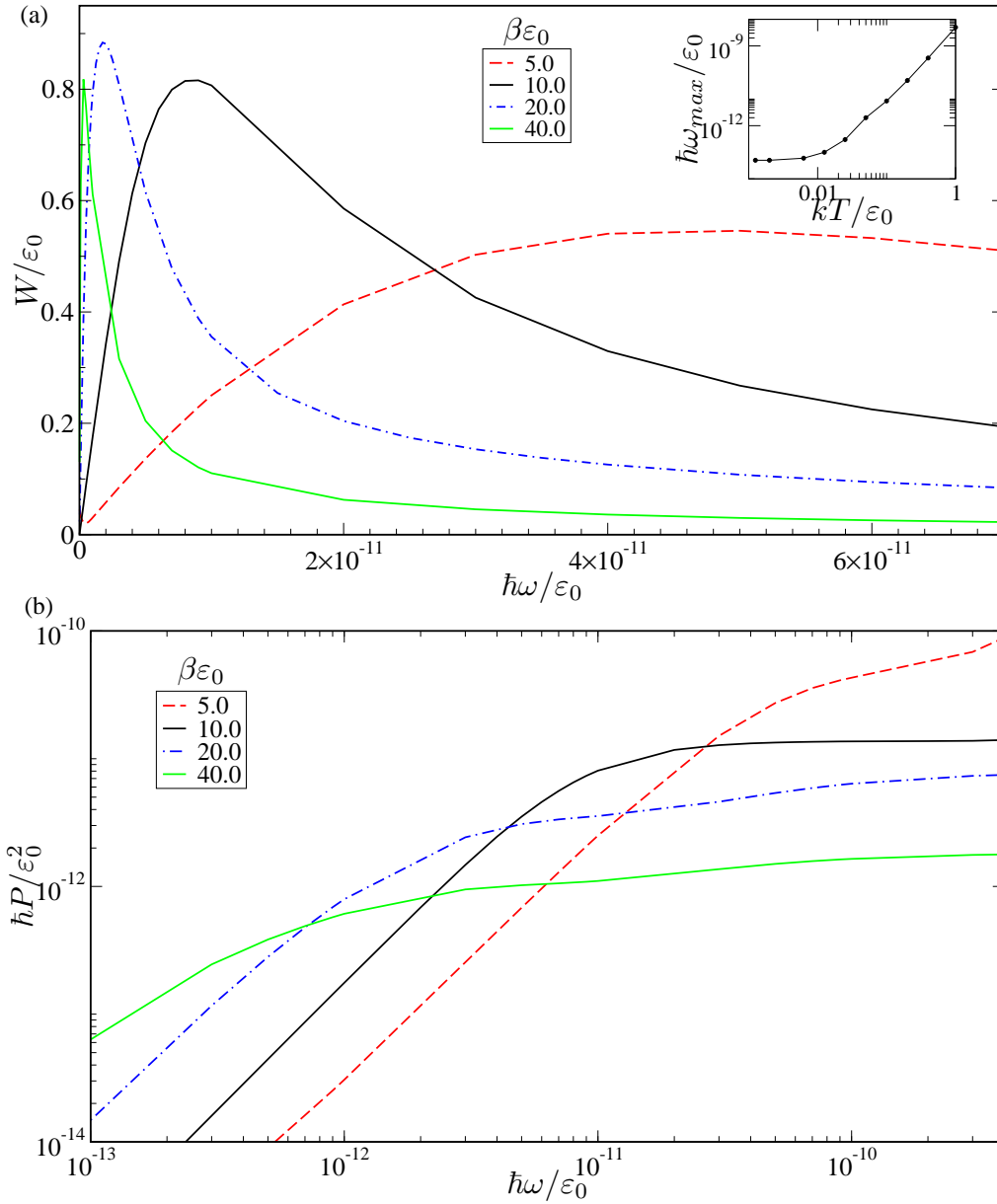
Figure 2.11: (a) Area of the hysteresis loop as a function of frequency for various values of β (see legend). Inset: Frequency of maximum area of the hysteresis loop as a function of the temperature T. (b) Dissipated power as a function of frequency for various values of β (see legend).

dissipation. We can see from the inset how the temperature dependence of the maximum dissipation frequency is compatible with the T-dependence of Γ (2.44).

Overall we can state that the dissipation mechanism we proposed satisfies all the prerequisites that were missing in the other models considered: it is clearly spin-dependent, unlike many other dissipation mechanisms usually considered in AFM experiments, it works down to low frequencies, which as shown in 2.2 is not true for the most natural choice of dissipation through spin-waves; and finally it has the right order of magnitude to fit the experimental data. We are therefore inclined to believe that this is a mechanism taking place in the MExFM experiment on NiO.

Chapter 3

Dissipative Quantum Pumping

In this chapter we consider another nanoscopic problem, this time electronic, and its behavior in presence of dissipation. This problem enters the general category of quantum pumping (QP): we refer to QP whenever we are forcing quantum particles through a system with a cyclic process, obtaining a direct current as a result. The case we will take into account, in which QP is performed in a circular system, is often referred to as quantum stirring. In section 3.1 we will describe the simple three-site model we will consider in our further treatment and the real systems it can describe, we will present the solution for the isolated system and a comparison to known results from the standard QP theory. We will then introduce in section 3.2 the presence of a bath to account for dissipation, showing how under quite general approximations the system can still be solved analytically and observing some interesting changes occurring in the system due to this coupling [4], we will then briefly explore some a possible experimental implementation.

3.1 Quantum Pumping in Three-Site Systems

3.1.1 From Three Sites to Two States

We will start by considering a model composed of three sites in a ring structure, as schematically represented in Fig. 3.1. We will consider two possible systems characterized by this structure that can be reduced to the same two-level Hamiltonian.

The most straightforward system showing these characteristics is a triple quantum dot, where all dots are interconnected in a ring structure. The experimental realization of such geometry is known to be feasible [28] and will be further investigated in section 3.2. We indicate with ϵ_i the external
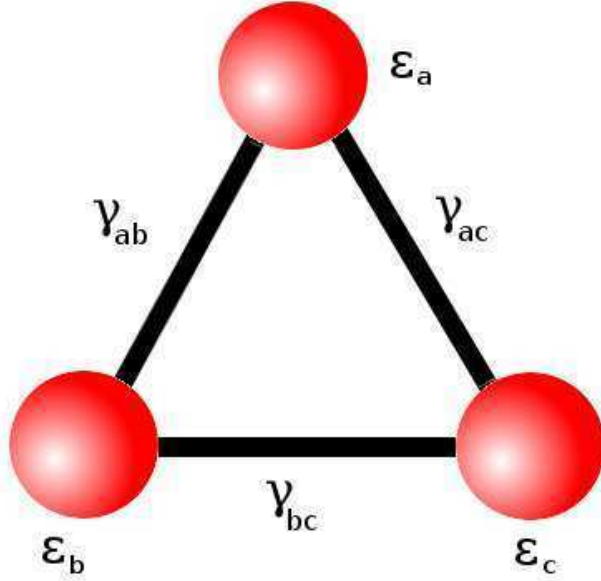
Figure 3.1: Schematic representation of the three-site model.

bias applied to each single-orbital dot i, and with γ_{ij} the hopping amplitude for an electron to jump between sites i and j. The Hamiltonian

$$
\mathcal{H}_0 = \begin{pmatrix} \epsilon_a & -\gamma_{ab} & -\gamma_{ac}^* \\ -\gamma_{ab}^* & \epsilon_b & -\gamma_{bc} \\ -\gamma_{ac} & -\gamma_{bc}^* & \epsilon_c \end{pmatrix} \tag{3.1}
$$

describes the one-electron dynamics. Without loss of generality, we can set $\sum_i \epsilon_i = 0$.

This Hamiltonian can be easily diagonalized in the fully symmetric case of equal hoppings $\gamma_{ij} = \gamma_0$ and energies $\epsilon_a = \epsilon_b = \epsilon_c = 0$, to give a ground state $|0\rangle = (|a\rangle + |b\rangle + |c\rangle)/\sqrt{3}$ with energy $-2\gamma_0$ and a degenerate doublet of excited levels with energy γ_0. We choose as a basis for the degenerate subspace

$$
\begin{cases} |x\rangle & = & \dfrac{|b\rangle - |c\rangle}{\sqrt{2}} \\[2mm] |y\rangle & = & \dfrac{2\,|a\rangle - |b\rangle - |c\rangle}{\sqrt{6}} \ . \end{cases} \tag{3.2}
$$

Neglecting electron-electron correlation effects, when three electrons occupy the system of the three quantum dots, two of them fill the state $|0\rangle$, and the third one remains free to move in the twofold-degenerate manifold $|x\rangle$, $|y\rangle$, which is therefore the one relevant for transport processes.

To act on this twofold degeneracy, experimentally the easiest way is to perturb the bias ϵ_i at each site. We can consider the perturbing Hamiltonian in the $|0\rangle$, $|x\rangle$, $|y\rangle$ basis:

$$
\mathcal{H}_{\text{bias}} = \begin{pmatrix} 0 & \frac{1}{\sqrt{6}}(\epsilon_b - \epsilon_c) & \frac{1}{\sqrt{2}}\epsilon_a \\ \frac{1}{\sqrt{6}}(\epsilon_b - \epsilon_c) & -\frac{1}{2}\epsilon_a & \frac{1}{2\sqrt{3}}(\epsilon_c - \epsilon_b) \\ \frac{1}{\sqrt{2}}\epsilon_a & \frac{1}{2\sqrt{3}}(\epsilon_c - \epsilon_b) & \frac{1}{2}\epsilon_a \end{pmatrix} . \tag{3.3}
$$

As long as the deviation from the unbiased system can be treated as a small perturbation with respect to the gap $3\gamma_0$, admixtures of state $|0\rangle$ produce negligible effects within the $|x\rangle$, $|y\rangle$ doublet. We can therefore restrict the treatment to the $|x\rangle$, $|y\rangle$ subspace. Here, the perturbing Hamiltonian takes the form:

$$
\mathcal{H}_{\text{QD}} = -\frac{1}{2\sqrt{3}} \begin{pmatrix} \sqrt{3}\epsilon_a & \epsilon_b - \epsilon_c \\ \epsilon_b - \epsilon_c & -\sqrt{3}\epsilon_a \end{pmatrix} . \tag{3.4}
$$

To realize the pumping (or stirring), we can cycle the external potentials according to

$$
\begin{cases} \epsilon_a(t) &= -\hbar\Delta\cos(\omega t) \\ \epsilon_b(t) &= -\hbar\Delta\cos\left(\omega t - \frac{2\pi}{3}\right) \\ \epsilon_c(t) &= -\hbar\Delta\cos\left(\omega t + \frac{2\pi}{3}\right) \end{cases} \tag{3.5}
$$

and, since the system is now equivalent to a spin-$\frac{1}{2}$, this reduces it to the two-level Hamiltonian:

$$
\mathcal{H}_S(t) = \frac{\hbar\Delta}{2}\left[\cos(\omega t)\sigma^z + \sin(\omega t)\sigma^x\right] , \tag{3.6}
$$

where we have used the Pauli matrices σ^z and σ^x. This is the Hamiltonian we will consider in our further treatment.

The second system that can be reduced to the same Hamiltonian is the molecular trimer: we consider a molecule such as H_3, Li_3 or Na_3 and its valence electronic states [29]. In this case, driving is achieved through the excitation of "rotating" vibrational modes and acts through the degenerate electron-vibration interaction, of the Jahn-Teller "$e \otimes E$" type [30].

A standard tight-binding model [31] provides a basic and fairly realistic picture of the molecular electronic structure. The relevant tight-binding Hamiltonian reads exactly like Eq. (3.1). A trimer of equal atoms has identical on-site energy $\epsilon_a = \epsilon_b = \epsilon_c = 0$.

To realize the pumping in this system, we change in time the hopping integrals γ_{ij}. The equilateral molecular geometry has identical hopping integrals $\gamma_{ij} = \gamma_0$, in these conditions the spectrum consists again of a singlet

ground state at energy $-2\gamma_0$ plus a twofold degenerate excited state at energy γ_0 as before. But upon molecular distortion, these overlaps may be assumed to change with distance approximately as

$$\gamma_{ij} \simeq \gamma_0 e^{-\kappa(d_{ij}-u_0)} , \qquad (3.7)$$

where d_{ij} is the instantaneous distance between atoms i and j, and u_0 is the equilibrium separation in the equilateral geometry.

To obtain time-dependent hoppings, we can consider the perturbation to the electronic levels induced by the a small-amplitude excitation of the vibrational modes of the trimer: excluding the uniform dilation, which does not split the degeneracy, the remaining two vibrational normal modes are degenerate in frequency. The associated atomic displaced positions can be described in terms of two normal coordinates Q_x and Q_y as follows:

$$\begin{cases} \mathbf{R}_a = (0,1)\dfrac{u_0}{\sqrt{3}} + \left(\dfrac{1}{\sqrt{3}},0\right)Q_x + \left(0,\dfrac{1}{\sqrt{3}}\right)Q_y \\[2mm] \mathbf{R}_b = -\left(\dfrac{\sqrt{3}}{2},\dfrac{1}{2}\right)\dfrac{u_0}{\sqrt{3}} - \left(\dfrac{1}{2\sqrt{3}},\dfrac{1}{2}\right)Q_x + \left(\dfrac{1}{2},-\dfrac{1}{2\sqrt{3}}\right)Q_y \\[2mm] \mathbf{R}_c = \left(\dfrac{\sqrt{3}}{2},-\dfrac{1}{2}\right)\dfrac{u_0}{\sqrt{3}} + \left(-\dfrac{1}{2\sqrt{3}},\dfrac{1}{2}\right)Q_x - \left(\dfrac{1}{2},\dfrac{1}{2\sqrt{3}}\right)Q_y \end{cases} \qquad (3.8)$$

The modified atomic positions result in modified overlap integrals estimated by substituting $d_{ij} = |\mathbf{R}_i - \mathbf{R}_j|$ into Eq. (3.7). We can compute the electron-phonon linear coupling by linearizing the coupling term for small Q_i. We obtain the following overlaps:

$$\begin{cases} \gamma_{ab} \simeq \gamma_0\left(1 - \kappa\dfrac{\sqrt{3}}{2}Q_x - \kappa\dfrac{1}{2}Q_y\right) \\[2mm] \gamma_{bc} \simeq \gamma_0\left(1 + \kappa Q_y\right) \\[2mm] \gamma_{ac} \simeq \gamma_0\left(1 + \kappa\dfrac{\sqrt{3}}{2}Q_x - \kappa\dfrac{1}{2}Q_y\right) \end{cases} \qquad (3.9)$$

The resulting Hamiltonian for perturbatively small displacement can be represented in the $|0\rangle$, $|x\rangle$, $|y\rangle$ basis by:

$$\mathcal{H}_{\text{lin}} = \gamma_0 \begin{pmatrix} -2 & \frac{1}{\sqrt{2}}\kappa Q_x & \frac{1}{\sqrt{2}}\kappa Q_y \\ \frac{1}{\sqrt{2}}\kappa Q_x & 1 + \kappa Q_y & \kappa Q_x \\ \frac{1}{\sqrt{2}}\kappa Q_y & \kappa Q_x & 1 - \kappa Q_y \end{pmatrix} . \qquad (3.10)$$

We can further restrict this linearized Hamiltonian to the $|x\rangle$, $|y\rangle$ subspace, where it takes the form:

$$\mathcal{H}_{\mathrm{MT}} = \kappa\gamma_0 \begin{pmatrix} Q_y & Q_x \\ Q_x & -Q_y \end{pmatrix} , \tag{3.11}$$

where we have omitted the trivial shift by γ_0.

Assuming to be able to excite a classical motion of the vibrational degrees of freedom, and choosing a time-dependent rotating combination of these vibrations with amplitudes

$$\begin{cases} Q_x &= \dfrac{\hbar\Delta}{2\kappa\gamma_0} \sin(\omega t) \\[2mm] Q_y &= \dfrac{\hbar\Delta}{2\kappa\gamma_0} \cos(\omega t) \end{cases} \tag{3.12}$$

we recover the pumping Hamiltonian in the form (3.6).

Since we want to estimate the pumping in the system, we need to find the operator corresponding to the current circulating in the ring structure. To do so, the simplest way is to consider the current between two sites, e.g. a and b, as:

$$I_{ab} = -iq\gamma_{ab} \left(c_b^\dagger c_a - c_a^\dagger c_b \right) , \tag{3.13}$$

where the $c_i^\dagger$ and c_i are creation and annihilation operators at site i and q is the charge. Applying the previous change of basis, we can therefore write I_{ab} in the $|0\rangle$, $|x\rangle$, $|y\rangle$ basis as:

$$I_{ab} = iq\gamma_{ab} \begin{pmatrix} 0 & \frac{1}{\sqrt{6}} & \frac{1}{\sqrt{2}} \\ -\frac{1}{\sqrt{6}} & 0 & -\frac{1}{\sqrt{3}} \\ -\frac{1}{\sqrt{2}} & \frac{1}{\sqrt{3}} & 0 \end{pmatrix} \tag{3.14}$$

which, restricted to the subspace $|x\rangle$, $|y\rangle$ and for fixed hopping γ_0, simply reads

$$I_{ab} = \frac{q\gamma_0}{\sqrt{3}} \begin{pmatrix} 0 & -i \\ i & 0 \end{pmatrix} = I_0\sigma^y , \tag{3.15}$$

with $I_0 = q\gamma_0/\sqrt{3}$. The quantity $\langle\sigma^y(t)\rangle$ will therefore be the one we will be measuring to estimate the current pumped in the system.

3.1.2 Solution for the Isolated System

We will now show the exact solution of the Hamiltonian (3.6). While one could clearly tackle the problem directly, a clever change of basis can make

the problem particularly easy: let us consider the operator

$$R_t = e^{-i\omega t \sigma^y/2} = \mathbb{I}\cos(\omega t/2) - i\sigma^y \sin(\omega t/2) \ , \tag{3.16}$$

representing a rotation of frequency ω around the y axis. If we apply this operator to the Hamiltonian we obtain:

$$\tilde{H}_S = R_t^{-1}\mathcal{H}_S(t)R_t = \frac{\hbar\Delta}{2}\sigma^z \ , \tag{3.17}$$

which is conveniently time-independent. Since our transformation is time-dependent, the states $|\tilde{\psi}(t)\rangle = R_t^{-1}|\psi(t)\rangle$ in the rotated frame obey a modified Schrödinger equation (due to the derivative of R_t):

$$i\hbar\frac{\partial}{\partial t}|\tilde{\psi}\rangle = \left[\tilde{\mathcal{H}}(t) - \frac{\hbar\omega}{2}\sigma^y\right]|\tilde{\psi}\rangle \ . \tag{3.18}$$

We can take into account this new term in the Schrödinger equation by considering a new effective Hamiltonian

$$\tilde{\mathcal{H}}_{\text{eff}} = \tilde{\mathcal{H}}_S - \frac{\hbar\omega}{2}\sigma^y = \frac{\hbar\Delta}{2}\sigma^z - \frac{\hbar\omega}{2}\sigma^y = \frac{\hbar\omega'}{2}\hat{\mathbf{n}}\cdot\vec{\sigma} \ , \tag{3.19}$$

where $\omega' = \sqrt{\Delta^2 + \omega^2}$, and $\hat{\mathbf{n}}$ is a versor in spin space with components $\hat{\mathbf{n}} = (0, -\omega/\omega', \Delta/\omega')$. It is trivial to solve this Hamiltonian, since the eigenstates are simply spin states directed along $\pm\hat{\mathbf{n}}$, call them $|\pm\mathbf{n}\rangle$, and have energies $\pm\hbar\omega'/2$.

We notice that the current operator σ^y is not affected by the rotation R_t since it is parallel to the rotation axis: this means that the observable we are interested in is still time-independent. It is also straightforward to estimate the current on the eigenstates of the effective Hamiltonian:

$$\langle\pm\hat{\mathbf{n}}|\sigma^y|\pm\hat{\mathbf{n}}\rangle = \mp\frac{\omega}{\omega'} \ . \tag{3.20}$$

If we start from the ground state of the original Hamiltonian:

$$|\tilde{\psi}(0)\rangle = R_t|-\hat{z}\rangle = \sin\left(\frac{\theta}{2}\right)|+\hat{\mathbf{n}}\rangle + \cos\left(\frac{\theta}{2}\right)|-\hat{\mathbf{n}}\rangle \ , \tag{3.21}$$

with $\theta = \arccos(\Delta/\omega')$, we get the current as a function of time as

$$\begin{aligned}
\langle\tilde{\psi}(t)|\sigma^y|\tilde{\psi}(t)\rangle = \ & \sin^2\left(\frac{\theta}{2}\right)\langle+\mathbf{n}|J|+\mathbf{n}\rangle + \cos^2\left(\frac{\theta}{2}\right)\langle-\mathbf{n}|J|-\mathbf{n}\rangle \\
& - \sin\left(\frac{\theta}{2}\right)\cos\left(\frac{\theta}{2}\right)\left(e^{-i\omega't}\langle+\mathbf{n}|J|-\mathbf{n}\rangle + c.c.\right) \ .
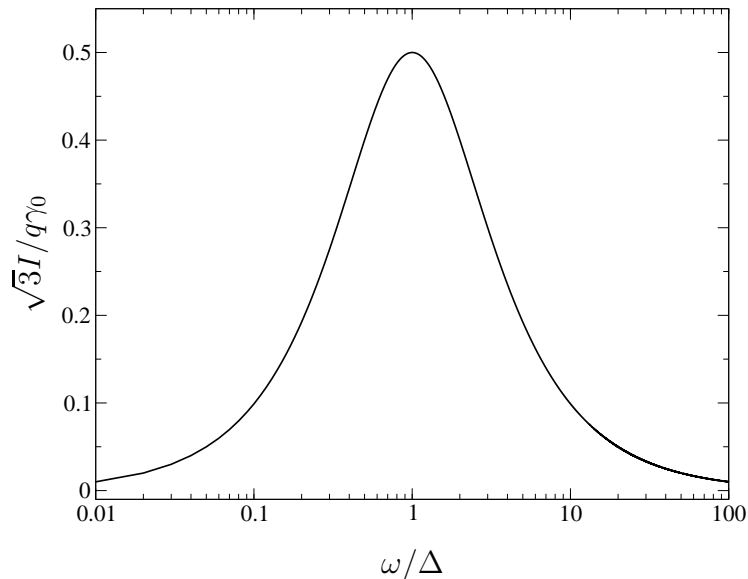\end{aligned} \tag{3.22}$$

Figure 3.2: DC current as a function of the pumping frequency as per Eq. (3.23).

This expression has a constant and an oscillating part. Since we are interested in the DC component due to pumping we can concentrate on the first two terms and get

$$J = \frac{\omega}{\omega'} \cos\theta = \frac{\omega\Delta}{\omega'^2} \ . \tag{3.23}$$

The oscillating component coming from the last term would have a frequency ω' and an amplitude $\omega\Delta/\omega'^2$, but is not our main interest now.

The DC current as a function of the pumping frequency ω is shown if Fig. 3.2: we can clearly see that the maximum current $J = 0.5$ is obtained for $\omega = \Delta$. The maximum in the final current is due to the interaction of two different effects: for increasing frequencies the maximum theoretical current ω/ω' increases as the effective quantization axis $\hat{\mathbf{n}}$ gets closer to the y direction; on the other side our choice of initial condition $|\phi(0)\rangle = |-\hat{z}\rangle$ has a smaller projection on the y axis as the frequency increases, so that the DC current decreases. A different choice of initial conditions would lead to currents up to ω/ω'.

3.1.3 Standard Quantum Pumping

To consider our problem from a viewpoint closer to the standard quantum pumping literature, we will re-derive our result in a different formalism, as presented by Cohen in [32], specialized for our system.

Let us start by considering a magnetic field threading our three-sites system for a flux Φ (in units of the flux quantum Φ_0): we can include this in our Hamiltonian by updating the hopping terms as $\gamma_0 e^{\pm 2\pi\Phi/3}$ in (3.1), assuming the dots to be equally spaced. By passing to the $|x\rangle$, $|y\rangle$ basis (3.2) we obtain a term

$$
\mathcal{H}_\Phi = -\gamma_0 \begin{pmatrix} \cos\left(\dfrac{2\pi\Phi}{3}\right) & -i\sqrt{3}\sin\left(\dfrac{2\pi\Phi}{3}\right) \\ i\sqrt{3}\sin\left(\dfrac{2\pi\Phi}{3}\right) & \cos\left(\dfrac{2\pi\Phi}{3}\right) \end{pmatrix} . \tag{3.24}
$$

Incidentally, we can recover through this the expression for the current operator: by considering charge and flux as conjugate variables we get

$$
J = -\left.\frac{\partial \mathcal{H}}{\partial \Phi}\right|_{\Phi=0} = \frac{2\pi\gamma_0}{\sqrt{3}}\sigma^y , \tag{3.25}
$$

and dividing by 2π over the circumference and multiplying by the charge unit q (we consider here a probability current) we find again the expression (3.15).

Neglecting the diagonal term (which is just a simple shift) we can introduce this into the Hamiltonian (3.6) by adding a term coupled to σ^y:

$$
\mathcal{H}'_S(t) = \frac{\Delta}{2}\left[\cos(\omega t)\sigma^z + \sin(\omega t)\sigma^x\right] + \frac{D}{2}\sigma^y , \tag{3.26}
$$

with $D = \sqrt{3}\gamma_0 \sin(2\pi\Phi/3)$. Passing to the rotating frame of reference of Eq. (3.16), since σ^y is not affected we simply get:

$$
\tilde{\mathcal{H}}'_S(t) = \frac{\omega'}{2}\sigma^z + \frac{D}{2}\sigma^y , \tag{3.27}
$$

and a further rotation around $\tilde{x}$ gives us the final

$$
\hat{\mathcal{H}}'_S(t) = \frac{\sqrt{\omega'^2 + D^2}}{2}\sigma^z; . \tag{3.28}
$$

The eigenvalues of this Hamiltonian are trivially $E_\pm = \pm\frac{1}{2}\sqrt{\omega'^2 + D^2}$, and we can apply the inverse rotations to get the eigenvectors in the original basis:

$$
|\tilde{\pm}\rangle = e^{i\frac{\omega t}{2}}\left\{\left[\cos\frac{\omega t}{2}C_\pm \mp i\sin\frac{\omega t}{2}C_\mp\right]|\uparrow\rangle + \left[\sin\frac{\omega t}{2}C_\pm \pm i\cos\frac{\omega t}{2}C_\mp\right]|\downarrow\rangle\right\} , \tag{3.29}
$$

with $C_\pm = \sqrt{(\sqrt{\omega'^2 + D^2} \pm \omega'^2)/(2\sqrt{\omega'^2 + D^2})}$ and where the first term is added to insure the single-valuedness of the wavefunction over the ring.

The space spanned by this Hamiltonian can be parametrized by 3 quantities: we will choose $\theta = \omega t$ (which is the term we use to achieve our pumping, with one cycle being 2π long), ω' and Φ. Without entering too much into the detail of the theory (for which we refer to [32]), we will state that within linear response theory, and in the DC limit, the current is proportional to the derivative of the parameters through a tensor called the conductance matrix. In the basis and with the pumping of our choice, only the term in θ is different from zero, and in the adiabatic limit it can be expressed as:

$$B^\theta = \Im\, 2\left(\frac{\partial}{\partial\theta}\langle\hat{-}|\right)\left(\frac{\partial}{\partial\Phi}|\hat{-}\rangle\right)\,. \tag{3.30}$$

With this it becomes easy to calculate the pumped charge as

$$Q = \int_{\text{cycle}} I \mathrm{d}t = \int_0^{2\pi} B^\theta \mathrm{d}\theta = \frac{4\pi^2\gamma_0}{\sqrt{3}\Delta}\,, \tag{3.31}$$

where we have taken the $D \to 0$ limit since we work at $\Phi = 0$. We can compare this result with Eq. (3.23): multiplying by $2\pi/\omega$ to get the pumped charge, plus a further 2π for the circumference, and taking the adiabatic limit $\omega \to 0$ we find the two results to coincide exactly.

3.2 Quantum Pumping in Presence of a Bath

3.2.1 Master Equation Description

We will now turn back to the Hamiltonian (3.6) to investigate what happens if we introduce dissipation in the system by coupling it to a bosonic bath in the form

$$
\begin{aligned}
\mathcal{H} =\ &\overbrace{\frac{\hbar\Delta}{2}\left[\cos(\omega t)\sigma^z + \sin(\omega t)\sigma^x\right]}^{\mathcal{H}_S} + \\
&+ \underbrace{\sum_{\xi=z,x}\sum_\nu\left[\frac{p_{\xi,\nu}^2}{2m} + \frac{m\omega_\nu^2 q_{\xi,\nu}^2}{2}\right]}_{\mathcal{H}_B} + \underbrace{\sum_{\xi=z,x}\sum_\nu\sqrt{\frac{2m\omega_\nu}{\hbar}}\lambda_{\xi,\nu} q_{\xi,\nu}\sigma^\xi}_{\mathcal{H}_{SB}}\,,
\end{aligned}
\tag{3.32}
$$

where q, p, m and ω are position, momentum, mass and frequency of the oscillators of the baths, λ represents the coupling constant and the sum over ξ stands for the presence of two noninteracting baths, labeled z and x and

coupled through σ^z and σ^x, respectively. Both baths will be once more taken as Ohmic, with the usual spectral density (1.10):

$$J_\xi(\omega) = \sum_\nu \lambda_{\xi,\nu}^2 \delta(\omega - \omega_\nu) = \hbar^2 \alpha_\xi \omega e^{-\omega/\omega_c} \qquad (3.33)$$

Since we have seen how the system Hamiltonian is much better handled in the rotating frame of reference defined by R_t (3.16), we will rotate the complete Hamiltonian obtaining $\tilde{\mathcal{H}} = \tilde{\mathcal{H}}_{\text{eff}} + \mathcal{H}_B + \tilde{\mathcal{H}}_{SB}(t)$, where the first term is (3.19) and the last one is modified by rotating the spin operators as:

$$\begin{cases} \tilde{\sigma}^z(t) & = & R_t^{-1} \sigma^z R_t = \sigma^z \cos(\omega t) - \sigma^x \sin(\omega t) \\ \tilde{\sigma}^x(t) & = & R_t^{-1} \sigma^x R_t = \sigma^x \cos(\omega t) + \sigma^z \sin(\omega t) . \end{cases} \qquad (3.34)$$

We will handle this system through the ME formalism introduced in section 1.3. Let us recall Eq. (1.29) and specialize it for our Hamiltonian:

$$\begin{aligned} \frac{\partial \rho_S(t)}{\partial t} &\approx -i[\mathcal{H}_{\text{eff}}, \rho_S(t)] - \frac{1}{\hbar^2} \int_0^\infty d\tau \sum_{\xi,\eta} \\ &\quad \left\{ g_{\xi\eta}(\tau) \left[\sigma^\xi(t), U^\dagger(-\tau) \sigma^\eta(t-\tau) U(-\tau) \rho_S(t) \right] \right. \\ &\quad \left. + g_{\xi\eta}^*(\tau) \left[\rho_S(t) U^\dagger(-\tau) \sigma^\eta(t-\tau) U(-\tau), \sigma^\xi(t) \right] \right\} , \end{aligned} \qquad (3.35)$$

where the ξ and η summation runs over the x and z indexes of the baths and we have dropped the tilde to lighten the notation, though all quantities are intended in the rotated frame of reference. One must pay attention to the two different time-dependences of the system operators σ^ξ: the one given by the rotation R_t, referred to implicitly in the equation above, and the one given by the ME itself, here stated explicitly by the application of the operator

$$U(t) = e^{i\omega' \hat{\mathbf{n}} \cdot \vec{\sigma} t/2} = \cos(\omega' t/2) \mathbb{I} - i \sin(\omega' t/2) \hat{\mathbf{n}} \cdot \vec{\sigma} . \qquad (3.36)$$

Since the baths are independent and identical, we have $g_{\xi\eta}(\tau) = \delta_{\xi,\eta} g(\tau)$, where $g(\tau)$ is defined as in (1.11). To proceed, it is convenient to name the

possible integrals we will find:

$$
\begin{cases}
g_{cc} &= \displaystyle\int_0^\infty g(\tau)\cos(-\omega\tau)\cos(-\omega'\tau)d\tau \\[2ex]
g_{sc} &= \displaystyle\int_0^\infty g(\tau)\sin(-\omega\tau)\cos(-\omega'\tau)d\tau \\[2ex]
g_{cs} &= \displaystyle\int_0^\infty g(\tau)\cos(-\omega\tau)\sin(-\omega'\tau)d\tau \\[2ex]
g_{ss} &= \displaystyle\int_0^\infty g(\tau)\sin(-\omega\tau)\sin(-\omega'\tau)d\tau \\[2ex]
g_{c0} &= \displaystyle\int_0^\infty g(\tau)\cos(-\omega\tau)d\tau \\[2ex]
g_{s0} &= \displaystyle\int_0^\infty g(\tau)\sin(-\omega\tau)d\tau.
\end{cases}
\tag{3.37}
$$

It is also convenient to choose a basis more appropriate for the frame of reference of the effective Hamiltonian: defining the vector perpendicular to both $\hat{\mathbf{n}}$ and x as $\hat{\mathbf{m}} = (0, \Delta/\omega', \omega/\omega')$, we can define the new operators (obeying the standard Pauli matrices commutation relations):

$$
\begin{cases}
\sigma^x &= \hat{\mathbf{x}}\cdot\vec{\boldsymbol{\sigma}} \\
\sigma^m &= \hat{\mathbf{m}}\cdot\vec{\boldsymbol{\sigma}} \\
\sigma^n &= \hat{\mathbf{n}}\cdot\vec{\boldsymbol{\sigma}}.
\end{cases}
\tag{3.38}
$$

In terms of these quantities we can explicit the ME (3.35) as:

$$
\begin{aligned}
\frac{\partial\rho_S(t)}{\partial t} =\ & -i\frac{\omega'}{2}[\sigma^n,\rho_S] - \Bigg[C_t\sigma^x + S_t\left(\frac{\Delta}{\omega'}\sigma^n + \frac{\omega}{\omega'}\sigma^m\right), \\
& \left\{\frac{\Delta}{\omega'}(S_t g_{c0} + C_t g_{s0})\sigma^n + \right. \\
& + \left(C_t g_{cc} - S_t g_{sc} + \frac{\omega}{\omega'}S_t g_{cs}\frac{\omega}{\omega'}C_t g_{ss}\right)\sigma^x + \\
& + \left.\left(S_t g_{ss} - C_t g_{cs} + \frac{\omega}{\omega'}S_t g_{cc} + \frac{\omega}{\omega'}C_t g_{sc}\right)\sigma^m\right\}\rho_S\Bigg] + \text{c.c.} + \\
& + \Bigg[-S_t\sigma^x + C_t\left(\frac{\Delta}{\omega'}\sigma^n + \frac{\omega}{\omega'}\sigma^m\right), \left\{\frac{\Delta}{\omega'}(C_t g_{c0} + S_t g_{s0})\sigma^n + \right. \\
& + \left(-S_t g_{cc} - C_t g_{sc} + \frac{\omega}{\omega'}C_t g_{cs} - \frac{\omega}{\omega'}S_t g_{ss}\right)\sigma^x + \\
& + \left.\left(S_t g_{cs} + C_t g_{ss} + \frac{\omega}{\omega'}C_t g_{cc} - \frac{\omega}{\omega'}S_t g_{sc}\right)\sigma^m\right\}\rho_S\Bigg] + \text{c.c.},
\end{aligned}
\tag{3.39}
$$

with $C_t = \cos(\omega t)$ and $S_t = \sin(\omega t)$.

We can consider the generic density matrix $\bar{\rho}_S = \frac{1}{2}\left(\mathbb{I} + a\sigma^x + b\sigma^m + c\sigma^n\right)$ as we did in section 1.3 to cast the master equation in the more manageable form: after evaluating the commutators and regrouping the terms we get

$$
\begin{aligned}
\frac{\partial\bar{\rho}_S}{\partial t} &= \\
&= -2\left\{\left(\frac{\Delta^2}{\omega'^2}\Re g_{c0} + \frac{\omega}{\omega'}\Re g_{ss} + \frac{\omega^2}{\omega'^2}\Re g_{cc}\right)a + \left(\frac{\omega'}{4} + \frac{\omega}{\omega'}\Re g_{sc} - \frac{\omega^2}{\omega'^2}\Re g_{cs}\right)b\right. \\
&\quad + \frac{\Delta}{\omega'}\left(\Re g_{sc} - \frac{\omega}{\omega'}\Re g_{cs}\right)c + \frac{\Delta}{\omega'}\left(-\frac{\omega}{\omega'}\Im g_{c0} + \Im g_{ss} + \frac{\omega}{\omega'}\Im g_{cc}\right)\right\}\sigma^x + \\
&\quad -2\left\{\left(-\frac{\omega'}{4} - \frac{\omega}{\omega'}\Re g_{sc} + \Re g_{cs}\right)a + \left(\frac{\Delta^2}{\omega'^2}\Re g_{c0} + \Re g_{cc} + \frac{\omega}{\omega'}\Re g_{ss}\right)b + \right. \\
&\quad - \frac{\Delta}{\omega'}\left(\frac{\omega}{\omega'}\Re g_{cc} + \Re g_{ss}\right)c + \frac{\Delta}{\omega'}\left(\Im g_{s0} + \Im g_{sc} - \frac{\omega}{\omega'}\Im g_{cs}\right)\right\}\sigma^m + \qquad (3.40) \\
&\quad -2\left\{-\frac{\Delta}{\omega'}\Re g_{s0}a - \frac{\omega}{\omega'}\frac{\Delta}{\omega'}\Re g_{c0}b + \left(\frac{\omega^2 + \omega'^2}{\omega'^2}\Re g_{cc} + 2\frac{\omega}{\omega'}\Re g_{ss}\right)c\right. \\
&\quad + \left.\left(-2\frac{\omega}{\omega'}\Im g_{sc} + \frac{\omega^2 + \omega'^2}{\omega'^2}\Im g_{cs}\right)\right\}\sigma^n .
\end{aligned}
$$

This is a simple equation with constant coefficients, we can therefore easily find the equilibrium state of the system by setting all derivatives to 0. To get a final simple result, we will recall that this theory is valid in the weak coupling limit, and observe that, since all the g's are of order α, the a and b terms clearly vanish at zeroth order, while the c term goes to a finite value that we can estimate:

$$
c_{\text{eq}} = \frac{(\omega' - \omega)^2 J(\omega' + \omega) + (\omega' + \omega)^2 J(\omega' - \omega)}{(\omega' - \omega)^2 J(\omega' + \omega)\coth\dfrac{\hbar(\omega' + \omega)}{2k_B T} + (\omega' + \omega)^2 J(\omega' - \omega)\coth\dfrac{\hbar(\omega' - \omega)}{2k_B T}} .
$$
$$(3.41)$$

To recover the current we just need to project this state over the initial y direction, acquiring a ω/ω' factor (plus the I_0 prefactor to obtain a charge current). We can observe some quite simple behaviors in different limits: for $T \to 0$, irrespective of ω/Δ and of the form of the spectral density, the stationary master equation operator is a projector onto the ground state $|-\hat{\mathbf{n}}\rangle$ and the current is therefore the maximum ω/ω' of Eq. (3.20).

For finite temperature, in the adiabatic limit $\omega \ll \Delta$, the effects of the pumping should be minimal, and in fact we find

$$
J \simeq \frac{\omega}{\omega'}\tanh\frac{\hbar\Delta}{2k_{\text{B}}T} , \qquad (3.42)
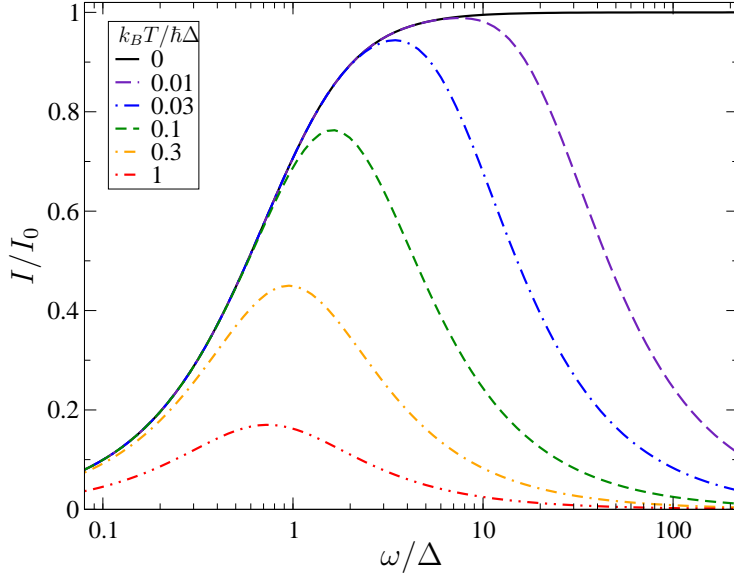$$

Figure 3.3: Steady-state DC circulating current I as a function of the pumping frequency ω. Solid line: $T = 0$ current, obtained by Eq. (3.20). Dashed and dot-dashed curves: pumped DC current for several temperatures, as obtained by the exact expression (3.41).

as is appropriate for a static Hamiltonian in thermal equilibrium.

Finally, in the high frequency antiadiabatic regime $\omega \gg \Delta$ we find a current

$$J \simeq \frac{\omega}{\omega'} \tanh \frac{\hbar(\omega' - \omega)}{2k_B T} . \tag{3.43}$$

This result is interesting, since it tells us that for fast driving, the spin reaches the thermal equilibrium of a static spin Hamiltonian characterized by an effective Larmor frequency

$$(\omega' - \omega) = \Delta \left[\frac{\Delta}{2\omega} + O\left(\frac{\Delta^3}{\omega^3} \right) \right] , \tag{3.44}$$

vanishing for large ω. The current, which coincides with the theoretical maximum for all large frequencies at $T = 0$, decays eventually at any finite T for large enough ω, as shown in Fig. 3.3. Faster and faster driving at finite temperature enhances the pumped current up to $\omega \simeq \hbar \Delta^2 / k_B T$. For larger driving frequencies, thermal fluctuations catch up and suppress J causing the pumped current to drop.

The reason why $(\omega' - \omega)$ determines the Boltzmann occupancy of the two levels split by $\hbar \omega'$ may be traced to the $-\omega \cdot \mathbf{M}$ term to be included in the thermodynamically relevant functions for a body rotating at frequency ω,

see e.g., §26 of Ref. [33], where $\mathbf{M}$ is the body angular momentum which, for our spin, coincides with $\hbar\boldsymbol{\sigma}$. This basically makes the energies of the spin states, as seen from the bath, be renormalized by a factor $-\hbar\omega$, and the equilibrium reached is changed accordingly. This effect is quite intuitive for the very high frequency limit where σ^n almost coincides with σ^y: shifting to the frame of reference where the bath is at rest is a rotation around the y axis with frequency ω, which in this limit clearly introduces the effective factor $-\hbar\omega$.

3.2.2   Numerical Results

While finding analytical results is quite elegant, it is nevertheless always useful to compare them with some numerical simulations, for the possibility to relax some approximations or, as in this case, to obtain information on the evolution rather than only on the asymptotic state. To this purpose, we numerically integrated Eq. (3.39) using the Runge-Kutta algorithm [27] for different values of α, T and ω: the first due check is that the system actually reaches the predicted asymptotic state. In Fig. 3.4 we can see the match of the asymptotic states found by simulating the whole evolution with the analytic solution of Eq. (3.41), already shown in Fig. 3.3. We find indeed a quite good agreement, with small discrepancies mainly due to the accumulation of numerical errors in the longer evolutions and the approximation of integrals.

Another opportunity of numerical integration is getting a better insight on the time-evolution of the system, as can be seen in Fig. 3.5. We can clearly observe how the presence of the bath leads to damped oscillations towards the asymptotic state. The relaxation time needed to reach the steady state is found to be decreasing with α, as could be expected, but also depending on the temperature, with lower temperature baths generally taking a longer time to equilibrate the system.

The final aspect we investigated numerically is the possibility of an anisotropic coupling to the bath, meaning the coefficients λ_ξ are different for the x and z direction. The result is shown in Fig. 3.6: the evolution does not completely damp the oscillations in the case of asymmetric baths, but goes to a steady oscillating state with frequency 2ω and amplitude growing with the anisotropy parameter. It can anyway be shown both numerically and analytically (by averaging out the oscillations in the asymmetric equivalent of Eq. (3.39)) that in the limit $\alpha_\xi \to 0$ (while keeping constant anisotropy) the oscillation amplitude goes to 0 and the zeroth order symmetric result (3.41) is recovered.
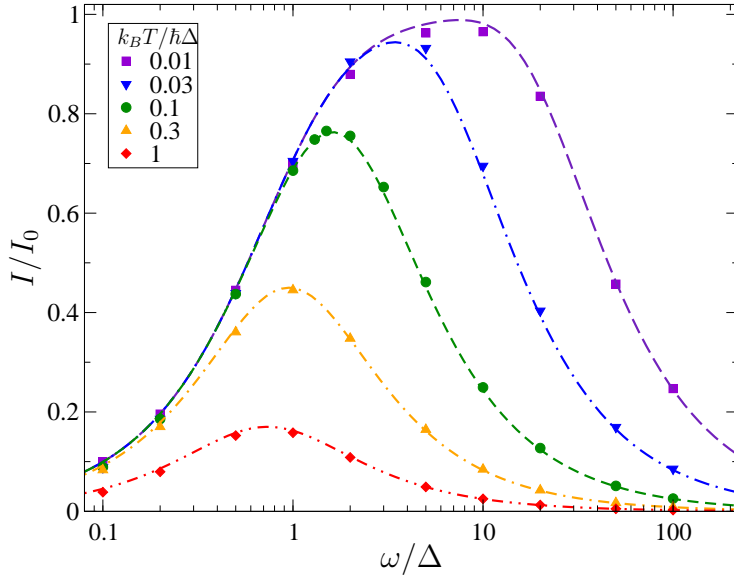
Figure 3.4: Asymptotic current I as a function of the pumping frequency ω. Curves: analytical results as obtained by the exact expression (3.41). Points: steady state of numerical simulations.

3.2.3 Experimental Feasibility

Quantum pumping is nowadays achievable at the experimental level in nanoscopic structures. We now ask ourselves whether the triple quantum dot setup we considered is realistic and the current we calculated measurable.

If we look at state-of-the-art quantum dot experiments, we can find realizations of triple quantum dots in a ring structure based on two-dimensional electron gas depleted by metallic gates [34, 35] as shown in the original Fig. 3.7. While the main focus of these experiments is charge transfer *through* the quantum dots, the same apparatus could in principle be used in a different setup, carefully changing the gate voltage to achieve the cyclic potential modulation we considered. In fact the presence of a state where changing only two gate potential can push the only excess electron in any of the three potential minima has been shown in [34].

We will therefore take this experiment as our reference to calculate the current which could be induced by our pumping. Starting from the observation of a 30 mT periodicity in the current when the ring is subject to an external magnetic field (due to Aharanov-Bohm effect), the estimated effective radius of the ring is $r_{\text{eff}} \simeq 200$ nm (compatible with the measured size of the system). To calculate the current, we need to know the entity of the hopping γ_0 between the dots: both experimental results [35] and an extensive
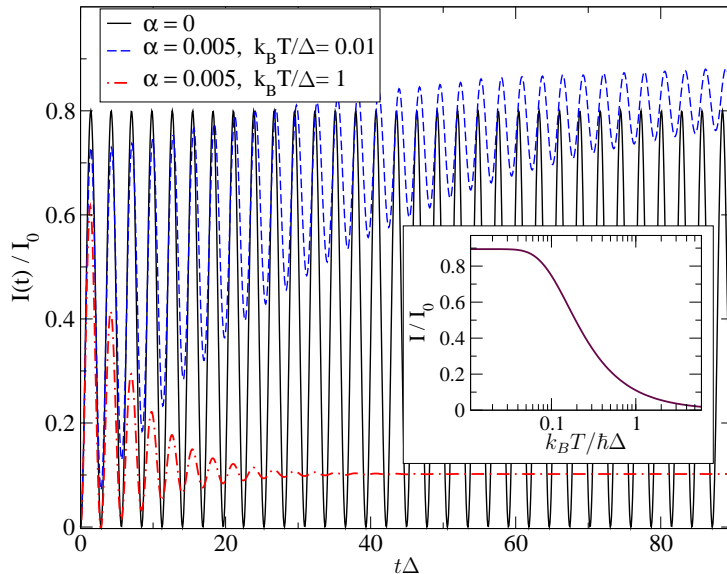
Figure 3.5: Time evolution of the current $I(t)$ for $\omega = 2\Delta$, in the dissipationless case ($\alpha = 0$, solid curve), and in the transient induced by weak dissipation ($\alpha = 0.005$), at low (dashed) and intermediate temperature (dot-dashed), starting from the initial $|-\hat{z}\rangle$ state. Inset: temperature dependence of the steady-state dc current I.

theoretical treatment [36] agree on a value $\gamma \simeq 0.05$ meV. From this we can easily calculate the maximum current using Eq. (3.15):

$$I_{\max} = \frac{e\gamma_0}{\sqrt{3}\hbar} \simeq 8\,\text{nA} \, , \tag{3.45}$$

where e is the electron charge.

We can now imagine to measure this current from the magnetic field it generates through the triple quantum dot (other measurement possibilities exist involving the use of a further lead, but they seem less applicable and more likely to perturb the system in such a complicated setup). We can imagine to measure this current through a Superconducting Quantum Interference Device (SQUID): we will model this as a ring with a 5 μm radius placed 5 μm over our system. All we need to do is calculate the flux though the SQUID of a 8 nA current circulating in a 200 nm ring. We know the flux can be calculated as $\Phi = \int_\Sigma \vec{A} \cdot d\vec{l}$, where Σ is the SQUID circuit and $\vec{A}$ the vector potential generated by the current. A simple integral yields the desired result $\Phi \simeq 4 \cdot 10^{-17}$ Wb, which corresponds to $0.02\,\Phi_0$ in terms of the flux quantum.

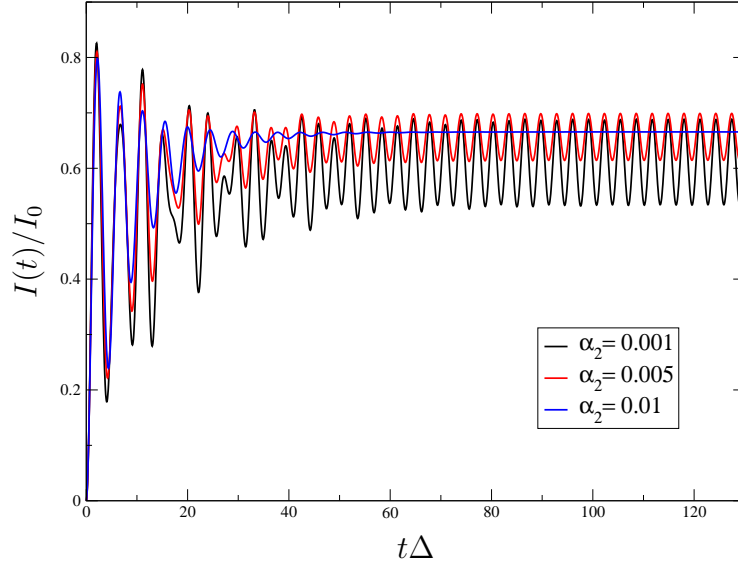Measurements of magnetic fields much smaller than $0.02\,\Phi_0$ are known

Figure 3.6: Time evolution of the current $I(t)$ for $\omega = \Delta$, $k_B T/\hbar\Delta = 0.1$ and two different bath couplings: $\alpha_1 = 0.01$ and three different α_2.

to be entirely feasible, so even accounting for some inaccuracy in our estimate we are confident that the effect we described could soon be observed experimentally, offering the intriguing possibility to investigate the effects of the unavoidable coupling to external sources of noise and compare it to our theory.
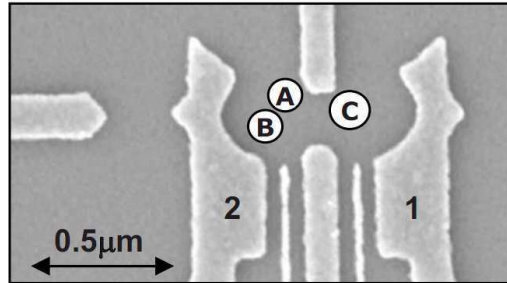

Figure 3.7: Experimental setup of a triple quantum dot. Reproduced from [35]

Chapter 4

Friction in Quantum-Classical Systems

In this chapter we will present another model for the description of dissipative systems which has been investigated, but for various reasons could not be brought to a complete description. The general idea is an attempt to explore a simple dissipative system where both a classical and a quantum description could be fully achieved, with the ultimate aim of finding some intrinsically quantum contribution to dissipation. The method employed, which will be briefly explained, is a known procedure for quantum-classical systems, which unfortunately proved computationally too heavy for a simple handling of the system. Although incomplete, we hope this idea, in line with the rest of the material presented, proves interesting for the reader and have a chance to be further expanded in the future.

The idea for this model came from an experiment by the R. Carpick group [37], where a nanoscale tip is slid over hydrogen- and deuterium-terminated single-crystal diamond and silicon surfaces in a contact-mode AFM experiment. The measured friction shows a clear dependence on the nature of the adsorbed atoms: specifically the hydrogen-terminated surface results in a higher friction (see Fig. 4.1). This effect is explained in terms of the different damping related to different masses which in turn translates in a different energy dissipation. Although this mechanism is consistent with the experiment, one is led to wonder if some specifically quantum effect could be observed when light particles like H or D are perturbed at low enough T.

Models of single impurities coupled to chains and baths are known in literature [38], but mainly in classical terms and rarely with a specific attention to frictional effects. Moreover the introduction of a quantum degree of freedom makes things more complicated: a complete quantum description, while optimal in principle, is clearly not feasible in a system governed by many
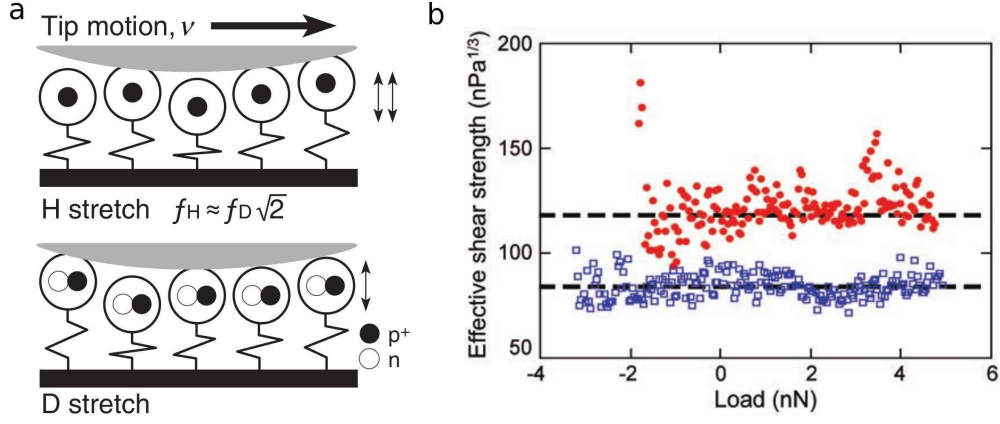
Figure 4.1: **a** Schematic representation of the experimental setup; **b** Measured effective shear strength for hydrogen (solid red dots) and deuterium (open blue squares) coated surfaces. Reproduced from [37].

different timescales; we therefore explore the option of a hybrid quantum-classical description of our system, in an effort to extrapolate the relevant physics. To further reduce the complexity of the model, we will consider a single quantum impurity attached to a classical atom chain, and we will mimic the effect of the nanoscale tip through a last classical atom slowly oscillating over the quantum particle.

The proposed model, shown in Fig.4.2, is composed of a big tip M governed by an external force $F(t)$, connected to a chain of smaller oscillators m_i through a much lighter particle μ, held in place by its own transverse potential, which we will regard as our quantum degree of freedom. The net effect of the movement of the tip (in the transverse direction) should be a sort of time-dependent double-well potential for the quantum particle: as the tip oscillates the light atom is pushed left and right, while having to avoid the position right under the tip. This effective double-well is the prototypical model for Caldeira-Leggett-like systems [7], but since we expect many levels to be involved in the dynamics, no simple treatment in terms of a spin-$\frac{1}{2}$, as presented in chapter 2, can be applied.

The model is described by the following Hamiltonian:

$$
\begin{aligned}
\mathcal{H}_{tot} = & \; \frac{P_0^2}{2M} + \frac{\hat{p}^2}{2\mu} + \sum_{i=1}^{N} \frac{P_i^2}{2m_i} + V_T(R_0, t) + \mathcal{H}_{TQ}(R_0, \hat{q}) + \\
& + V_Q(\hat{q}) + \mathcal{H}_{QS}(\hat{q}, R_1) + V_S(R_i, \dots, R_n) + \\
& + \mathcal{H}_{SB}(R_n, R_{n+1}) + V_B(R_{n+1}, \dots, R_N),
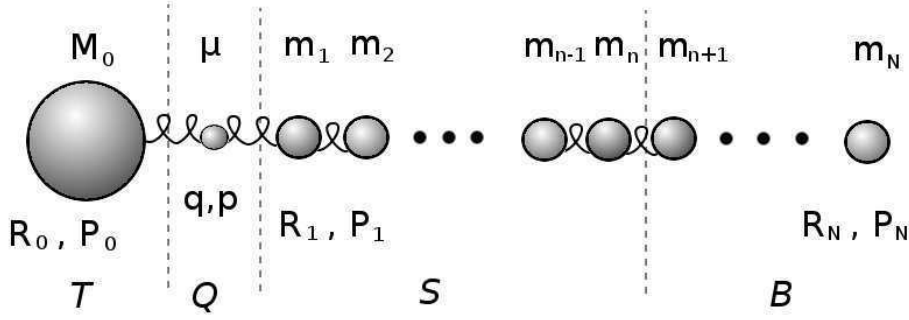\end{aligned}
\tag{4.1}
$$

Figure 4.2: The system under investigation: a quantum particle Q connected to a classical system S (and bath B) and under the effect of a classical tip T.

where we have divided the system in four components

- The tip T of mass M and coordinates $\{R_0, P_0\}$

- The quantum particle Q of mass μ and coordinates $\{\hat{q}, \hat{p}\}$

- The first n oscillators S of masses m_i and coordinates $\{R_i, P_i\}_{i=1..n}$

- The remaining $N - n$ oscillators B of coordinates $\{R_i, P_i\}_{i=n+1..N}$ and masses m_i

and the various terms represent the kinetic component of each part, its external potential (where needed to hold it in place in the transverse direction) and internal couplings V_X and the interaction terms among them $\mathcal{H}_{XY}$. In particular for the external force $F(t) = -\partial V_T(R_0, t)/\partial R_0$ it the driving transverse perturbation.

The reason for dividing the oscillators in two parts is to allow for the possibility of treating some of them explicitly while transforming the rest in an effective bath later in the calculation following one of the many simplifying schemes to remove this kind of degrees of freedom [39].

The easiest and most direct way to tackle a quantum-classical problem would be in the direction of the so-called Ehrenfest dynamics. In this method the classical and quantum subsystems are evolved according to their respective Hamiltonians with the interaction term taking the instantaneous classical values for the quantum system and the average over the quantum wavefunction of the coupling observable for the classical system. For example for a two-level system coupled to some classical degrees of freedom $\{q, p\}$ and described by the wavefunction $\psi(t) = c_\alpha(t)\alpha_q + c_\beta(t)\beta_q$, where α_q and β_q are

the instantaneous eigenfunctions of the Hamiltonian with eigenvalues ε_α and ε_β, the time evolution would be given by

$$\frac{\mathrm{d}c_{\alpha,\beta}(t)}{\mathrm{d}t} = -\frac{i}{\hbar}\varepsilon_{\alpha,\beta}c_{\alpha,\beta} \mp \dot{q}d_{\alpha\beta}c_{\beta,\alpha}, \tag{4.2}$$

with $d_{\alpha\beta} = \langle\alpha_q|\nabla_q\beta_q\rangle$. Conversely, the evolution of the classical degrees of freedom would be modified with the instantaneous expectation value of the quantum system like, e.g.,

$$\dot{p} = \frac{\partial V(q)}{\partial q} - (\varepsilon_\beta - \varepsilon_\alpha)d_{\alpha\beta}(c_\alpha^* c_\beta + c_\beta^* c_\alpha), \tag{4.3}$$

depending on the shape of the coupling [40].

While this is a reasonable first approximation if we want to deal with wavefunctions, it does not behave well for a system that is supposed to thermalize to the right statistical description in terms of a density matrix. The reason behind this is that the evolution of the quantum state is ultimately determined simply by a time-dependent Hamiltonian, so that a pure state can never evolve into a mixed state and achieve the right thermal equilibrium.

In order to find a more complete description of quantum-classical dynamics, able to achieve the correct thermodynamic state, we will follow a more general procedure for mixed quantum-classical systems introduced by Kapral [41]: we will start from a completely quantum description of the system and convert some degrees of freedom to their classical equivalent through a Wigner transformation, this will allow us to keep the interesting physics and in some reasonable limit obtain a manageable expression.

Let us consider just the Q and S parts of our model as a single quantum system described by a density matrix $\rho(t)$ starting from a factorized initial state $\rho(0) = \rho_Q(0) \otimes \rho_S(0)$. A Wigner transformation over the S degrees of freedom is defined as

$$\rho_W(R_i, P_i, t) = \frac{1}{(2\pi\hbar)^n} \int \prod_{i=1}^n dy_i e^{iP_i y_i/\hbar} \left\langle R_i - \frac{y_i}{2}\middle| \rho(t) \middle| R_i + \frac{y_i}{2}\right\rangle \tag{4.4}$$

and it obeys an equivalent of the Liouville equation:

$$\frac{\mathrm{d}\rho_W(R_i, P_i, t)}{\mathrm{d}t} = -\frac{i}{\hbar}\left(H_W e^{-i\hbar\Lambda/2}\rho_W - \rho_W e^{-i\hbar\Lambda/2}H_W\right) \tag{4.5}$$

where H_W is the Wigner transform of the Hamiltonian and $\Lambda = \overleftarrow{\nabla}_P \cdot \overrightarrow{\nabla}_R - \overleftarrow{\nabla}_R \cdot \overrightarrow{\nabla}_P$ is an operator similar in spirit to the Poisson bracket.

If now consider the m_i masses of the S system to be much bigger than the μ mass of the Q system, we can justify the classical treatment of the former

with respect to the latter and write the evolution as a quantum-classical Liouville equation:

$$
\begin{aligned}
\frac{\mathrm{d}\rho_W(R_i, P_i, t)}{\mathrm{d}t} &= -\frac{i}{\hbar}[H_W, \rho_W(t)] + \frac{1}{2}(\{H_W, \rho_W(t)\} - \{\rho_W(t), H_W\}) \equiv \\
&\equiv -i\mathcal{L}\rho_W(t) ,
\end{aligned}
\tag{4.6}
$$

where $\{\cdot, \cdot\}$ is the Poisson bracket.

This equation properly accounts for the evolution of the system treating the S part as classical (Poisson bracket) and the Q part as quantum (commutator) and it can lead from a pure state to the correct thermodynamical mixed state because we can properly explore all the elements of the density matrix.

The direct integration of Eq. (4.6) is computationally quite heavy, since each element of the density matrix needs to be evolved and can affect every element of its row or column, plus having a different contribution to the evolution of the classical subsystem. We will therefore present a possible algorithm to efficiently obtain the evolution of the density matrix in a statistical way.

As a first step, we can write explicitly the terms of the Liouville operator (4.6) for the various elements of the density matrix in the form $\left(\frac{\mathrm{d}\rho_W}{\mathrm{d}t}\right)_{\beta,\beta'} = i\mathcal{L}_{\alpha\alpha',\beta\beta'}(\rho_W)_{\alpha\alpha'}$ considering the instantaneous eigenstates of the quantum subsystem $h_W|\alpha_R\rangle = E_\alpha(R)|\alpha_R\rangle$ in the adiabatic base at a given R:

$$
\begin{aligned}
i\mathcal{L}_{\alpha\alpha',\beta\beta'} &= i\mathcal{L}^0_{\alpha\alpha'}\delta_{\alpha\beta}\delta_{\alpha'\beta'} - J_{\alpha\alpha',\beta\beta'} = i(\omega_{\alpha\alpha'} + L_{\alpha\alpha'})\delta_{\alpha\beta}\delta_{\alpha'\beta'} - J_{\alpha\alpha',\beta\beta'} = \\
&= \left(i\frac{E_\alpha(R) - E_{\alpha'}(R)}{\hbar} + \frac{P}{m}\frac{\mathrm{d}}{\mathrm{d}R} + \frac{1}{2}(F_W^\alpha + F_W^{\alpha'})\frac{\mathrm{d}}{\mathrm{d}P}\right)\delta_{\alpha\beta}\delta_{\alpha'\beta'} + \\
&\quad + \left[d_{\alpha\beta}\delta_{\alpha'\beta'} + d_{\alpha'\beta'}^*\delta_{\alpha\beta}\right]\left(\frac{P}{m} + \frac{E_\alpha - E_\beta}{2}\frac{\mathrm{d}}{\mathrm{d}P}\right) ,
\end{aligned}
\tag{4.7}
$$

where $\omega_{\alpha\alpha'} = (E_\alpha(R) - E_{\alpha'}(R))/\hbar$, $F_W^\alpha = \langle\alpha_R|\frac{\mathrm{d}V_W}{\mathrm{d}R}|\alpha_R\rangle$, and $d_{\alpha\beta}(R) = \langle\alpha_R|\frac{\mathrm{d}}{\mathrm{d}R}|\beta_R\rangle$, and where we have considered a single classical degree of freedom for sake of simplicity. We can identify a first term of simple propagation plus a second term that actively accounts for quantum transitions between different elements of the density matrix.

Let us consider the propagator from time 0 to time t as the product of smaller propagators over N time-steps $\Delta t = t_j - t_{j-1}$: from an initial density

matrix element (α_0, α'_0) to the final (α_N, α'_N) we will have

$$\left(e^{i\mathcal{L}t}\right)_{(\alpha_0,\alpha'_0),(\alpha_N,\alpha'_N)} = \sum_{(\alpha_1,\alpha'_1)\ldots(\alpha_{N-1},\alpha'_{N-1})} \prod_{j=1}^{N} \left(e^{i\mathcal{L}(t_j-t_{j-1})}\right)_{(\alpha_{j-1},\alpha'_{j-1}),(\alpha_j,\alpha'_j)} \cdot$$
(4.8)

If we now consider Δt to be "small enough" (formally we operate a truncation of the Dyson expansion of the exponential) we can rewrite each term plugging (4.7) in the exponential and expanding:

$$\left(e^{i\mathcal{L}(t_j-t_{j-1})}\right)_{(\alpha_{j-1},\alpha'_{j-1}),(\alpha_j,\alpha'_j)} \simeq e^{i\omega_{\alpha_{j-1}\alpha'_{j-1}}\Delta t} e^{iL_{\alpha_{j-1}\alpha'_{j-1}}\Delta t}$$
$$\left(\delta_{\alpha_j\alpha'_j}\delta_{\alpha_{j-1}\alpha'_{j-1}} - \Delta t J_{\alpha_{j-1}\alpha'_{j-1},\alpha_j\alpha'_j}\right) \cdot$$
(4.9)

The simulation scheme we would like to follow represents the product of these terms as an ensemble of surface hopping trajectories, which can be sampled quite easily through a sort of Monte Carlo method to achieve the evolved state of the system. Assuming to start from a system with classical coordinates (R, P) and density matrix element $\alpha_0\alpha'_0$, the computational procedure is as follows:

- We evolve the quantum state with $e^{i\omega_{\alpha_0\alpha'_0}\Delta t}$ (namely a phase factor) and the classical system with $e^{iL_{\alpha_0\alpha'_0}\Delta t}$

- We choose with probability $1/2$ if we consider the transition $\alpha_0 \to \alpha_1$ or $\alpha'_0 \to \alpha'_1$, where α_1 and α'_1 are chosen uniformly among the allowed final states

- We calculate the transition probability π and the momentum exchange ΔP (explained later) and cast a random number $p \in [0, 1]$ to see if the transition occurs:

  - If the transition is not energetically allowed or if $p > \pi$ we continue the trajectory adiabatically: the classical variables remain the same and the quantum state gains a factor $(1 - \pi)^{-1}$ (the weight of the step).

  - If the transition is energetically allowed and $p < \pi$ we compute the transition: the classical momentum is updated based on the momentum exchange $P(t + \Delta t) \to P(t + \Delta t) + \Delta P$ and the quantum state gains a factor $w_{\alpha_0\alpha'_0,\alpha_1\alpha'_1}\pi^{-1}$ (the weight of the step considering the allowed jumps).

The nonadiabatic transition probability π introduced above is defined as (for a $\alpha_0 \to \alpha_1$ transition):

$$\pi = \left| \frac{P(t + \Delta t)}{m} d_{\alpha_0 \alpha_1}(R(t + \Delta t)) \right| \Delta t \left(1 + \left| \frac{P(t + \Delta t)}{m} d_{\alpha_0 \alpha_1}(R(t + \Delta t)) \right| \Delta t \right)^{-1}$$
$$(4.10)$$

and the weight of the accepted transition is further multiplied by

$$w_{\alpha_0 \alpha_0', \alpha_1 \alpha_1'} = \mathcal{N} \frac{P(t + \Delta t)}{m} d_{\alpha_0 \alpha_1}(R(t + \Delta t)) \Delta t, \qquad (4.11)$$

where $\mathcal{N}$ is the total number of allowed final states.

The easiest way to calculate the last missing quantity, the momentum exchange ΔP, is called momentum-jump approximation and basically relies on $(E_\alpha - E_\beta)\frac{m}{P}$ being small enough, so that we can convert the last terms of J in eq.(4.7) in exponentials. In this case we can write the momentum increment for a nonadiabatic jump as (skipping over some vectorial notation for the multidimensional case):

$$\Delta P = d_{\alpha\beta} \left[\text{sgn}(Pd_{\alpha\beta}) \sqrt{(Pd_{\alpha\beta})^2 + E_\beta - E_\alpha} - (Pd_{\alpha\beta}) \right] \qquad (4.12)$$

where $d_{\alpha\beta}$ is the matrix element defined before. This automatically ensures that the dynamics takes place on energy-conserving surfaces.

The last needed remark is about the energetic feasibility of the transition: if $E_\beta - E_\alpha < 0$ the quantum system is getting energy from the system, so that there is a chance that $(Pd_{\alpha\beta})^2 < |E_\beta - E_\alpha|$ and the transition cannot occur because there is not enough kinetic energy in the classical system to balance it. If we select a sufficient number of initial states their average at time t will represent the final evolved state of the system.

Since our final goal would be to treat some of the classical degrees of freedom as an effective bath, we will see how it is possible to do this within the same quantum-classical dynamics framework introduced up to now. The basic idea behind this is to separate the classical system in two parts (our H_S and H_B) and trace away the bath degrees of freedom to get a simple modification of the dynamics of the classical system.

We start by applying the usual Wigner transformation over the classical degrees of freedom of both subsystems to obtain $\rho_W(R, P, t)$. We will divide the total Liouville operator $\mathcal{L}$ in two parts: the one corresponding to terms that do not include the bath degrees of freedom $\mathcal{L}'$ and the bath and bath-system interaction part $\mathcal{L}_0$ (for ease of notation in the following we will indicate with a prime X' all quantities related only to H_S and with a double

prime X'' all quantities related only to the bath; quantities with no primes generally refer to the whole system). The part of the density matrix we want to get an equation for is

$$\rho'_W(R', P', t) = \int dR'' dP'' \rho_W(R, P, t). \qquad (4.13)$$

To find an equation for this we will define the equilibrium density matrix ρ_{We}, satisfying $i\mathcal{L}\rho_{We} = 0$, and we will assume that this can reasonably be expressed as the product $\rho_{We} = \rho'_{We}(R', P')\rho_0(R, P)$ where the first term is the equilibrium density matrix for the quantum-classical system $i\mathcal{L}'\rho'_{We}(R', P') = 0$ and the second is the equilibrium density matrix for the bath on a fixed system configuration $i\mathcal{L}_0\rho_0(R, P) = 0$ (this can be actually justified a posteriori as keeping the lowest order in $\hbar$). We will also consider the projection of the overall equilibrium density matrix on the subsystem of our interest $\rho_c = \int dR'' dP'' \rho_{We}$.

We can now define the projector $\mathcal{P}$ on a generic f_W as:

$$\mathcal{P}f_W(R, P) = \frac{1}{2}\left[\rho_{ce}\left(\int dR'' dP'' f_W\right) + \left(\int dR'' dP'' f_W\right)\rho_{ce}^\dagger\right], \qquad (4.14)$$

where $\rho_{ce}(R, P) = \rho_{We}(R, P)\rho_c^{-1}(R', P')$. By applying this projector (and applying the Nakajima-Zwanzig identity [42]) we can verify that the projection over the subspace of our interest of the density matrix obeys the equation:

$$\frac{d\rho'_W(R', P', t)}{dt} = \left[-i\mathcal{L}' - F_{SB}^0 \frac{d}{dP'} + \zeta\frac{d}{dP'}\left(\frac{P'}{m} + K_B T\frac{d}{dP'}\right)\right]\rho'_W, \qquad (4.15)$$

where $F_{SB}^0 = \left\langle\frac{dV_{SB}}{dR'}\right\rangle_0$ (the average is over $H_0 = H_B + H_{SB}$), and ζ is the fixed particle friction tensor of the bath $\zeta(R') = \frac{1}{K_B T}\int_0^\infty dt \left\langle\delta F_{SB}e^{-i\mathcal{L}_0 t}\delta F_{SB}\right\rangle_0$, δF_{SB} being the difference between the actual forces on the system and their H_0 average: $\delta F_{SB} = F_{SB}^0 - F_{SB}$. The position dependence of the friction tensor has been dropped.

To obtain this final form, we have also made the approximation that the characteristic relaxation time of the bath τ_B is much smaller than the typical timescale of the rest of the system τ_{QS} (basically to ignore the term depending on the initial conditions).

With respect to the previous equation (4.7), the presence of the bath basically only changes the evolution of the classical system by considering both external forces $F_{tot}^\alpha = F_W^\alpha + F_{SB}^0$ and adding the term due to the tracing away of the bath, so that we can rewrite (4.7) (with the previous notation) as:

$$i\tilde{\mathcal{L}}_{\alpha\alpha',\beta\beta'} = i(\omega_{\alpha\alpha'} + \tilde{L}_{\alpha\alpha'})\delta_{\alpha\beta}\delta_{\alpha'\beta'} - J_{\alpha\alpha',\beta\beta'} \qquad (4.16)$$

with

$$i\tilde{L}_{\alpha\alpha'} = \frac{P}{m}\frac{\mathrm{d}}{\mathrm{d}R} + \frac{1}{2}(F_{tot}^{\alpha} + F_{tot}^{\alpha'})\frac{\mathrm{d}}{\mathrm{d}P} - \zeta\frac{\mathrm{d}}{\mathrm{d}P}\left(\frac{P}{m} + K_B T\frac{\mathrm{d}}{\mathrm{d}P'}\right). \qquad (4.17)$$

The algorithm for the computation can be therefore easily changed accordingly.

The theory here presented allows to describe mixed quantum-classical systems in presence of a bath, in a way that preserves the density matrix structure of the quantum state. Coming back to the initial model: we would describe the quantum system Q as a single particle on a grid, solving the relevant Schrödinger equation to find the adiabatic basis; the T and S system would form our classical terms, while B would be absorbed in the way presented for baths. Finally, we would like to apply Eq. (4.16) through the sampling method proposed.

The approximations made should be reasonable for our system, given the proper ratio between the masses is considered and a sufficient number of paths with small enough time-steps is computed. Unfortunately, preliminary results seem to show that the needed number of paths is indeed very large: as with many Monte Carlo methods, the weights of the paths tend to diverge and need to be treated carefully, so that a good sampling of the trajectory space becomes quite heavy even for short evolutions. While this approach has been used to reproduce the evolution of spin-boson systems [43], treating systems with more degrees of freedom seems quite unfeasible.

Ultimately, we were expecting from this model to show a sort of frictional force on the tip due to the presence of the quantum particle. This could happen, e.g., in a regime where the motion of the quantum particle is damped by the presence of the bath as was the case for the spin of chapter 2: whether this is realistic or not for this system still has to be understood. This should in principle be confronted with a classical treatment of the light particle to see if some inherently quantum effect is present. Unfortunately, until we find a lighter approach or a different implementation of the one presented here, the exploration of this effects has to be delayed.

Conclusion

In this thesis we have presented two examples of dissipative quantum systems. Although both cases have been reduced to an "innocent looking" spin-$\frac{1}{2}$ coupled to a bosonic bath, they were derived from very different starting models and proved to be characterized by very different features. This shows the importance of the right description of the coupling between system and environment and how the presence of other degrees of freedom can have non-negligible effects even on the simplest Hamiltonian, completely changing the isolated behavior of the system.

In the MExFM case, we have seen that strong coupling can significantly slow down the response of a spin, so that an apparently adiabatic perturbation can become nonadiabatic in presence of a bath. We have shown how this effect can directly lead to dissipation by creating an hysteresis loop. In doing so, we have found a low-frequency spin-dependent dissipation mechanism, compatible with the experimental findings.

In the quantum pumping case, we have seen how a weak coupling can allow for relaxation of a spin to its ground state, but we have also showed that in presence of a fast rotation, the relevant energy scale might not straightforwardly correspond to the one of the isolated system. Once more this nonintuitive effect shows the importance of correctly accounting for the form of the bath. In our ideal system, this effect leads to a non-monotonicity of the pumped current as a function of frequency, an interesting effect which, as we have shown, could lead to experimental tests in the near future.

While both these applications are quite self-contained, further exploration of both systems could be interesting, especially if supported by experimental findings. On a larger scheme, the treatment of quantum dissipative systems is a rapidly growing area of research and both of these models could, with more or less extensive modifications, be applied to different systems and hopefully describe some other interesting effects.

Appendix A

The Influence Functional

In this appendix we will briefly derive Eq. (1.52). Our derivation will start from the general equation (1.50) for a path integral without further derivation and will outline the main steps needed to obtain the expression we used; we refer the interested reader to [2] and [10] for a more complete treatment and discussion of the general properties and limits of influence functionals.

Expending Eq. (1.50) for a system with a generic variable q (the spin in our case) and a bath with coordinates X_t and wavefunctions $\chi(X_t)$ from 0 to t we obtain:

$$
\begin{aligned}
P_{fi} \quad = \quad & \int \chi_f^*(X_t)\chi_f(X_t')e^{\frac{i}{\hbar}[S_0(q)-S_0(q')+S_B(X)-S_B(X')+S_I(q,X)-S_I(q',X')]} \\
& \chi_i^*(X_0')\chi_i(X_0)dX_0dX_0'dX_t\mathcal{D}q\mathcal{D}q'\mathcal{D}X\mathcal{D}X' ,
\end{aligned}
\tag{A.1}
$$

where $S_{0,B,I}$ are the actions of the system, bath and interaction parts, respectively, and once more the $\mathcal{D}\cdot$ represent integrals over the paths.

If we factor out all the parts belonging to the bath, we can obtain an expression for the influence functional by direct comparison with (1.51):

$$
\begin{aligned}
\mathcal{F}[q,q'] \quad = \quad & \int \chi_f^*(X_t)\chi_f(X_t')e^{\frac{i}{\hbar}[S_B(X)-S_B(X')+S_I(q,X)-S_I(q',X')]} \\
& \chi_i^*(X_0')\chi_i(X_0)dX_0dX_0'dX_t\mathcal{D}X\mathcal{D}X' ,
\end{aligned}
\tag{A.2}
$$

or better, since we are working with density matrices,

$$
\mathcal{F}[q,q'] = \int \rho_B(X_0, X_0')F(q; X_t, X_0)F^*(q'; X_t, X_0')dX_0dX_0'dX_t,
\tag{A.3}
$$

in term of the density matrix ρ_B of the bath and defining

$$
F(q; X_f, X_i) = \int e^{\frac{i}{\hbar}[S_B(X)+S_I(q,X)]}\mathcal{D}X .
\tag{A.4}
$$

We can now specialize this general form for a harmonic bath: for a bath of N oscillators with mass m_α and frequency ω_α coupled to a variable q (the spin in our case), we consider the Lagrangian of the bath and interaction as

$$
\begin{cases}
\mathcal{L}_B &= \dfrac{1}{2}\displaystyle\sum_{\alpha=1}^{N} m_\alpha \left(\dot{X}_\alpha^2(t) - \omega_\alpha^2 X_\alpha^2(t) \right) \\[2ex]
\mathcal{L}_I &= \displaystyle\sum_{\alpha=1}^{N} \left(c_\alpha X_\alpha(t) q(t) - \dfrac{1}{2}\dfrac{c_\alpha^2}{m_\alpha \omega_\alpha^2} q^2(t) \right) \ ,
\end{cases}
\tag{A.5}
$$

where the c_α's of the coupling correspond to our parameter λ and the second term in the coupling just ensures the correct minimum for the potential of the system. By assuming the bath at time 0 to be thermalized we can compute for the density matrix

$$
\begin{aligned}
\rho_B(X, X') &= \prod_{\alpha=1}^{N} \frac{1}{Z_\alpha} \sqrt{\frac{m_\alpha \omega_\alpha}{2\pi\hbar \sinh(\omega_\alpha \hbar\beta)}} \exp\left\{ -\frac{m_\alpha \omega_\alpha}{2\hbar \sinh(\omega_\alpha \hbar\beta)} \right. \\
&\quad \left. \left[(X_\alpha^2 + X_\alpha'^2)\cosh(\omega_\alpha \hbar\beta) - 2 X_\alpha X_\alpha' \right] \right\}
\end{aligned}
\tag{A.6}
$$

where Z_α is the partition function. We can then compute the other terms of the influence functional from the Lagrangians:

$$
\begin{aligned}
F(q; X^f, X^i) &= \\
&= \prod_{\alpha=1}^{N} \sqrt{\frac{m_\alpha \omega_\alpha}{2\pi\hbar \sin(\omega_\alpha t)}} \exp\left\{ \frac{i m_\alpha \omega_\alpha}{2\hbar \sin(\omega_\alpha t)} \left[(X_\alpha^{i2} + X_\alpha^{f2})\cos(\omega_\alpha \hbar\beta) \right.\right. \\
&\quad \left. -2 X_\alpha^i X_\alpha^f \right] + \frac{i X_\alpha^i c_\alpha}{\hbar \sin(\omega_\alpha t)} \int_0^t \sin\left(\omega_\alpha(t-t')\right) q(t') \\
&\quad + \frac{i X_\alpha^f c_\alpha}{\hbar \sin(\omega_\alpha t)} \int_0^t \sin\left(\omega_\alpha t'\right) q(t') - \frac{i c_\alpha^2}{2\hbar m_\alpha \omega_\alpha^2} \int_0^t q^2(t') dt' \\
&\quad \left. - \frac{i c_\alpha^2}{\hbar m_\alpha \omega_\alpha \sin(\omega_\alpha t)} \int_0^t dt' \int_0^{t'} dt'' \sin\left(\omega_\alpha(t-t')\right)\sin(\omega_\alpha t'')q(t')q(t'') \right\} .
\end{aligned}
\tag{A.7}
$$

By substituting the expressions (A.6) and (A.7) in (A.5) we finally find the form:

$$
\begin{aligned}
\mathcal{F}[q, q'] &= \exp\left\{ -\int_0^t dt' \int_0^{t'} dt'' \, [q(t') - q'(t')] \right. \\
&\quad \left. [L(t' - t'')q(t'') - L^*(t' - t'')q'(t'')] \right\}
\end{aligned}
\tag{A.8}
$$

with

$$L(t) = \frac{1}{\pi} \int_0^\infty d\omega \, J(\omega) \left(\coth \frac{\omega \beta}{2} \cos(\omega t) - i \sin(\omega t) \right) , \qquad \text{(A.9)}$$

as reported in Eq. (1.52) used in the text.

Bibliography

[1] R. Zwanzig, *Nonequilibrium Statistical Mechanics* (Oxford University Press, 2001).

[2] U. Weiss, *Quantum Dissipative Systems* (World Scientific, 1999).

[3] F. Pellegrini, G.E. Santoro, and E. Tosatti, Phys. Rev. Lett. **105**, 146103 (2010).

[4] F. Pellegrini, C. Negri, F. Pistolesi, N. Manini, G.E. Santoro, and E. Tosatti, Phys. Rev. Lett. **107**, 060401 (2011).

[5] C. Cohen-Tannoudji, J. Dupont-Roc, and G. Grynberg, *Atom-Photon Interactions: Basic Processes and Applications* (Wiley, New York, 1998).

[6] A. Caldeira and A. J. Leggett, Phys. Rev. Lett. **46**, 211 (1981).

[7] A. Leggett, S. Chakravarty, A. Dorsey, M. Fisher, A. Garg, and W. Zwerger, Rev. Mod. Phys. **59**, 1 (1987).

[8] M. Grifoni and P. Hänggi, Phys. Rep. **304**, 229 (1998).

[9] R.P. Feynman and A.R. Hibbs, *Quantum Mechanics and Path Integrals* (McGraw-Hill, 1965).

[10] R.P. Feynman and F.L. Vernon, Jr., Ann. Phys. (N.Y.) **24**, 118 (1963).

[11] M. Grifoni, M. Sassetti, J. Stockburger, and U. Weiss, Phys. Rev. E **48**, 3497 (1993).

[12] M. Grifoni, M. Sassetti, P. Hänggi, and U. Weiss, Phys. Rev. E **52**, 3596 (1995).

[13] M. Grifoni, M. Winterstetter, and U. Weiss, Phys. Rev. E **56**, 334 (1997).

[14] U. Kaiser, A. Schwarz, and R. Wiesendanger, Nature **446**, 522 (2007).

[15] R. Wiesendanger, Rev. Mod. Phys. **81**, 1495 (2009).

[16] H. Momida and T. Oguchi, Surf. Sci. **590**, 42 (2005).

[17] D. Ködderitzsch, W. Hergert, W.M. Temmerman, Z. Szotek, A. Ernst, and H. Winter , Phys. Rev. B **66**, 064434 (2002).

[18] T. Yamada, J. Phys. Soc. Jpn. **21**, 650 (1966); T. Yamada, S. Saito, and Y. Shimomura, J. Phys. Soc. Jpn. **21**, 672 (1966).

[19] W.L. Roth, Phys. Rev. **111**, 772 (1958); W.L. Roth, and G.A. Slack, J. Appl. Phys. **31**, S352 (1960).

[20] E. Uchida, N. Fukuoka, H. Kondoh, T. Takeda, Y. Nakazumi, T. Nagamiya, J. Phys. Soc. Jpn. **23**, 1197 (1967).

[21] M.T. Hutchings and E.J. Samuelsen, Phys. Rev. B **6**, 3447 (1972).

[22] T. Yamada, J. Phys. Soc. Jpn. **18**, 520 (1963).

[23] M.E. Lines and E.D. Jones, Phys. Rev. **139** A1313 (1965).

[24] D.C. Mattis, *The Theory of Magnetism* (Springer-Verlag, 1988).

[25] T. Holstein and H. Primakoff, Phys. Rev. **58**, 1098 (1940).

[26] F. Guinea, Phys. Rev. B **32**, 4486 (1985).

[27] W.H. Press, B.P. Flannery, S.A. Teukolsky, and W.T. Vetterling, *Numerical Recipes in FORTRAN: The Art of Scientific Computing (2nd ed.)* (C.U.P., 1992).

[28] L. Gaudreau, S. A. Studenikin, A. S. Sachrajda, P. Zawadzki, A. Kam, J. Lapointe, M. Korkusinski, and P. Hawrylak, Phys. Rev. Lett. **97**, 036807 (2006).

[29] W. H. Gerber and E. Schumacher, J. Chem. Phys. **69**, 1692 (1978).

[30] R. Englman, *The Jahn Teller Effect in Molecules and Crystals* (Wiley, London, 1972).

[31] N. W. Ashcroft and M. D. Mermin, *Solid State Physics* (Holt-Saunders, Philadelphia, 1976).

[32] D. Cohen, Phys. Rev. B **68**, 155303 (2003).

[33] L.D. Landau and E.M. Lifshitz, *Statistical Physics, Part 1, Course of Theoretical Physics, Vol. 5* (Pergamon, Oxford, 1980).

[34] L. Gaudreau, S.A. Studenikin, A.S. Sachrajda, P. Zawadzki, A. Kam, J. Lapointe, M. Korkusinski, and P. Hawrylak, Phys. Rev. Lett. **97**, 036807 (2006).

[35] L. Gaudreau, A.S. Sachrajda, S. Studenikin, A. Kam, F. Delgado, Y.P. Shim, M. Korkusinski, and P. Hawrylak, Phys. Rev. B **80**, 075415 (2009).

[36] F. Delgado, Y.P. Shim, M. Korkusinski, and P. Hawrylak, Phys. Rev. B **76**, 115332 (2007).

[37] Rachel J. Cannara, Matthew J. Brukman, Katherine Cimatu, Anirudha V. Sumant, Steven Baldelli, and Robert W. Carpick, Science **318**, 780 (2007).

[38] A. Nitzan, M. Shugard, and J.C. Tully, J. Chem. Phys. **69**, 2525 (1978).

[39] A. Benassi, A. Vanossi, G.E. Santoro, and E. Tosatti, Phys. Rev. B **82**, 081401(R) (2010).

[40] P.V. Parandekar and J.C. Tully, J. Chem. Phys. **122**, 094102 (2005); P.V. Parandekar and J.C. Tully, J. Chem. Theory Comput. **2**, 229 (2006).

[41] R. Kapral and G. Ciccotti, J. Chem. Phys. **110**, 8919 (1999).

[42] S. Nakajima, Prog. Theor. Phys. **20**, 948 (1958); R. Zwanzig, Physica **30**, 1109 (1964).

[43] D. Mac Kernan, G. Ciccotti, and R. Kapral, J. Chem. Phys. **116**, 2346 (2002).